DIAGENESIS IN SEAGRASS VEGETATED SEDIMENTS:

BIOGEOCHEMICAL PROCESSES ON DIURNAL TIME SCALES

A Dissertation

by

ANDREW BRIAN HEBERT

Submitted to the Office of Graduate Studies of
Texas A&M University
in partial fulfillment of the requirements for the degree of

DOCTOR OF PHILOSOPHY

August 2004

Major Subject: Oceanography

DIAGENESIS IN SEAGRASS VEGETATED SEDIMENTS:

BIOGEOCHEMICAL PROCESSES ON DIURNAL TIME SCALES

A Dissertation

by

ANDREW BRIAN HEBERT

Submitted to Texas A&M University
in partial fulfillment of the requirements for the degree of

DOCTOR OF PHILOSOPHY

Approved as to style and content by:

John W. Morse (Chair of Committee)	James L. Pinckney (Member)
Richard H. Loeppert, Jr. (Member)	Steven F. DiMarco (Member)
Peter M. Eldridge (Member)	Wilford Gardner (Head of Department)

August 2004

Major Subject: Oceanography

ABSTRACT

Diagenesis in Seagrass Vegetated Sediments: Biogeochemical Processes on Diurnal Time Scales.

(August 2004)

Andrew Brian Hebert, B.S., Northwestern State University of Louisiana;

M.S., Texas A&M University

Chair of Advisory Committee: Dr. John W. Morse

Seagrass productivity is largely limited by nutrient and light availability. However, increasing evidence suggests that sedimentary geochemical processes may play an essential role in seagrass productivity/health. Much of this work has been largely phenomenalistic and has not clearly identified the spatio-temporal behavior of the major geochemical parameters involved in diagenesis of seagrass sediments. In this study, a much broader range of both dissolved and solid phase chemical parameters in eelgrass vegetated sediments was investigated. Parallel measurements were made on adjacent unvegetated sediments (<10 m) to more clearly refine the specific influences of seagrass (*Zostera marina*) on chemical gradients in associated sediments. Previous studies have pointed strongly toward diurnal "ventilation" of sediments vegetated with seagrass by the exudation of photosynthetically produced oxygen. However, strong lateral variability of sediment geochemical parameters among and between seagrass vegetated and unvegetated sediments made the observation of diurnal effects sufficiently difficult. Changes resulting from temporal variability were difficult to discern within the spatial variability.

A critical question that is often not dealt with in the study of the early diagenesis of sediments is what spatial and temporal sampling intervals are required to account for the dominant source of variability. The auto-covariance function (ACF) was used to determine the optimum scaling length for sample intervals (Δx) of ΣH_2S and Fe^{2+}. Characteristic scale lengths obtained for sediments from seagrass environments are not significantly different from those observed for unvegetated sediments and averaged 13.7± 2.2 mm. Lateral variations in our scales analyses showed that scale length approximated our sampling interval and that lateral sampling intervals were smaller than the vertical sampling intervals. Our results indicate that macrofauna dwelling in the sediment, the seagrass root/rhizomes, and aggregations of bacteria, microalgae, and meiofauna may be responsible for the vertical and lateral variability. Model calibrations and sensitivity analyses from a sediment-seagrass diagenetic model revealed that changes in physical parameters of the sediments (irrigation, advection, and porosity, for example) had the greatest effect on organic carbon and total dissolved sulfides. This study revealed that sedimentary geochemical parameters that are both vertically and laterally heterogeneous may also affect seagrass productivity.

DEDICATION

To my wife, Elizabeth, without whom everything else is meaningless

ACKNOWLEDGEMENTS

I would like to acknowledge my committee chair, Dr. John W. Morse, for his invaluable advice and financial support from the Louis and Elizabeth Scherck Endowed Chair. Special recognition should be given to Drs. James L. Pinckney and Peter Eldridge along with the rest of my committee, Drs. Steven F. DiMarco and Richard H. Loeppert, Jr. for their continued support and instruction. I would also like to thank Bryan Brattin and Dr. Robert Taylor of the Trace Element Research Laboratory (TERL), Dr. Luis Cifuentes and Brian Jones for their contributions.

Jim Kaldy and Bruce Boese at USEPA, Karen Sell, Rolf Arvidson, Alyce Lee, Amy Degeest, and Sandy Drews all deserve appreciation. Thanks to Dwight Gledhill, who has always taken the time to help and Megan Singer who always made sure I had clean equipment and supplies and helped with some of the analyses. Particular credit and recognition go to all my family and friends for their encouragement and support, especially my parents, brothers, and my wife Elizabeth, who have always inspired me to do my best.

This research was supported financially by the USEPA and Louis and Elizabeth Scherck Endowed Chair. I am grateful to the Oceanography Graduate Council for providing mini-grant funds to aid in the completion of this research.

TABLE OF CONTENTS

CHAPTER Page

Page

LIST OF FIGURES

FIGURE Page

LIST OF TABLES

TABLE Page

CHAPTER I

INTRODUCTION

Objectives

The primary objective of this research was to better understand the complex relationship between seagrass meadows and their underlying sedimentary geochemical processes. Within this general objective, most of the critically important oxidation/reduction reactions in seagrass sediments and in reference (unvegetated) sites on varying spatial and temporal scales received primary attention.

This research was motivated by the severe limitation of management strategies based on sediment geochemical data from seagrass meadows, and broadens the range of sedimentary geochemical parameters sampled than previous investigations. The information developed in this study was used to address geochemical processes in early diagenesis of seagrass sediments. Spatio-temporal scales of the variability of geochemical parameters were also determined, the results were used to develop, calibrate and simulate a seagrass/sediment diagenetic model that links temperate seagrass physiology to sedimentary geochemical processes. In addition, this study characterized estuarine seagrass communities and habitats and examined potential impacts of multiple stressors such as nutrient availability, turbidity, and sediment phytotoxin concentration that may adversely impact seagrass ecosystems. Phytotoxin concentration, e.g. H_2S, has been shown to be responsible for reductions in leaf surface nutrient and carbon cycling, and because of the limited and/or contradictory studies on

---

This dissertation follows the style of *Geochimica et Cosmochimica Acta*.

inhibition effects on seagrass productivity due to sediment toxicity, nutrient limitation, and/or other aquatic stressors reassessment is require (Goodman et al., 1995; Erskine and Koch, 2000).

Carbon, oxygen, nitrogen, iron, and sulfur are among the most important of many elements that are cycled in most sediments, thus play a fundamentally active role in diagenesis among seagrass vegetated sediments. The majority of seagrass research has largely focused on biomediated processes that tend to neglect chemical equilibria processes and abiotic reactions. Because geochemical processes in seagrass vegetated sediments are almost never at steady-state due to spatial and temporal scale differences as well as continual biological activity (bacterial respiration, localized inputs of seagrass exudates, and bioturbation/irrigation, for example) it is important to know how biomediated processes and pore water/solid abiotic reactions function in conjunction with in the diagenesis of seagrass vegetated sediments. This study focused on the extensive interactions between seagrasses and associated sedimentary geochemical processes.

Background on Seagrass/Sediment Interactions

Seagrass meadows are often considered to be the most valuable component of shallow water ecosystems and are frequently used as sensitive bioindicators of water and sediment quality (Hammerstrom et al., 1998; Fourqurean and Cai, 2001). Other studies showed that benthic net primary production of seagrasses was strongly correlated with water column respiration, mainly due to bacterioplankton that were responsible for

carbon remineralization of more than 50% of the DOC released from the benthos (Ziegler and Benner, 1999).

Seagrass-sediment interaction: sulfide connection

Seagrass productivity is largely limited by light and nutrient availability. However there is increasing evidence that hydrogen sulfide, produced by sulfate reducing bacteria (SRB), may also play an essential role in seagrass productivity and health. Sulfide in sediments can impede seagrass growth rate and influence morphology (Goodman et al., 1995; Terrados et al., 1999; Erskine and Koch, 2000; Lee and Dunton, 2000; Koch and Erskine, 2001). Experiments in which sedimentary sulfide concentrations were manipulated have demonstrated that dissolved sulfide can cause a reduction in plant biomass and have negative effects on plant physiology (Goodman et al., 1995; Erskine and Koch, 2000; Lee and Dunton, 2000; Koch and Erskine, 2001). However, as seagrass leaves photosynthesize during light periods, oxygen is produced and translocated by diffusional processes to the rhizosphere for root respiration via lacunae within the seagrass (Smith et al., 1984; Connell et al., 1999). As a consequence, redox reactive chemical constituents in the pore water can become oxidized (Lee and Dunton, 2000; Hebert and Morse, 2003).

Based on extensive observations of the biogeochemistry of sediments associated with both seagrass vegetated and unvegetated sediments, in Laguna Madre, TX, Eldridge and Morse (2000) produced a diagenetic model for the root-zone of vegetated sediments that required substantial diurnal inputs of oxygen from the rhizomes to maintain the observed chemical conditions. In the same region, Lee and Dunton (2000) examined

sulfide-seagrass interactions of a sub-tropical seagrass *Thalassia testudinum* in relation to diel changes in sediment pore water sulfide concentrations. They observed that sulfide concentrations were higher in seagrass sediment as opposed to adjacent unvegetated areas and mid-day depressions in sulfide concentrations corresponded with subsequent transport and release of oxygen to the sediments. Similarly, Hebert and Morse (2003), using microelectrodes as described by Brendel and Luther (1995) demonstrated that sediments vegetated with a temperate seagrass *Zostera marina* in Yaquina Bay, OR contained pore water concentrations of Fe^{2+} and H_2S that varied by an order of magnitude or more within 1.5 cm horizontally. Despite, the high spatial variability in vegetated sediments, temporal signatures existed among Fe^{2+} and H_2S concentrations within the vegetated sediments but not in nearby (<10 m) unvegetated sediments (Hebert and Morse, 2003).

Hebert and Morse (2003) showed for vegetated sediments, H_2S and Fe^{2+} concentrations in the upper 5 cm exhibited a diurnal cycle, most likely in response to photosynthetic oxygen input, similar to those observed in previous studies. During periods of light exposure, Fe^{2+} concentrations were often approximately inversely related to H_2S concentrations. A possible explanation for that observation was that as H_2S was produced or oxidized, the Fe^{2+} concentration decreased or increased in response to iron sulfide mineral (e.g., amorphous FeS or mackinawite) precipitation and dissolution. Thus changes in pore water concentrations of Fe^{2+} and H_2S did not necessarily represent the total change in the dissolved plus solid phase concentrations of these components. Labile iron sulfide minerals could play an important role as sinks and buffers for

dissolved Fe^{2+} and H_2S concentrations that may have also varied on similar time scales. Equilibria constraints between solid and dissolved components significantly complicate interpretation of their variability in sediments simply by dissolved phase biomediated redox processes (Hebert and Morse, 2003).

Seagrass-sediment interaction: infaunal irrigators

The benefit of seagrass as a source of nutrition and refuge to infaunal communities has been demonstrated in numerous studies (Webster et al., 1998; Mattila et al., 1999; Bostrom et al., 2002). Fewer studies, however, have demonstrated the benefits that seagrasses derive from the presence and activity of infaunal organisms. Peterson and Heck (2001) found a positive relationship between infaunal nutrient cycling and seagrass productivity. Eldridge et al. (in press) suggest that seagrass derive additional benefits from irrigating infauna through the introduction of oxidants from the water column into the root zone. The additional complement of oxidants in the rhizosphere helps maintain low levels of sulfides and other reduced toxicants (Eldridge and Johnson, 2004).

Seagrass-sediment interaction: seagrass as sequesters of particles

Seagrasses produce more organic matter than is used by water-column, epifaunal, and infaunal organisms. Much of this organic matter is sequestered in the sediments (Moriarty et al., 1986, Boschker et al., 2000; for example). Particulate deposition is further enhanced by the capacity of seagrass to directly retain sestonic particles. In addition to the settling of particles due to decrease turbulence and current flow (Terrados and Duarte, 2000; Koch, 2001), particles physically adhere to seagrass leaf surfaces or

are trapped by protozoa that reside on leaves. These trapping mechanisms may be the dominant particle trapping mechanism in seagrass canopies and add significantly to the high total organic carbon input into seagrass sediments (Agawin and Duarte, 2002; Eldridge and Johnson, 2004).

Seagrass-sediment interaction: nutrient effects

Mineralization processes in sediments are largely responsible for supplying nutrients to the seagrass root zone (Short, 1987; Perez et al., 1994; Holmer et al., 2001). Because of the abundance of sulfate in seawater, much of the mineralization of organic material in near-shore sediments results from sulfate reduction. This process may inhibit seagrass growth through sulfide toxicity (Holmer and Bondgaard, 2001). The high concentration of sulfate in the seawater-column insures that the in-sediment zone of sulfate reduction is much thicker than that for nitrate and oxy-hydroxy-metals (Berner 1980). Although sulfate competes poorly as an oxidant, its prevalence ensures that sulfate reduction is the dominant process in near shore sediments (Berner 1980). However, the extrapolation of the general trends in near shore sediment diagenesis to seagrass sediments is equivocal. While Holmer et al. (2001) found that the depth distribution of sulfate reduction in a tropical seagrass (*Cymodocea rotundata*) was positively correlated with below ground biomass, they also found that sulfate reduction was not the major diagenetic process leading to nutrient remineralization possibly because of the seagrasses ability to inject O_2 and other oxidants into the root zone. The ability of seagrass to promote mineralization of organic material while regulating sulfate

reduction in the root zone may be an important mechanism to insure seagrass survival in high total organic loading areas (Eldridge and Johnson, 2004).

The ability of seagrasses to regulate organic carbon mineralization depends on a number of factors including canopy irradiance and sediment organic enrichment (Koch 2001; Holmer and Laursen, 2002). In low (less than about 2.5 wt % (Koch, 2001 and references within)) organic sediments with seagrasses receiving high canopy irradiance, stable isotope data from several studies suggests that there is a strong linkage between seagrass production and sediment biogenic processes (Holmer and Lauren, 2002; Kaldy et al., unpublished data). Significant levels of seagrass root exudates can be sequestered in sediment bacteria (Kaldy et al., unpublished data), but the level of coupling between seagrass and biogenic processes is dependent on the seagrass irradiance field and the level of sediment organic loading (Holmer and Laursen, 2002). The interaction between seagrass production and percent organic matter is highly variable and there are studies that show healthy seagrass in highly organic sediments (Koch, 2001). It is assumed that either the organic matter in these sediments is relatively unreactive or that infaunal irrigating (filter feeders) are aerating the sediments in the vicinity of the seagrass (Eldridge and Johnson, 2004).

Seagrass-sediment interaction: role in bed migration

In many shallow estuaries there is an obvious migration of seagrass patches often in the direction of dominant wind flow. Similarly, in seagrass meadows there are often bare areas formed by macroalgae smothering of seagrass or dredge spoil deposits that also migrate in the direction of the dominant wind flow. While the mechanism for these

migrations is poorly understood, it is assumed to be mechanical in nature. The rationale for this process is as follows. Initially, there is net growth on the edge of a seagrass patch or bare area (a.k.a. "pane" in the nomenclature of marsh ecology) which is most sheltered by the seagrass from erosion and there is loss of seagrass at the edge of the patch or pane where physical disturbance is greatest. The result is that patches and panes migrate in the direction of the current which in shallow waters is approximately the same as the wind flow. To provide a framework for discussing seagrass patches and panes, the upwind edge of each is defined as the leading edge. Preliminary studies (Hebert et al., in prep.; Hebert and Morse, 2003) suggest that there are other chemical factors that relate to the migration of seagrass patches and panes. The reduction in light due to resuspension of sediment can reduce the irradiance at the leading edge of the patch or trailing edge of a pane. This reduces the flow of oxygen and other oxidants into the seagrass root zone. The interaction of the seagrass root zone and sediment geochemistry is highly variable (Hebert and Morse, 2003), but it is well known that highly organic sediments are geochemically uncoupled from seagrass production processes. That is, sediment organic matter inputs from seagrass are too small or refractory to affect sediment diagenetic processes (Holmer et al., 2001). This is probably why seagrass is rarely found in sediment with greater than 5% organic matter (Hemminga and Duarte, 2000). Generally seagrass meadows can be maintained through relatively severe organic loading events as long as there are high levels of light, and hence seagrass productivity, causing strong flux of O_2 through the lacunae to the root zone. However, when dredging or macroalgae erode or smother a portion of a seagrass

meadow, the reduction of O_2 flux into the sediment may set up a cascade of events that can require relatively benign sediment conditions for the seagrass to re-grow. Thus if a pane or bare area is subjected to high organic loading due to eutrophication, the expectation would be that the pane would become larger over time due to the reduction in seagrass re-growth (Eldridge and Johnson, 2004).

Pathway to a management criterion

The interaction of seagrass with its sedimentary environment has been explored in earlier sections of this chapter to provide a foundation for the development of management criterion that could be used to evaluate the "health" of *Z. marina* meadows.

Eldridge and Johnson (2004) define health in this regard in terms of maintaining healthy levels of biomass and productivity and further in terms of maintaining a continuous areal coverage to a reasonable depth limit in an estuary – the actual depth limit is dependent on the use attainment goal set for a region. In this section, the concern lies with sediment geochemical factors that affect seagrass production. The seagrass light field and percent organic matter are probably the most important factor affecting seagrass productivity (Dennison, 1987; Ziegler and Benner, 2000). The availability of light to seagrasses is directly related to photosynthesis and has been shown to be directly related to the seagrasses ability to protect itself from high levels of sulfide in the root zone. The percent organic matter in sediments is related to the potential sulfate reduction potential and hence to the sulfide concentrations in the sediment. Many biotic and physical processes that modify the interaction of seagrasses with its sedimentary environment have been discussed. In developing criterion that will be protective of the

seagrass it is necessary to take some of these factors into consideration. Factors related to seagrass sediment interaction could include (from Eldridge and Johnson, 2004):

1) disturbance – once seagrass is lost it is often difficult to get it to regenerate or re-grow.

2) total suspended solids – which reduce light field and photosynthesis and increase organic matter loading to the sediments.

3) percent organic loading – the greater the organic loading to the sediments the greater the potential for high sulfide concentrations that could inhibit seagrass production.

4) infaunal populations – the irrigating (filter feeding) infauna may be the most important of the infaunal organisms for maintaining continuous and productive seagrass meadows because of their ability to aerate the sediments.

Methods to evaluate these four factors in a way that scales them to nutrients, suspended sediment input, and other anthropogenic stressors are needed and these factors will be efficient tools for developing environmental criteria.

Research Summary

This dissertation focuses on a broad sampling of sedimentary geochemical parameters and assesses their spatial and temporal variability among and between seagrass and adjacent unvegetated sediments. The next chapter will address the sedimentary geochemical parameters and how they change with respect to space and time. Chapter III will illustrate the appropriate scale length for ΣH_2S associated with

these sediments using the autocovariance function (ACF). Chapter IV will attempt to model processes so that the geochemical parameters that are most sensitive to changes in sedimentary processes can be observed.

CHAPTER II

SPATIO-TEMPORAL CHANGES IN SEDIMENTARY GEOCHEMISTRY OF A TEMPERATE EELGRASS (*Zostera marina*) BED AND UNVEGETATED SEDIMENTS

Introduction

Seagrass productivity is largely limited by nutrient and light availability. However, there is increasing evidence that sedimentary geochemical processes may play an essential role in seagrass productivity/health as mentioned in the previous chapter (Pulich, 1989; Goodman et al., 1995; Holmer and Nielsen, 1997; Madureira et al., 1997; Blaabjerg et al., 1998; Terrados et al., 1999; Erskine and Koch, 2000; Lee and Dunton, 2000; Holmer et al., 2001). These processes can vary on small spatial (<1 mm) and temporal (< 1 hour) scales (Harper et al., 1999; Shuttleworth et al., 1999; Hebert and Morse, 2003; Morse et al., 2003). Sediment phytotoxin concentration (e.g. H_2S), if high enough, can lead to reductions in leaf surface area, necrotic tissue development, and overall biomass, as well as loss of acreage of seagrass meadows (Goodman et al., 1995; Erskine and Koch, 2000; Koch and Erskine, 2001).

However, sediment nutrient, carbon, iron, and sulfur cycling, and their relationship to seagrass productivity are poorly understood. Geochemical processes in seagrass vegetated sediments are generally not at steady-state, and are spatially and temporally heterogeneous due to biological activity, such as bacterial respiration, localized inputs of seagrass exudates, and bioturbation/bioirrigation.

The majority of the literature examining diurnal effects of geochemical changes in seagrass sediments has primarily focused on dissolved phase geochemical parameters, which typically represents only a small fraction of the total. However, the concentration of solid compounds such as sulfide minerals may also vary on similar time scales, and the interaction of seagrass with a potentially much larger reservoir of redox reactive components has not yet been determined. This study focused on the geochemical transformations (C, H, N, S, and reactive metals) in seagrass sediment and their spatial and temporal changes on diurnal time scales. The purpose was to examine on a diel cycle the spatial and temporal distribution of large range of sedimentary geochemical parameters at a seagrass site and adjacent unvegetated site. This was done to determine how geochemistry affects the seagrass and seagrass affects the geochemistry.

Methods

Study area and sampling strategy

The study focused on subtidal sediments vegetated with *Zostera marina* (eelgrass) at Idaho Point which is on the south side of the Yaquina Bay estuary in Newport, OR ($44^{o}37.125'$ N, 124^{o} 01.847' W) (Fig. 2.1) during August 2003. Samples were taken from the middle of a dense eelgrass bed (>~50 shoots $\cdot m^{-2}$) and unvegetated sediments 10 m from the edge of the bed. The sediments at both locations were dominantly fine-grained sand mixed with silt with a very dark color (see Kulm (1965) for mineralogy). Cores were taken avoiding, as much as possible, obvious macrostructures (e.g., burrows). Much of the unvegetated site was covered with benthic

micro- and macroalgal mats which were also avoided as reasonable achievable, hence unvegetated might be a misnomer. For the purposes of this dissertation, unvegetated sediments refer to non-seagrass sediments. Cores were taken at mid-day (~12:00 pm) and at night (~4:00 am) to examine both light and dark conditions. At each time and for each sediment type (seagrass vegetated (SG) or unvegetated (UV)), a variety of cores were taken for three different experiments (1) two cores (14 cm x 40 cm)were taken for microprofiles, (2) two cores (3 cm x 30 cm) with siliconed injection ports (2 cm depth intervals), were taken and processed for the determination of sulfate reduction rates, and (3) two Plexiglas core liners (7 cm x 40 cm) were taken and processed for pore water and solid geochemical analyses (Fig. 2.2).

Microprofiles

The cores used for the determination of dissolved O_2, Mn^{2+}, Fe^{2+}, ΣH_2S, and pH were immediately placed in aquaria with filtered seawater water of the same salinity and maintained at *in situ* temperature. The lighting was supplied by 1000 watt metal halide bulbs with a measured irradiance of ca. 400 µmol photons$\cdot m^{-2}\cdot s^{-1}$ with a 12/12 h on/off system. Seagrass leaves were allowed to extend out of the core as they do during low tide exposure. Gold-mercury amalgam, solid-state voltammetric microelectrodes were used to measure pore water dissolved O_2, Mn^{2+}, Fe^{2+}, and ΣH_2S. Microelectrodes were calibrated against reagent grade standard curves (Brendel, 1995; Brendel and Luther, 1995; Hebert and Morse, 2003). Sediments in both the seagrass and unvegetated cores were profiled every four hours for a 24 h period. Three near-simultaneous (<5 s lag) microelectrode measurements were obtained for each time point.

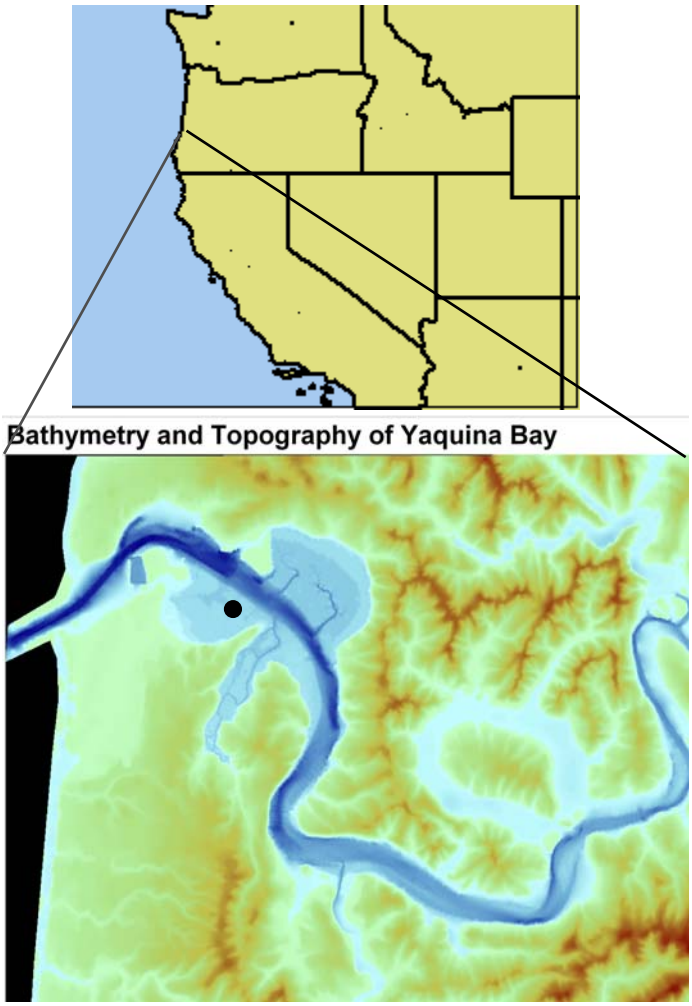

Fig. 2.1 Yaquina Bay, OR, USA (● denotes Idaho Point and sampling site)

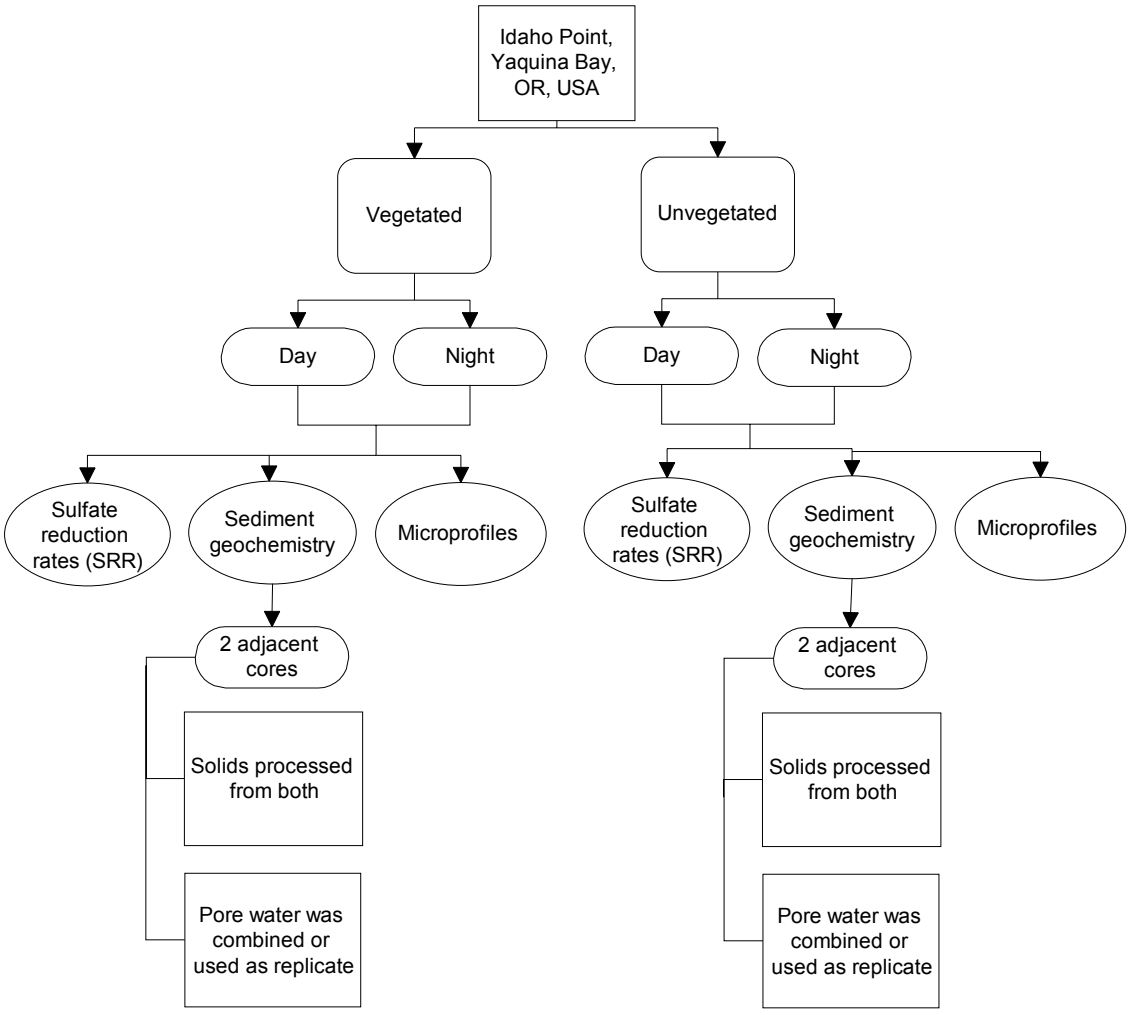

Fig. 2.2 Flow diagram of sampling scheme

Measurements for each profile were made at 2 mm depth increments down to 50 mm, at which point 5 mm depth increments were made to a total depth of 150 mm. The experiment was replicated a week later with fresh cores from the same location. A Corning combination pH microelectrode was used in conjunction with a Thermo Orion 230A+ pH meter to profile pH at 2 cm intervals. An ATC probe was used for

temperature compensation and Hannson's buffer was used to calibrate the electrode for seawater (Hannson, 1973).

Biomass data were obtained from the seagrass cores at the end of the experiment. Sediments were rinsed with deionized water from the rhizome and roots and epiphytic alga was removed from seagrass leaves by scraping. The shoots and leaves were dried and weighed as grams dry weight (gdw) of aboveground biomass normalized to core area. Roots and rhizomes were divided and dried separately. Percent total sulfur (%TS) of combusted plant parts, assumed to be largely organic-S because of reduced sulfur oxidation under aerobic conditions and plant rinsing (removes inorganic sulfur), was determined by combusting plant material in a UIC furnace against sulfur standards.

Sulfate reduction rates

Sulfate reduction rates (SRR) were determined using the radiotracer ^{35}S method of Jørgensen (1978) and Canfield et al. (1986). After the cores were obtained in the field, they were brought back to the laboratory (<2 h) and processed immediately. Cores for SRR determination were injected with 10 μCi of $Na_2{}^{35}SO_4$ every 2 cm, then incubated for 12 hours, quickly frozen, and shipped back on dry ice to Texas A&M University. The SRR were determined following the laboratory distillation and separation process using the boiling Cr $(II)^+$ acid method of Canfield et al. (1986). Once the separation of the radiolabeled sulfate and sulfide fractions was made, the samples were then diluted with zinc acetate, pippetted into scintillation vials with scintillation cocktail, well mixed, and measured on a LKB Wallack 1219 Rackbeta liquid

scintillation counter. The ratio of the radiolabeled H_2S/SO_4 fractions was calculated and the rates determined by activity and initial SO_4^{2-} concentrations.

Sediment pore water and solids geochemistry

7 cm diameter core liners were used to obtain sediments for the majority of chemical analyses to be performed. The cores were sectioned at 2 cm intervals to a final depth of 20 cm under a nitrogen environment and Reeburgh (1967) squeezers were used to extract pore water. The pore water was then syringe-filtered (0.45 μm) and separated into appropriately labeled glass vials with septa, spiked with mercuric chloride when appropriate (e.g. DIC), and frozen or refrigerated until analysis. Solids were placed in whirl bags under nitrogen and frozen.

Dissolved inorganic carbon (DIC) was determined by coulometric titration (UIC Inc. CO_2 Coulometer). An acid blank value was determined and subtracted from the samples. Both samples and standards were analyzed in identical fashion. The instrument was standardized by analyzing aliquots of reagent grade Na_2CO_3 (Aldrich) solution (Dickson and Goyet, 1994). A Shimadzu TOC- 5000 analyzer was used to determine dissolved organic carbon (DOC). Standards from 0-20 ppm of potassium biphthalate (Fisher) were used to develop a standard curve and blanks. SO_4^{2-}/Cl^- was measured using a DIONEX Ion Chromatograph while using reagent grade sodium sulfate (Aldrich) and sodium chloride (Fisher) for standard (calibration) curves. Ammonium-N was determined spectrophotometrically by the phenol-hypochlorite method using nitroprusside as a catalyst according to Strickland and Parsons (1972). Pore water was diluted to 1:20 mL and standard curves were generated using A.C.S. reagent-grade

ammonium chloride (Aldrich) (Strickland and Parsons, 1972). Nitrate was determined as NO_3^- + NO_2^- - N using a Clark-type nitrate sensor (Unisense) and a picoameter PA2000 (Unisense). A calibration curve was generated using various concentrations of a sodium nitrate solution (Aldrich). Phosphate was determined as soluble reactive PO_4^{3-} - P using ammonium molybdate, ascorbic acid, and trivalent antimony in a spectrophotometer (Varian DMS 100S UV-visible spectrophotometer) (Strickland and Parsons, 1972).

Similar procedures to those of Canfield et al. (1986) and Cornwell and Morse (1987) were used to determine TRS and AVS, respectively. Frozen sediments were digested to liberate sulfides and trapped in solution. An aliquot of the trap solution was then injected into a UIC sulfur coulometer and counted as µg S. Na_2S (Fisher) standards were used to verify accuracy and precision of the analysis and instrumentation. AVS was determined using a room temperature 6N HCl+$SnCl_2$ for 1 hour (see Cornwell and Morse (1987) for review). The chromium reduction of Canfield (1986) was used for the determination of TRS. Total organic carbon (TOC) was calculated as weight percent carbon by combusting acidified and unacidified dried sediment samples in a UIC furnace coupled to a UIC carbon coulometer. Reactive metals were extracted from the sediments using two different techniques, cold HCl and citrate dithionite (Raiswell et al., 1994). Once the samples were extracted they were analyzed using ICP-OES. Iron data reported will be distinguished henceforth by CDE-Fe (iron extracted by citrate dithionite for 2 hours) and HCl-Fe (iron extracted by 1M HCl for 24 hours) (Fig. 2.3). Previous porosity data from earlier in the year from the site was used. Grain size analysis was

determined by wet sieving the sand fraction and pippette analysis for silt and clay fractions.

Results

Microprofiles

Dissolved oxygen (O_2) and manganese (Mn^{2+}) concentrations were below detection (<5 μM) at the sediment-water interface and in the pore water so data are not presented. Sulfide in sediments (measured as ΣH_2S) and dissolved iron (Fe^{2+}) occurred concomitantly in many cases as well as a dissolved, unquantifiable FeS signal at -1.1 volts.

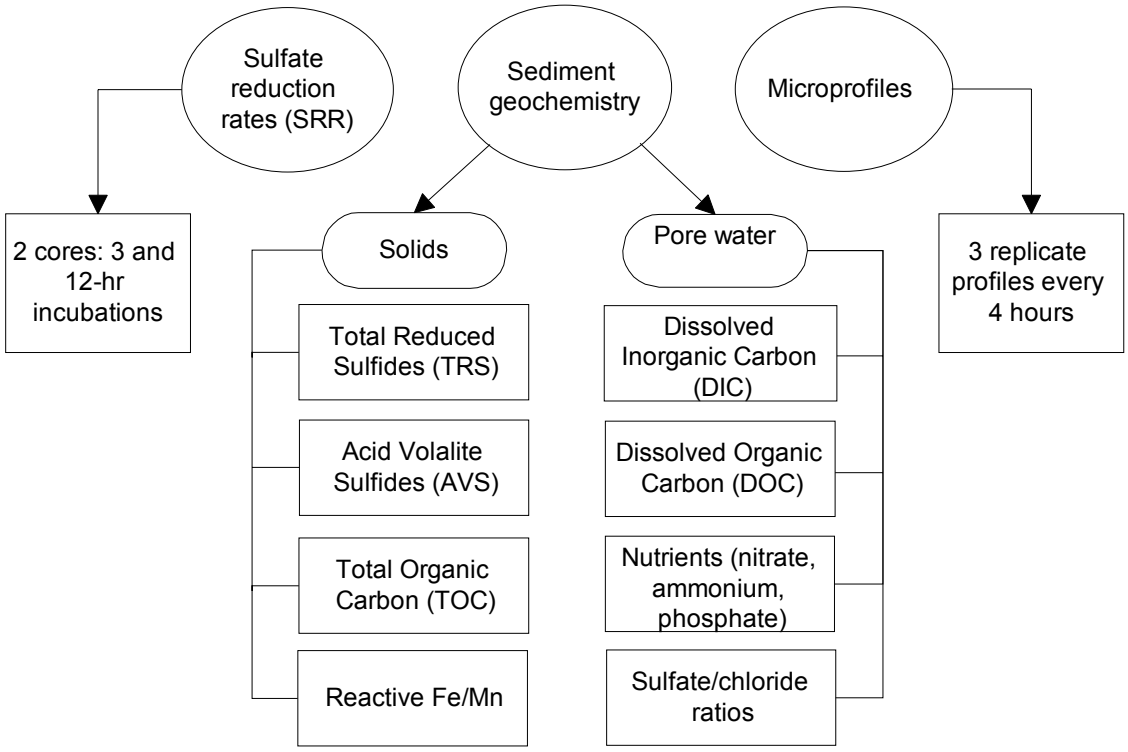

Fig. 2.3 Flow diagram of sample processing

Dissolved Fe^{2+} and ΣH_2S

The spatial heterogeneity in most cases was too large to distinguish from diurnal changes for seagrass pore water ΣH_2S and Fe^{2+} concentrations (Figs. 2.4-2.9). However, the general trend in profiles was that the standard deviation (as determined between three profiles for each time point) of depth-profiles was largest in the root zone (5-10 cm) of seagrass sediments, and was much smaller below the root zone from 10-15 cm depth. However, the coefficient of variation showed for some profiles that the standard deviation may have been a function of the mean. The variance to mean ratio is >>1 indicating that microdistributions of SRB may be responsible for the observed variability in ΣH_2S. Chapter III elaborates on the confounding factors of scale. Unvegetated sediments were also spatially heterogeneous, however, the average standard deviation from unvegetated sediments was smaller than the seagrass sediments. Fe^{2+} was present in the first seagrass core in high concentrations (0-6 mM) but was not detected in the other seagrass cores. The first unvegetated core, UV1-6, indicated lower Fe^{2+}concentrations (0-600 μM) in deeper sediments (10-15 cm) (data not shown) that occurred in patchy distributions. It should be noted that in almost all cases where ΣH_2S and $Fe^{2+}$are detected simultaneously, a signal for FeS occurred indicating the presence of iron sulfide clusters (Morse and Rickard, in prep.). Light and dark profiles of two seagrass cores (SG1 and SG2) were averaged separately and integrated into three depth bins (0-5 cm, 5-10 cm, and 10-15 cm). In UV1, concentrations steadily increased under both light and dark conditions, but were slightly higher in concentration for the dark.

Conversely, UV2 had higher sulfide concentrations in the light than in the dark, with little variability with depth.

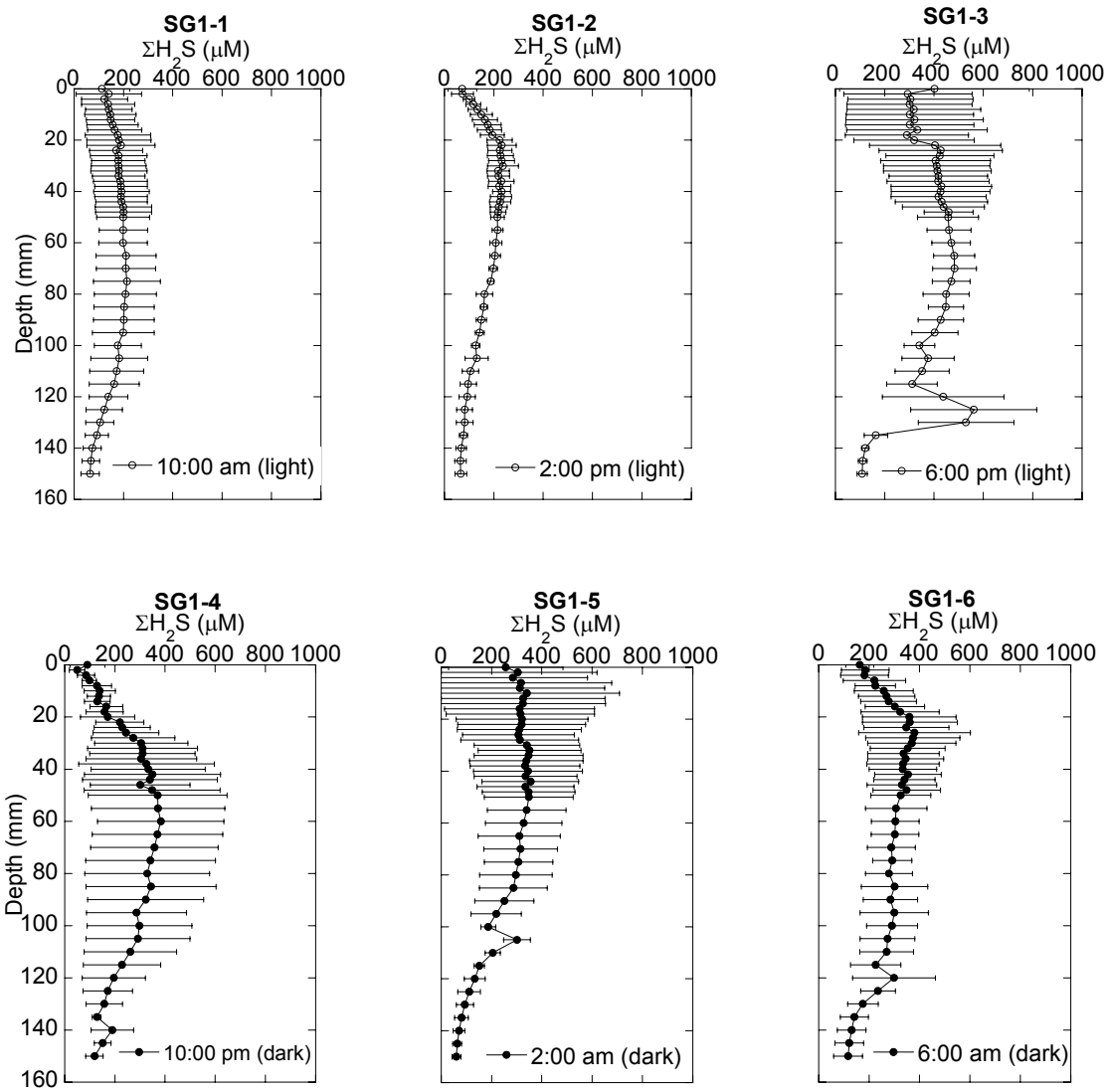

Fig. 2.4 Average dissolved pore water ΣH_2S for a seagrass core (SG1) in a 24 hr. period (bars represent ± standard deviation between three profiles)

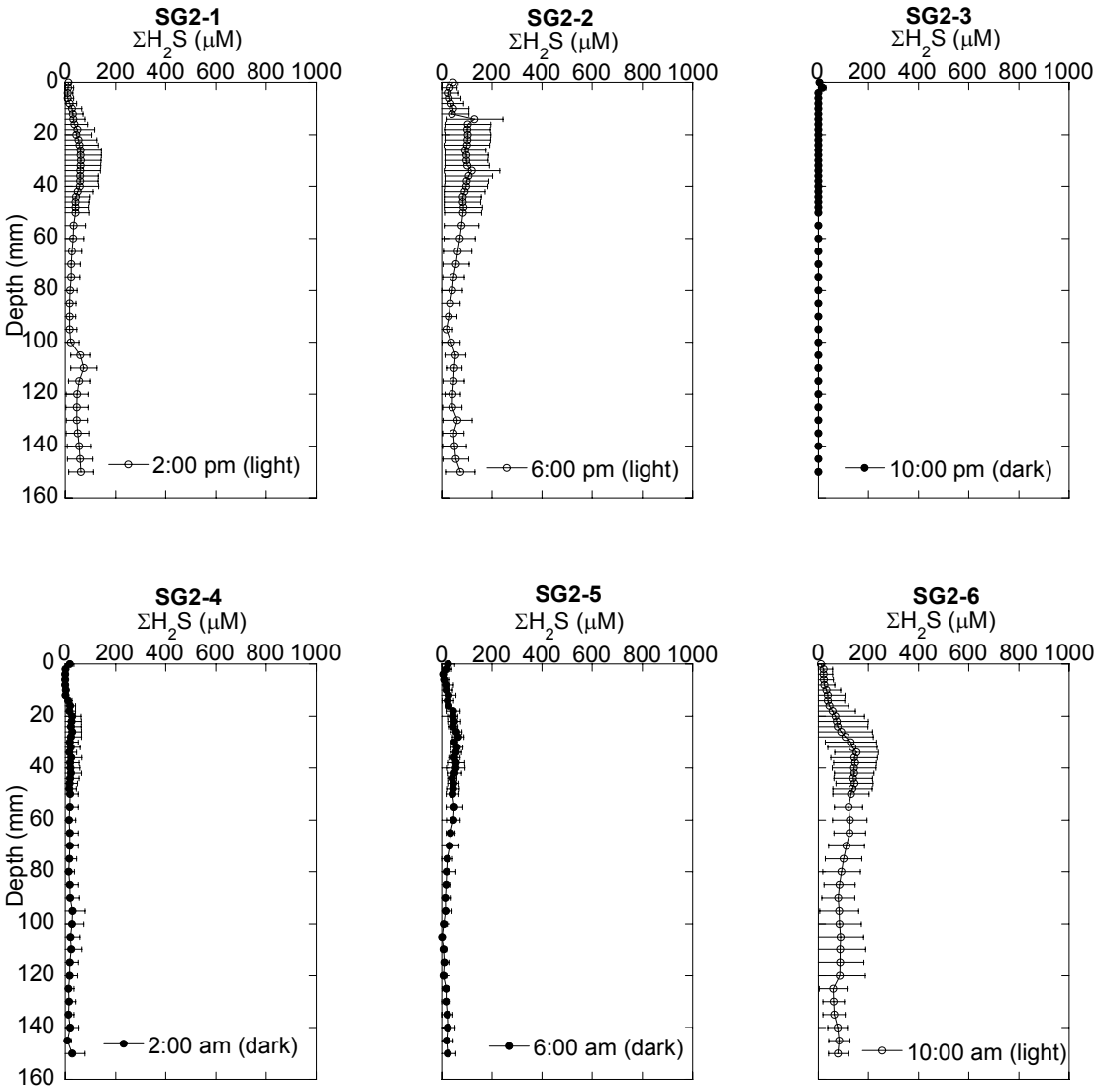

Fig. 2.5 Average dissolved pore water ΣH_2S for a seagrass core (SG2) in a 24 hr. period (bars represent ± standard deviation)

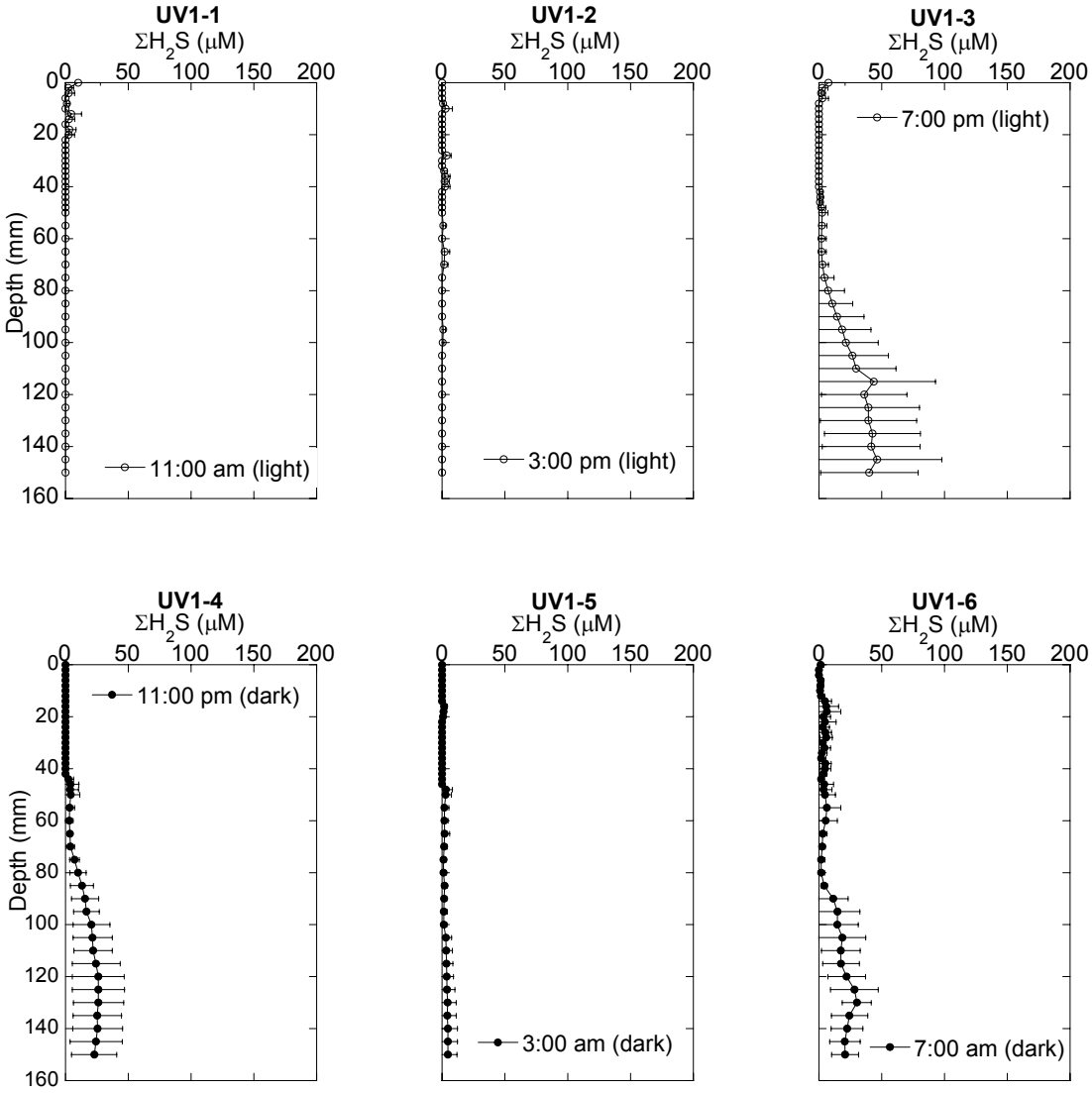

Fig. 2.6 Average unvegetated sediment (UV1) pore water ΣH_2S in a 24 hr. period (bars represent ± standard deviation)

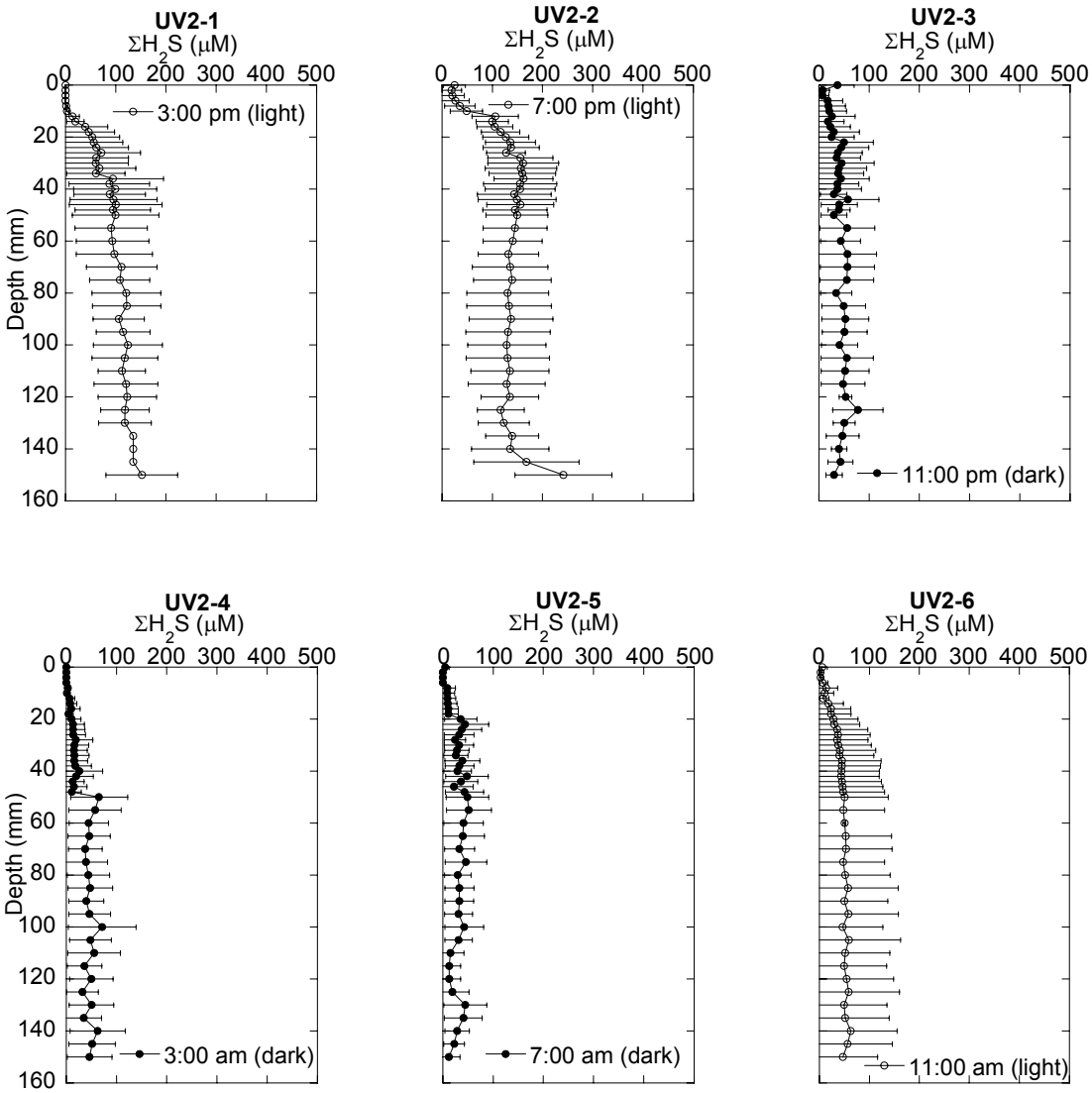

Fig. 2.7 Average unvegetated sediment (UV2) pore water ΣH_2S in a 24 hr. period (bars represent ± standard deviation)

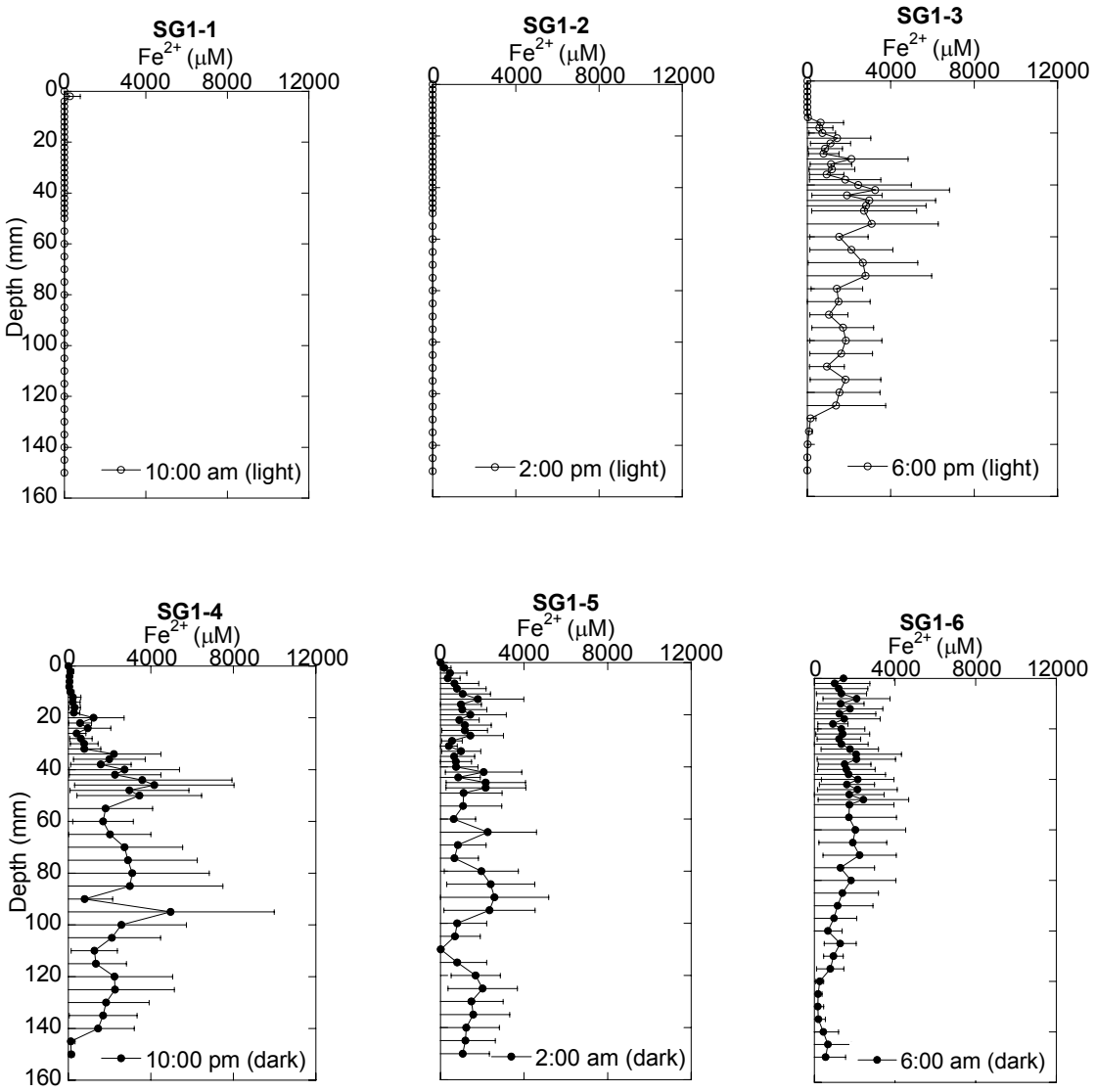

Fig. 2.8 Average dissolved pore water Fe^{2+} for a seagrass core (SG1) in a 24 hr. period (bars represent ± standard deviation)

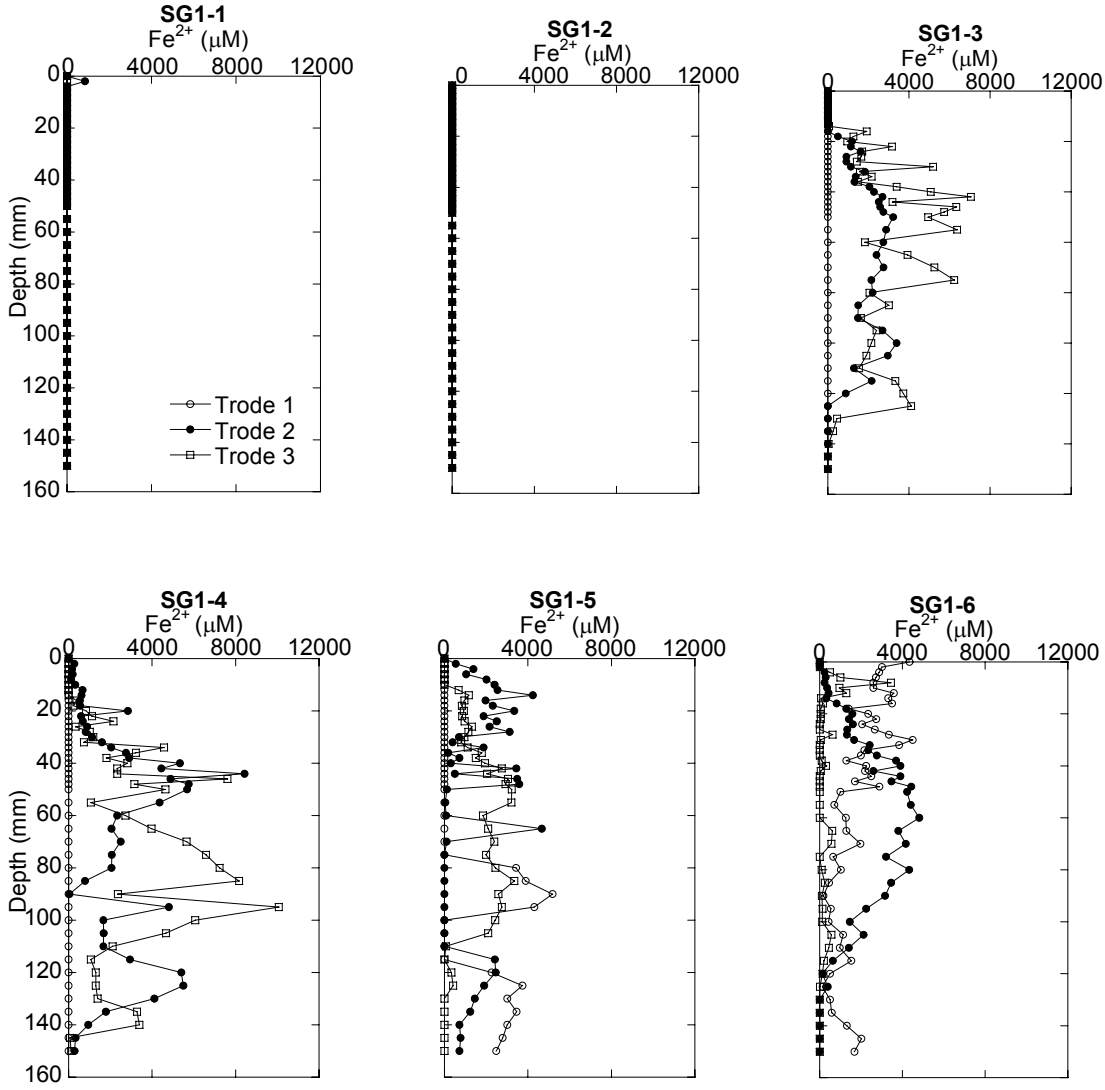

Fig. 2.9 Dissolved pore water Fe^{2+} for a seagrass core (SG1) in a 24 hr. period showing all three profiles

pH

The mean pH was 7.0±0.2, however the unvegetated sediments showed slightly more basic conditions within the top 2 cm of the sediment-water interface. The seagrass sediments showed a drop in pH during photoperiods which corresponds with increased

SRR, and increased to neutral in the dark. Light periods in the seagrass sediments varied more with depth in pH compared to dark periods of seagrass sediments and light/dark periods of unvegetated sediments (Fig. 2.10).

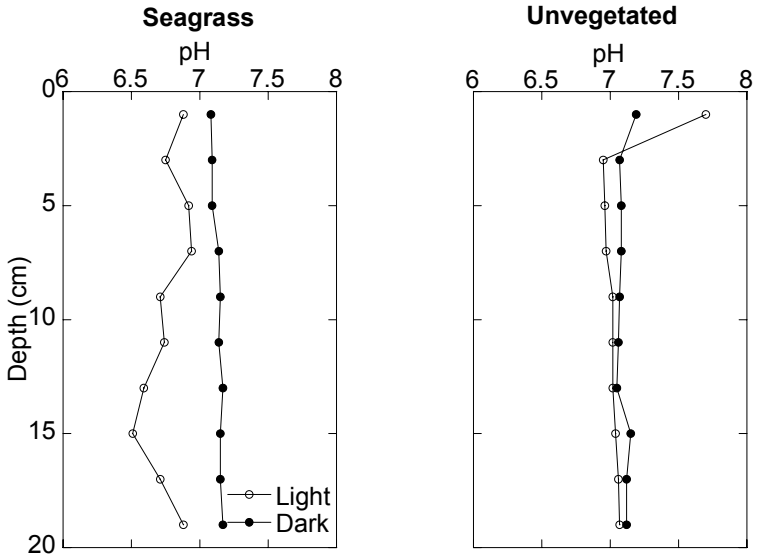

Fig. 2.10 pH profiles for seagrass and unvegetated sediments (light and dark profiles obtained ~12:00 pm and ~3:00 am, respectively)

Biomass

Aboveground, rhizome, and root biomass data were obtained from the microprofile cores (Table 2.1). Aboveground biomass was substantially the largest portion of overall biomass in the seagrass sediments. Typical rhizome depths were ~4-5 cm deep with roots extending down to ~10 cm. The leaves averaged ~1 m in length, and observationally ranged in epiphytic density. Biomass variation between seagrass cores was ~3 times the total biomass, and belowground biomass only comprised 10- 25% of

the total plant biomass. %TS of seagrass roots was higher in the seagrass cores with the larger dissolved sulfide concentration and lower root biomass.

Table 2.1 Biomass data from microelectrode cores and %TS (RR:tot=root and rhizome biomass to total biomass; %TS is the percent total sulfur content of combusted plant parts)

	SG1		SG2	
	g DW ▪ m^{-2}	%TS	g DW ▪ m^{-2}	%TS
Aboveground biomass	246.2	0.04	738.0	No data
Rhizome biomass	39.6	0.12	77.4	No data
Root biomass	19.9	1.83	28.5	1.27
Total Biomass	305.7		843.9	
RR:tot (%)	19.5		12.6	

Sulfate reduction rates

SRR showed similar trends observed in previous studies (Blaabjerg et al., 1998; Blaabjerg and Finster, 1998), where rates were higher in the light than in the dark for vegetated sediments. Unvegetated sediments did not show the same diurnal changes in SRR, and were less variable with depth than seagrass sediments. There were two subsurface maxima in the seagrass sediments around 3 and 11 cm sediment depth (Fig. 2.11). Table 2.2 clearly shows diurnal changes in SRR from depth-integrated values. SRR also agreed well with the percent sulfate loss shown in Table 2.3.

Sediment pore water and solids geochemistry

Porosity cores had shifted during transport and mixed sediment depths so data were obtained from an earlier study at the same site. Porosity was ~0.7 for all depths 0-20 cm. Grain size was determined in the top 2 cm for seagrass and unvegetated

sediments. For the unvegetated sediments, the distribution was 79% sand (2.5-3 φ (>63 μm), 21% silt (4-62 μm), and no clay (<4 μm). The seagrass sediment grain size distribution was 72% sand (2.5-3 φ), 27% silt and 1% clay (Fig. 2.12). Overlying surface water was ~5.4 mg L^{-1} O_2, S=34.2, and T=17.4° C.

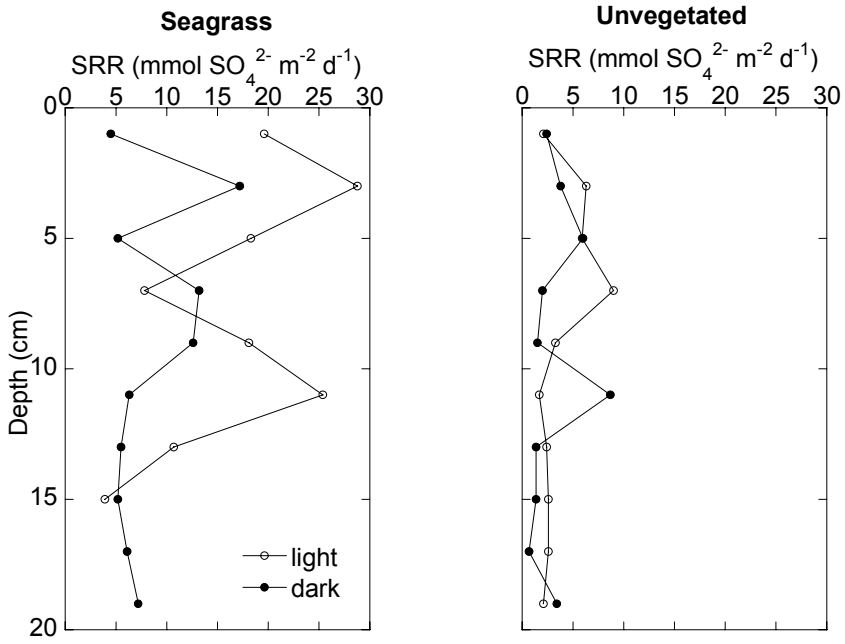

Fig. 2.11 SRR for seagrass and unvegetated sediments

Table 2.2 Integrated (0-15 cm) sulfate reduction rates (mmol SO_4^- m^{-2} d^{-1})

Seagrass		Unvegetated	
Light	Dark	Light	Dark
241.7	129.7	61.8	50.5

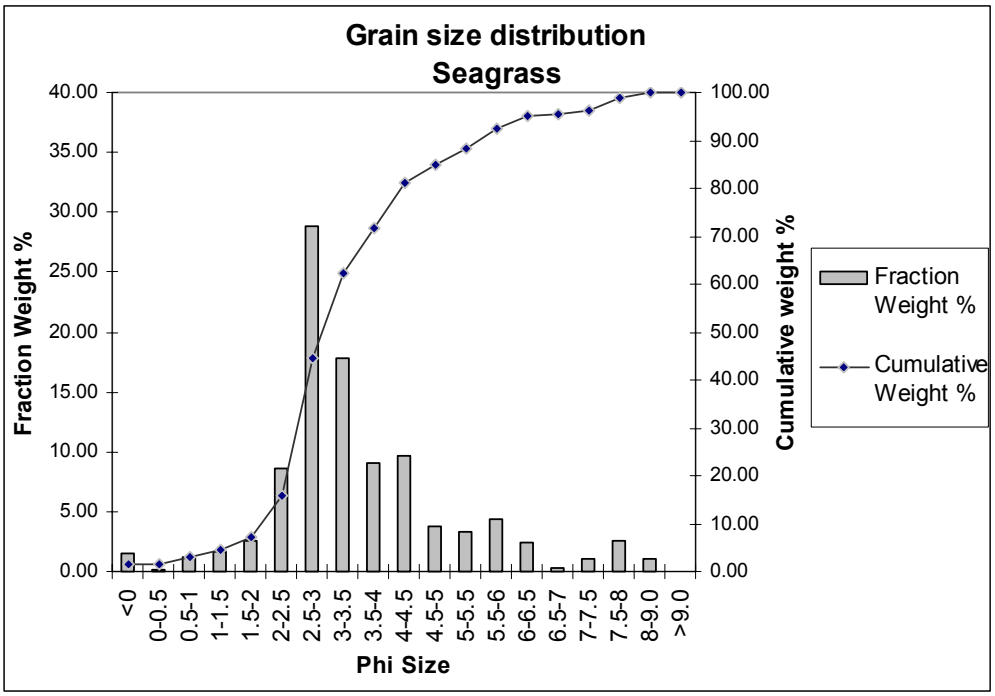

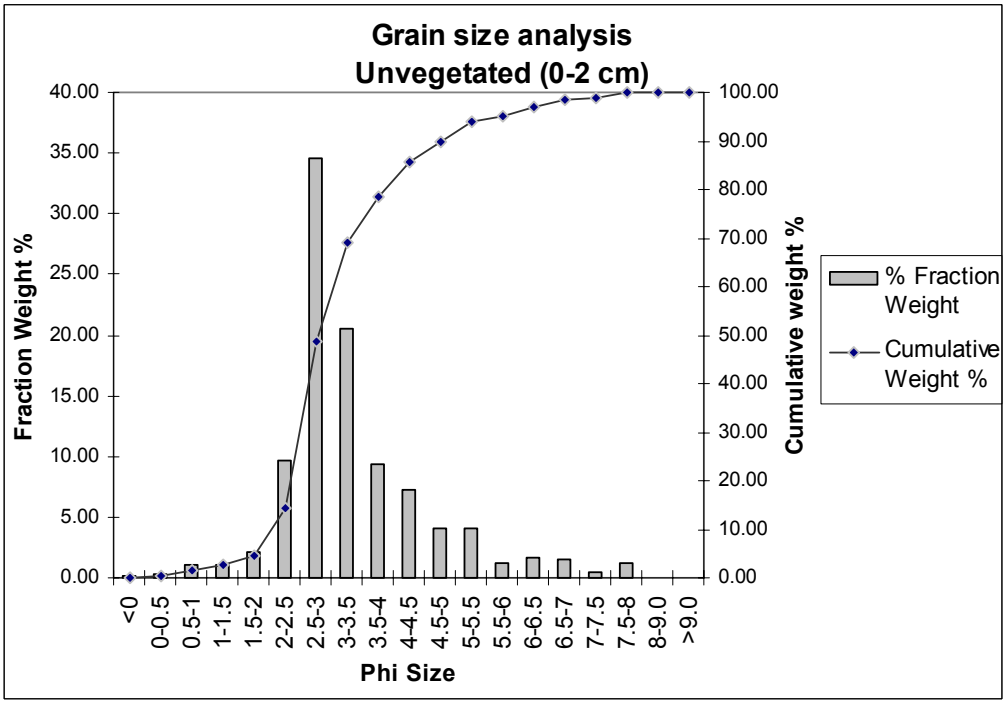

Fig. 2.12 Grain size distribution

Nutrients

Ammonium-N (NH_4^+) under light conditions of the seagrass sediment increased to ~2.5 mM throughout the first several centimeters of sediment depth and then decreased to 0.5 mM at 11 cm depth (Fig. 2.13). A small increase followed at 13 cm depth to ~1.2 mM and then decreased again to about 0.9 mM. In seagrass sediments, NH_4^+ was higher during the light periods than in the dark except at 17 cm depth where a maximum of 2.2 mM occurred for dark conditions. The unvegetated sediments did not exhibit the same diurnal changes that the seagrass sediment pore water exhibited. Light and dark concentrations of pore water NH_4^+ followed the same depth trends for the unvegetated sediments with some variability with depth. Concentrations were similar in magnitude for the two sediment types.

Nitrate (NO_3^-+NO_2^-) for light and dark seagrass sediments had subsurface maxima of ~40 and 8 μM, respectively, just below the water-sediment interface (Fig. 2.13). The rest of the depth profile was below detection (0.2 μM). The unvegetated sediments showed more variability with depth compared to the seagrass sediments. A nitrate peak occurred at around 10 cm depth for both light and dark times in the unvegetated sediments.

Phosphate (PO_4^{3-}) strongly resembled NH_4^+ concentrations in seagrass sediments (Fig. 2.13). For the seagrass sediments, PO_4^{3-} was higher during light periods with a subsurface maximum of 327 μM at ~3 cm depth, and dark concentrations were depressed and increased slightly with depth. The unvegetated sediments showed the

opposite trend where dark concentrations of PO_4^{3-} were higher than the concentrations in the light, similar in pattern to NH_4^+ concentrations.

Dissolved carbon pools

DIC was distinctly different for light and dark conditions for the seagrass sediment (Fig. 2.14). DIC in the light exposed seagrass sediments exhibited the highest concentrations in the top 4 cm and at 13 cm of the sediment at 16 and 9 mM, respectively. The concentrations of DIC in the dark seagrass sediments were lower overall (~2.2-5.4 mM) and less variable with depth. Similar trends were observed in the unvegetated sediments, with higher DIC in the dark than in the light.

DOC was much more variable in the seagrass sediments for both light and dark conditions than the unvegetated sediments (Fig. 2.14). DOC in the unvegetated sediments was similar in magnitude although slightly less than the DOC in seagrass sediments, with a mean value of 1539 μM in unvegetated sediments compared to 2222 μM in seagrass sediments.

Sulfate/chloride ratios

Sulfate to chloride ratios indicated that the greatest percent of sulfate loss occurred in the top 4 cm of the seagrass sediments exposed to light (Table 2.3). SO_4^- profiles indicated greater sulfate depletion in the upper 10 cm for light conditions than in dark and seagrass sediment sulfate concentration were generally the same as unvegetated sediment pore water (Fig. 2.15). Variability within the ratios may have resulted from signal to noise ratios of the Dionex ion chromatagraph, although there is some evidence

suggesting groundwater might be a significant factor in changing sedimentary geochemical constituents thus confounding interpretation of processes.

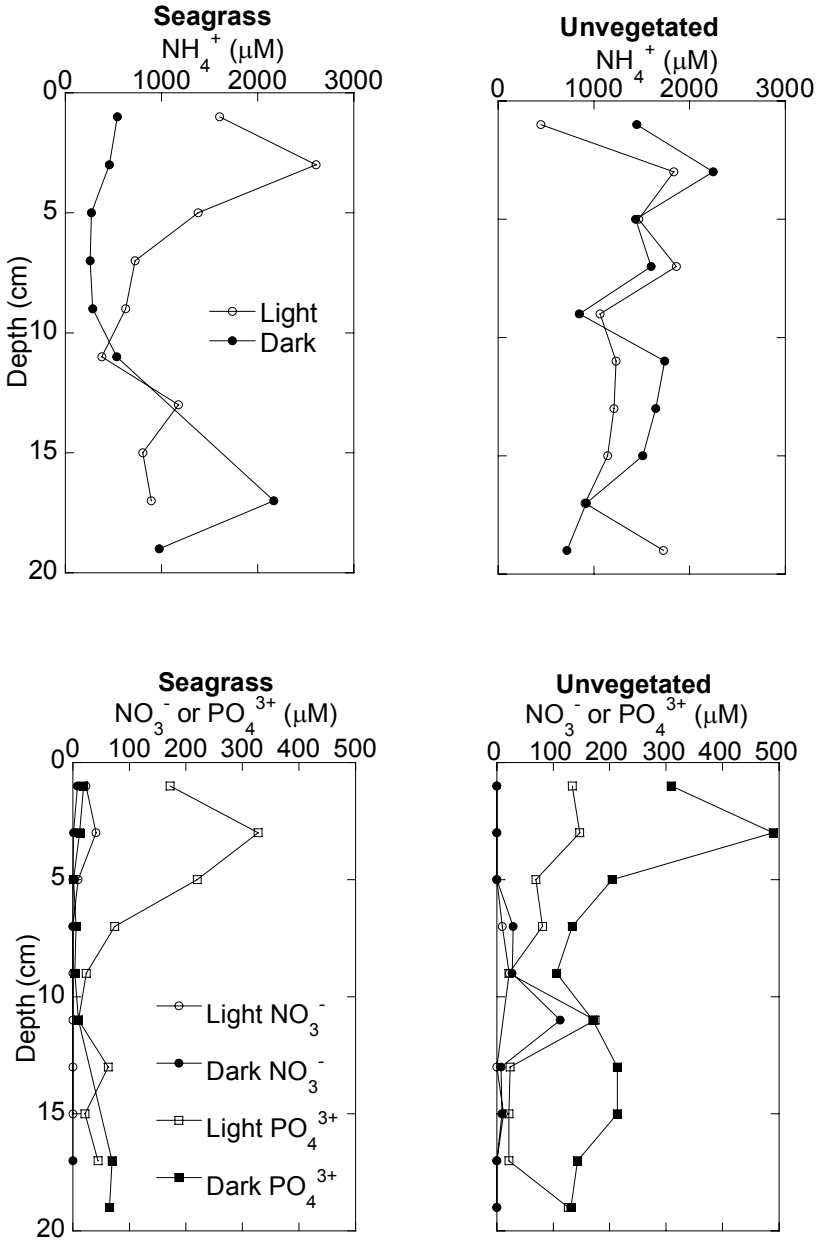

Fig 2.13 Nutrient concentrations for seagrass and unvegetated sediments

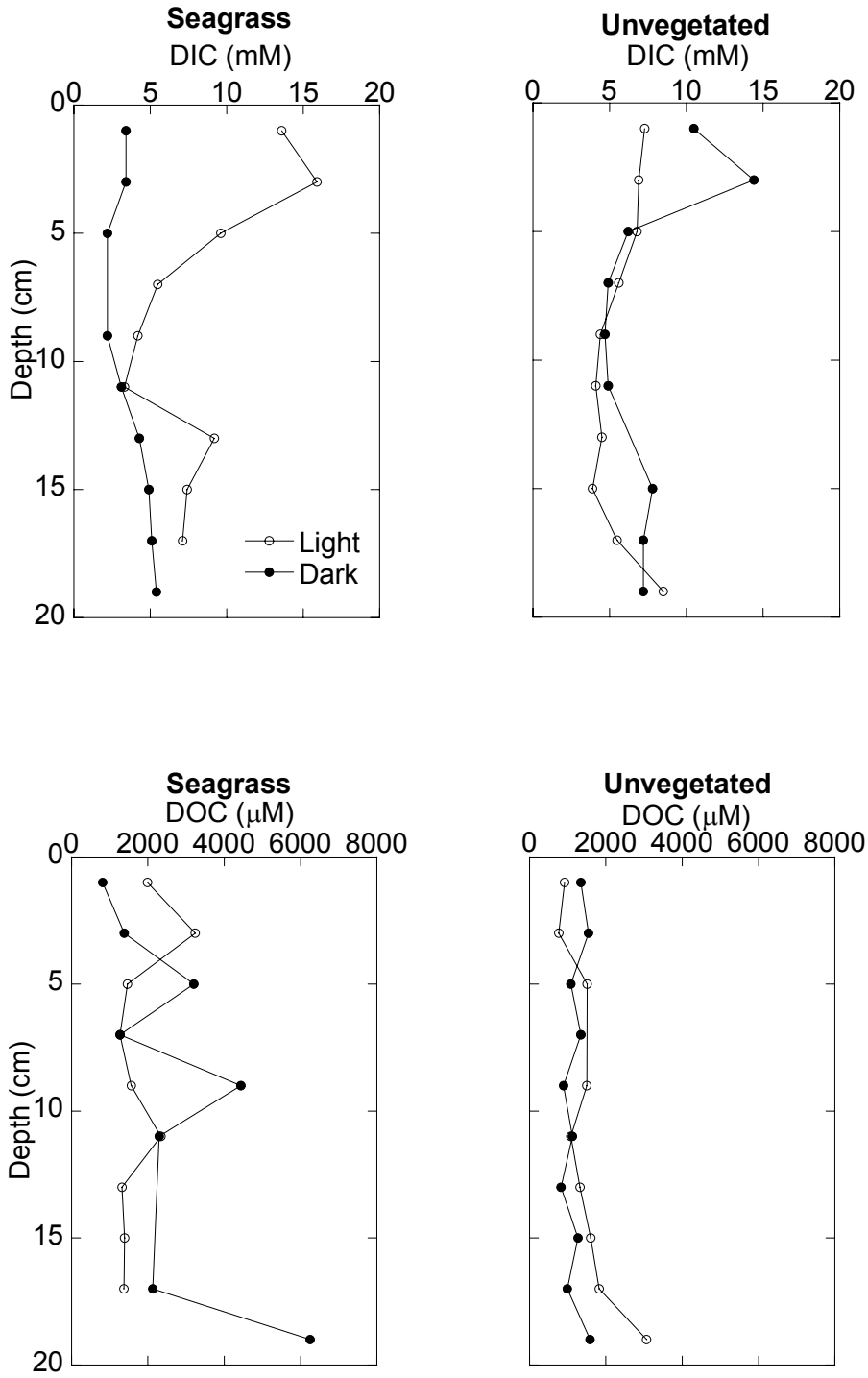

Fig. 2.14 DIC and DOC concentrations for seagrass and unvegetated sediments

Table 2.3 Sulfate and chloride ratios showing % sulfate loss with depth (LSG=light seagrass, LUV=light unvegetated, DSG=dark seagrass, and DUV=dark unvegetated)

Sample				
LSG	**Cl^- (mM)**	**SO_4^{2-} (mM)**	**SO_4^{2-}/Cl^-**	**% Sulfate loss**
0-2	520.84	20.70	0.040	23.1
2-4	691.88	22.91	0.033	36.0
4-6	461.72	23.26	0.050	2.6
6-8	439.88	24.34	0.055	7.0
8-10	425.19	22.83	0.054	3.8
10-12	625.96	33.43	0.053	3.3
12-14	582.89	31.21	0.054	3.5
14-16	592.51	32.28	0.054	5.3
16-18	632.02	32.96	0.052	0.8
LUV				
0-2	560.18	27.54	0.049	4.9
2-4	577.17	29.35	0.051	1.7
4-6	500.34	26.32	0.053	1.7
8-10	598.66	28.98	0.048	6.4
10-12	446.37	24.46	0.055	6.0
12-14	526.73	29.99	0.057	10.1
14-16	468.46	25.68	0.055	6.0
16-18	801.04	47.58	0.059	14.9
18-20	432.75	20.15	0.047	9.9
DSG				
0-2	676.26	37.76	0.056	8.0
2-4	392.10	22.82	0.058	12.5
4-6	514.77	26.64	0.052	0.1
6-8	466.65	27.67	0.059	14.6
16-18	459.60	25.55	0.056	7.5
DUV				
0-2	539.37	25.40	0.047	9.0
2-4	487.46	22.00	0.045	12.7
4-6	444.16	17.64	0.040	23.2
6-8	495.99	19.14	0.039	25.4
8-10	429.27	18.62	0.043	16.1
10-12	422.24	19.14	0.045	12.3
12-14	552.76	23.01	0.042	19.5
14-16	453.32	17.62	0.039	24.8
16-18	475.99	21.66	0.046	12.0
18-20	533.30	21.77	0.041	21.1

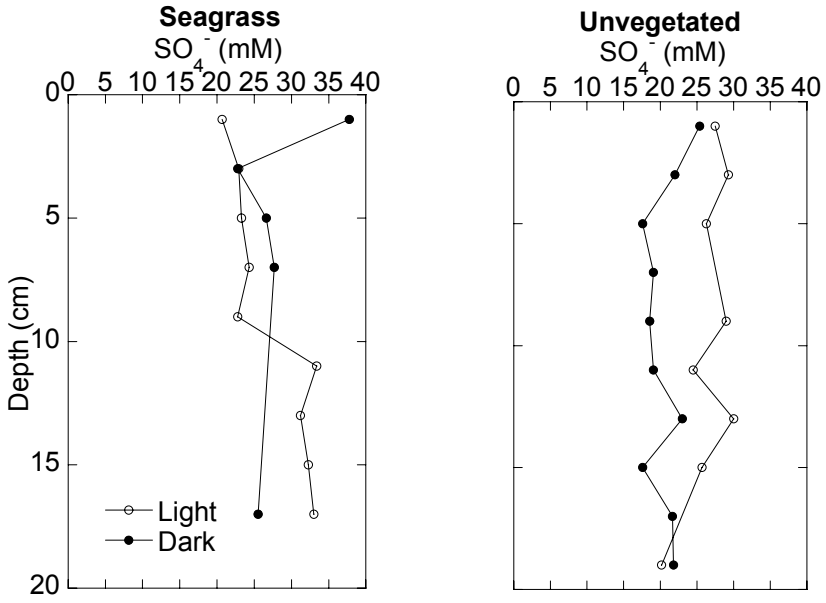

Fig. 2.15 SO_4^- concentration profiles for seagrass and unvegetated sediments

Total organic carbon

The TOC content of did not show a large difference between seagrass and unvegetated sediments. The mean weight percent of carbon content was slightly greater in the seagrass sediments with a mean of 1.3±0.3% in seagrass sediments and 1.2±0.3% in unvegetated sediments, however the range was greater in unvegetated sediments (Fig. 2.16).

AVS and TRS

There was some variability in TRS for light and dark cycles, and the standard deviation of TRS in seagrass sediments was much higher than the unvegetated cores. This further indicates the greater lateral heterogeneity associated with seagrass

sediments (Fig. 2.17). AVS accounted for ~5-25% of TRS, typical of many estuarine sedimentary environments.

Reactive metals

Reactive manganese was less than 1.25 μmol gdw^{-1} for all cores, and therefore the data were not shown. Iron ranged from 124-177 μmol gdw^{-1} in the acid-extracted samples (HCl-Fe). The citrate dithionite iron extractions (CDE-Fe) were typically half that of the acid-extracted samples (Fig 2.18). Table 2.4 shows the average degree of pyritization (DOP utilizing CDE-Fe, =0.5*(TRS-AVS)) for two sediment types under two different light conditions. Degree of pyritization ranged from ~0.3 - ~0.6 for both sediment types indicating that reactive iron may limit pyrite formation. Table 2.5 shows selected metal concentrations and significant changes between light and dark cycles. Fe, Zn, and Ni as well as TRS and pyrite-Fe indicated diurnal changes in seagrass sediments ($P<0.05$, one-way ANOVA) while Zn, TRS and pyrite-Fe showed diurnal changes in the unvegetated sediments. Results for other metal concentrations may be seen in Appendix III.

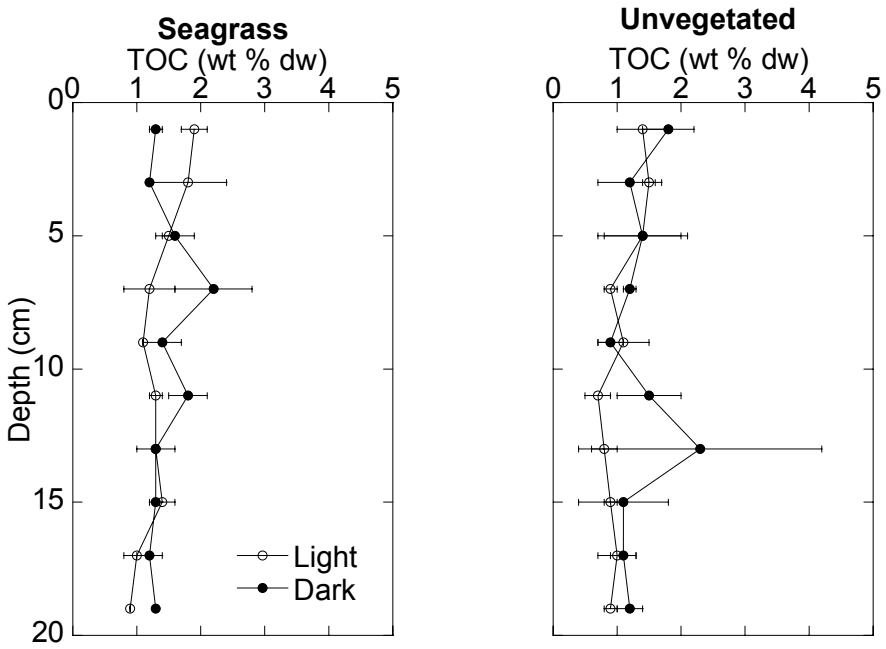

Fig. 2.16 TOC content for seagrass and unvegetated sediments (bars represent ± standard deviation)

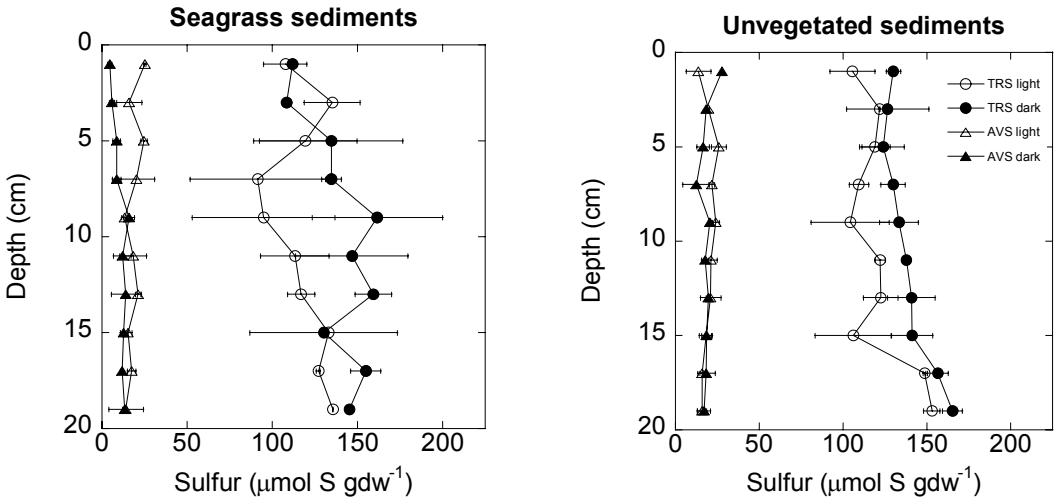

Figure 2.17 Reduced sulfur pool for seagrass and unvegetated sediments (bars represent ± standard deviation)

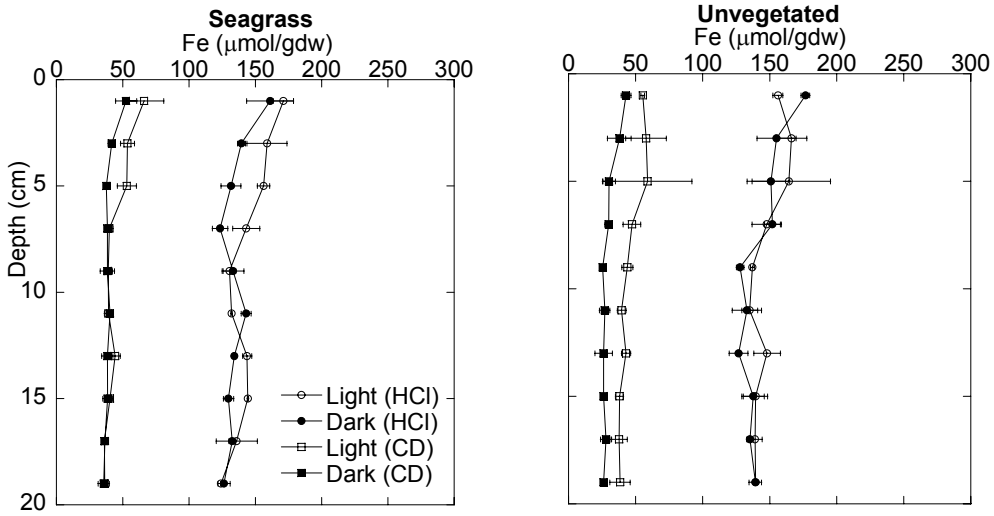

Fig. 2.18 Reactive iron for seagrass and unvegetated sediments (bars represent ± standard deviation)

Table 2.4 Average degree of pyritization (DOP) for seagrass and unvegetated sites ± standard deviation

Depth interval (cm)	Seagrass (light)		Seagrass (dark)		Unvegetated (light)		Unvegetated (dark)	
0-2	0.29	±0.02	0.38	±0.01	0.32	±0.04	0.40	±0.01
2-4	0.43	±0.08	0.40	±0.01	0.38	±0.07	0.45	±0.12
4-6	0.40	±0.02	0.49	±0.14	0.36	±0.11	0.50	±0.10
6-8	0.38	±0.08	0.51	±0.03	0.32	±0.02	0.53	±0.02
8-10	0.40	±0.01	0.55	±0.05	0.31	±0.09	0.56	±0.04
10-12	0.45	±0.09	0.49	±0.07	0.42	±0.03	0.56	±0.06
12-14	0.43	±0.11	0.54	±0.02	0.39	±0.04	0.59	±0.04
14-16	0.44	±0.00	0.43	±0.16	0.32	±0.14	0.56	±0.03
16-18	0.45	±0.01	0.55	±0.01	0.52	±0.05	0.59	±0.02
18-20	0.50	±0.00	0.52	±0.02	0.43	±0.10	0.65	±0.01

Table 2.5 Mean trace metal concentrations, reduced sulfur and standard deviations (SG=seagrass, UV=unvegetated). Asterisk indicates significant differences (P <0.05, one-way ANOVA)

	Seagrass		Unvegetated	
μmol/gdw	Light	Dark	Light	Dark
Fe	144 ±15*	136 ±11	147 ±11	144 ±15
Mn	0.949 ±0.10	0.909 ±0.10	0.964 ±0.10	0.908 ±0.09
Zn	2.99 ±1.4*	0.778 ±0.09	1.10 ±0.25*	2.89 ±1.3
Cu	13.2 ±3.4	12.2 ±3.4	11.3 ±2.0	12.6 ±5.9
Ni	0.208 ±0.02*	0.186 ±0.03	0.195 ±0.02	0.194 ±0.02
Cr	0.250 ±0.07	0.211 ±0.01	0.242 ±0.03	0.284 ±0.06
TRS	117.5 ±15.9*	138.9 ±18.4	121.3 ±17.2*	138.6 ±13.3
Pyrite-Fe	29.9 ±6.3*	38.6 ±6.9	28.4 ±6.7*	35.1 ±5.7

Discussion

ΣH_2S and plant biomass

An interesting topic for discussion is the substantial difference between SG1 and SG2 ΣH_2S concentrations despite the fact that the cores were obtained at the same site. Previous studies have observed diurnal changes in seagrass sediment ΣH_2S. However, SG1 did not show any temporal changes in ΣH_2S, or that any temporal variation that occurred was lost in the spatial heterogeneity, while SG2 showed the opposite of what was expected with lower ΣH_2S in the dark than in light. This agreed well with increased SRR in the seagrass sediments under light conditions.

Lee and Dunton (2000) showed that *Thalassia testudinum*, when shaded, did not exhibit changes in pore water sulfide. In addition, *T. testudinum* usually has much more belowground biomass than *Z. marina* that may impact the sediments more (>50% compared to <30%, respectively). Low light availability from the combination of lower incident sun angles, overcast Pacific Northwest, and from substantial self-shading and epiphytic biomass in *Z. marina* may decrease productivity and the subsequent translocation of oxygen to the sediments.

The literature is relatively replete with studies that define the tolerance of seagrass and in particular *Z. marina* to soluble sulfides. While there is some evidence that 1 to 2 mM H_2S may inhibit seagrass growth or cause death of *Z. marina* (Goodman et al., 1995), there are few definitive studies that show dose-response of this seagrass in long-term controlled-environment exposure studies. Holmer and Bondgaard (2001)

showed that photosynthesis stopped after 6 days at sulfide concentrations between 100 and 1000 μM. This study was done at saturating irradiance (400-500 μmol photon m^{-2} s^{-1}) so that these observations, while informative, do not provide a way of estimating the *Z. marina* response to sulfides in a reduced light environment as might occur in a system undergoing eutrophication.

Koch and Erskine (2001) provide observations of *T. testudinum* response to sulfides under varying conditions of light, salinity, and temperature. Interestingly, the *T. testudinum* showed no response to sulfides until the dose reached 6 mM concentration and this occurred only in their high temperature treatment. This result contradicts longer-term studies by Carlson et al. (1988) where *T. testudinum* died when exposed to ~2 mM sulfide concentrations.

Little is known about how light, salinity, temperature, and pH affect the tolerance of *Z. marina* to sulfides. While the available literature that pertains to light effect on sulfide toxicity in seagrass has already been addressed, no studies that address the temperature and pH effects on toxicity have been found. It is tacitly assumed that there will be an increase in toxicity with temperature similar to the Q_{10} relationship for seagrass metabolism with temperature. Likewise pH affects on sulfide toxicity on seagrasses have not been investigated. The pH effect may be important since it affects the speciation of the sulfide species. HS^- has been shown to be more toxic to some faunal species than the other sulfide species (Bagarinao, 1992). Therefore, higher pH conditions that favor the production of HS^- relative to H_2S will likely have a more deleterious effect on seagrasses (Eldridge and Johnson, 2004).

It can be observed from Fig. 2.19, although there are few data points, that as belowground biomass increases, sediment ΣH_2S decreases. This will eventually need to be substantiated by a more complete data set, however appears to be true for these data. In addition, %TS of plant roots increased for roots exposed to higher pore water ΣH_2S suggesting that the protective oxidized layer associated with seagrass roots and iron concretions essentially titrate out among the extremely reduced nature of these sediments which allows for sulfur intrusion into root biomass. In other words, the oxidative capacity surrounding the root zone is not sufficient enough to prevent sulfide intrusion into plant tissue. A Critical Biomass Index (CBI) is proposed:

$$CBI = \frac{\overline{[H_2S]}}{BGB} \tag{2.1}$$

where mean ΣH_2S (over the depth zone of the rhizosphere) in μM is divided by the belowground biomass (BGB) in gdw m^{-2}. As an arbitrary approximation, values greater than 1 (random selection that needs to be substantiated with more data) could lead to seagrass mortality and necrotic tissue development due to stress of anaerobiosis. However, it is still uncertain whether seagrass belowground biomass is low due to toxic effects of ΣH_2S, or ΣH_2S is high because no belowground biomass is present to oxidize it. However, because the unvegetated sediments had low ΣH_2S, the former is proposed. Values less than 1 may indicate a more healthy system where control of toxic sulfides is maintained by the seagrass. A more accurate index may be obtained when relative oxygen translocation rates are better understood, and inputs of O_2 from aboveground biomass may effect sulfide concentrations by supplying more O_2 to respiratory processes

of roots and rhizomes. Table 2.6 shows average ΣH_2S for light and dark conditions at binned depth intervals (recall 5-10 depth bin constitutes the majority of the belowground biomass). The large standard deviations associated with ΣH_2S with depth make it difficult to discern temporal variations from spatial variations.

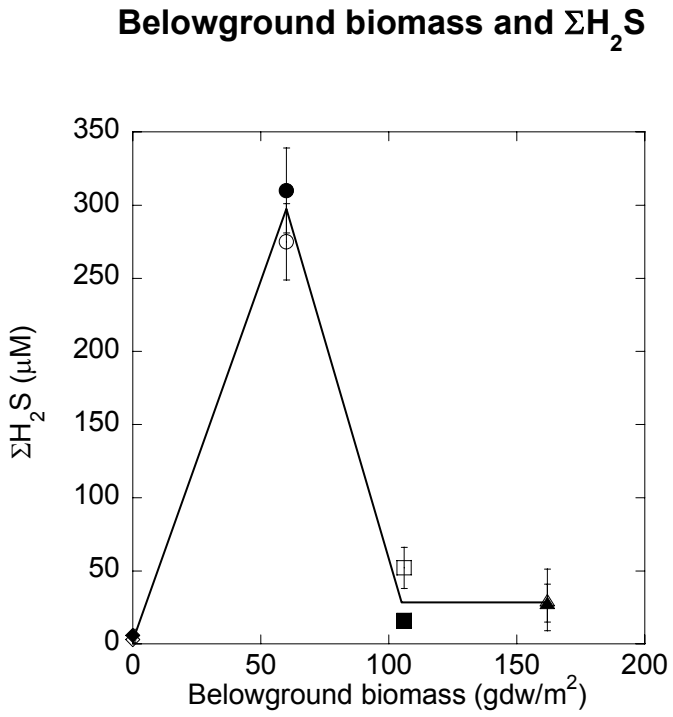

Fig. 2.19 ΣH_2S and biomass for three seagrass cores (◊,♦=UV1, ○,●=SG1, □,■=SG2, and △,▲=IDPT (from Hebert and Morse, 2003). Open symbols represent light conditions and closed symbols represent dark conditions (bars represent ± standard deviation)

Table 2.6 Average ΣH_2S over different depth bins (± standard deviation)

	Seagrass								Unvegetated							
	SG1				SG2				UV1				UV2			
Depth (cm)	**Light**		**Dark**		**Light**		**Dark**		**Light**		**Dark**		**Light**		**Dark**	
0-5	247	±41	287	±58	57	±25	19	±8	1	±1	1	±1	66	±34	23	±12
5-10	275	±26	310	±29	52	±14	16	±4	3	±2	6	±4	97	±7	45	±5
10-15	175	±17	180	±65	43	±5	11	±3	12	±3	11	±1	108	±15	41	±6

Behavior of carbon, nutrients, reactive metals, and reduced sulfur

High spatial and temporal variability existed in both seagrass and adjacent unvegetated sediments. Because of preferential uptake of DIN by seagrass from either the water column or the pore water, daytime NH_4^+ uptake from the pore water appeared minimal (or was < production), consequently NH_4^+ increased during the day most likely because of increased anaerobic bacterial respiration in the sediments associated with the daytime input of labile DOC by seagrass. This also agrees with increased DIC, sulfate reduction rate increase, and pH decrease during photic periods of seagrass sediments. The unvegetated sediments showed the opposite effect where DIC, NH_4^+, and PO_4^{3-} were more concentrated during the dark than at night most likely attributed to nocturnal respiration.

Despite the fact that these sediments are vegetated with seagrass, they are largely heterotrophic sediments with much of the organic matter produced or present rapidly mineralized by anaerobic bacteria. Although the total carbon content of the sediments appears low for seagrass sediments, sulfate reduction rates are relatively high which roughly approximates (using an average daytime sulfate reduction rate of 16.6 mmol

$SO_4^{2-} \cdot m^{-2} \cdot d^{-1}$) 0.4 $g \cdot m^{-2}$ of carbon consumption per day. Productivity of eelgrass in another Pacific Northwest estuary was determined as ~5 g $C \cdot m^{-2} \cdot d^{-1}$ (Nelson and Waaland, 1997). If all of the carbon SRB oxidize comes from seagrass, then SRB are responsible for mineralizing 8% of total seagrass productivity which agrees well with Holmer et al. (2001).

An important note of discussion is the %TRS as AVS in the seagrass core (16.3% and 16.7% for light and dark, respectively) and in the unvegetated core (7.7% and 13.7% for light and dark, respectively), since AVS classically comprises only about 5-10% of the total reduced sulfur pool in many coastal areas (Lin and Morse, 1991). Another important factor is that TRS is much more spatially heterogeneous in seagrass sediments than in adjacent unvegetated. The degree of variability among the seagrass vegetated sediments is consistent with the variability seen in pore waters from previous studies and indicates that much more than the pore water is affected on diel time scales. Unstable and metastable AVS are constantly exposed to varying redox states from tidal flushing of oxic waters, bioturbation/bioirrigation, and for these sediments, seagrass exudation of photosynthates, primarily oxygen and DOC. Intermediate polysulfides may form because dissolved H_2S in sediment pore waters from bacterially mediated sulfate reduction co-occurs with oxygen exuded into the root zone of sediments by the seagrass. Dissolved polysulfides were detected by microelectrodes in the pore waters, but were not quantified and can only be reported from this data as current (nA) (data not shown, see Luther et al., 2001). The polysulfidic pathway to pyrite formation is slow which may be an explanation for the high %TRS as AVS in seagrass sediments. In addition, DOC in

the pore water was high (~2-4 mM) which has been suggested to accelerate the sulfidation rate of goethite, but depress the formation of pyrite (Morse and Wang, 1997). Because of the reduced nature of the sediments, oxygen is rapidly consumed either by biological oxygen demand or chemical oxygen demand, and these dynamic reactions complicate the interpretation of sulfur cycling and perhaps inhibiting pyrite formation (TRS), the main sink for toxic sulfides.

The reactivity of trace metals and their chemical speciation (dissolved, adsorbed, and/or co-precipitated) in the marine environment plays a critically active role in determining toxicity and bioavailability. Huerta-Diaz and Morse (1992) demonstrated that the formation of pyrite can be a significant process for the removal of toxic trace metals and sulfides (Huerta-Diaz and Morse, 1992; Morse, 1994). Another study indicated that all metastable iron sulfide minerals and a considerable fraction of pyrite can become oxidized when exposed to oxic conditions (Morse, 1991). This has important implications for seagrass sediments where pyrite is a sink for toxic sulfides and trace metals that can later become liberated when photosynthetically produced oxygen is released into the sediments from roots and rhizomes.

Many studies have focused on quantifying various trace metal concentrations in seagrass tissue and uptake rates (Brinkhuis et al., 1980; Brix et al., 1983; Faraday and Churchill, 1979; Lyngby and Brix, 1982; Ward, 1987). Few studies, however, have incorporated sedimentary trace metal concentration because of its subsequent removal by adsorption or co-precipitation, and most of the concern was with water column exposure and uptake rates. Large reservoirs of reduced sulfur and dissolved iron in

anoxic sediments lead to pyrite formation. The oxidative capacity for seagrass by the exudation of photosynthetically produced oxygen into anoxic sediments causes metastable iron sulfides and perhaps even pyrite to dissociate and release trace metals into pore waters where they can become bioavailable. This was true for Fe, Zn, and Ni for the seagrass site where TRS was significantly changing on diurnal time scales, and Zn in unvegetated sediments, which also exhibited diurnal time scales in TRS. A closer examination of trace metal release on smaller time scales may be important in determining bioavailability.

Summary

Seagrass habitats are now being used as bioindicators for estuarine health. Loss of seagrass acreage has been observed in many systems which may serve as a proxy for the persistence of aquatic stressors. As such, the burial of toxic sulfides by way of pyritization from the sediments is an important sink that will affect the fate of seagrass survival and propagation. These analyses provide better insight into a dynamic system where sulfur and carbon cycling vary on short space and time scales. Belowground biomass may be correlated with ΣH_2S which may aid in the development of a Critical Biomass Index to determine geochemical indicators of seagrass health. Finally, diurnal variations were difficult to discern due to the large spatial variability which has important implications on the scale of biogeochemical processes in these sediments.

CHAPTER III

OPTIMUM VERTICAL AND LATERAL SCALE LENGTH OF TEMPERATE SEAGRASS SEDIMENT PORE WATERS*

Introduction

A fundamental problem, in studying benthic-pelagic coupling in the marine environment and early diagenesis in sediments, is determining optimum sampling intervals, both in space and time. If a system is under-sampled, critical information regarding processes of primary importance may be missed, whereas, if a system is over-sampled, a major waste of time and resources can occur. Therefore, quantitative approaches need to be developed for determining what intervals in time and space are needed to answer specific questions in a given environment. Such choices can significantly influence results in the marine environment (e.g., Fonseca, 1996, Whitlatch et al., 2001; Zajac, 2001) and are one of the most crucial decisions that researchers make (Dayton et al., 1992).

Scale theory is a rapidly developing field in both the natural and social sciences which addresses these types of problems. It deals primarily with grain (or resolution, e.g. the number of pixels per given area) and extent in space and/or time (e.g., the size of a

---

* Reprinted in part with kind permission of Kluwer Academic Publishers from *Aquatic Geochemistry* 9, 2003, 41-57, Determination of the optimum sampling intervals in sediment pore waters using the autocovariance function. Morse, J.W., Dimarco, S.F., Sell, K.S., and Hebert, A.B. Figures 3.1 and 3.3. © 2003 *Kluwer Academic Publishers.*

picture). Scaling deals with the translation or extrapolation of information between different scales. Wu and his associates (Wu, 1999; Wu and Qi, 2000; Wu et al., 2000) have written excellent reviews and discussions of scale theory, with applications to the conceptually similar field of landscape ecology. These papers, along the paper of Fonseca (1996) on the application of scaling methods to the study of seagrass systems, provide a good introduction to this field.

One-dimensional steady-state diagenetic models have been the most commonly used approach used for interpreting observations of sediment geochemistry, and understanding early diagenetic and biogeochemical processes in sediments for over a third of a century (e.g., Berner, 1964, 1974, 1980; Boudreau, 1997). However, there has been a growing body of evidence that in many instances this approach is not an accurate representation of what is occurring (e.g., Lavigne et al., 1997; Mannino and Montagna, 1997; Aller et al., 1998; Harper et al., 1999; Shuttleworth et al., 1999; Eldridge and Morse, 2000; Koenig et al., 2001). Spatial heterogeneities occur on scales that range from individual sediment grains to regional basin (Fig. 3.1). Important non-steady-state processes can occur over time ranges from minutes to centuries. How best to design sampling patterns and diagenetic models for sediments from complex natural systems presents a major challenge that has generally not been well addressed by benthic biogeochemists. Our own experience in several research projects consists of attempts to describe temporal changes which were all too often overwhelmed by lateral heterogeneity (e.g., Cooper and Morse, 1996; Eldridge and Morse, 2000; Hebert and Morse, 2003). A basic problem is how to establish an optimal sampling step size that

will maximize the amount of useful information returned and minimize the number of samples needed to describe the dominant variability. A practical example of the application of this approach is, when designing a study, calculating what level of effort will be required to successfully test a set of hypotheses.

A potentially powerful approach to this problem, which has its origins in signal theory, has been developed and tested by physical oceanographers faced with generically similar problems associated with the dynamic processes that occur in the water column (Denman and Feeland, 1985; Povlain and Niiler, 1989). This approach, which is discussed in detail in the next section, uses correlation statistics and "scale theory" to determine, for a selected parameter or set of parameters, the optimal size of spatial or temporal steps which can describe the dominant variability of the parameter(s). In this paper, examples of this scaling method's application to pore water chemistry are provided. Data obtained using anodic stripping voltammetry for dissolved sulfide (H_2S) and iron (Fe^{2+}) at two seasonally hypoxic sites in Corpus Christi Bay, Texas, and the Louisiana shelf near the Mississippi river delta, and a seagrass meadow with adjacent non-seagrass containing sediments in Yaquina Bay, Oregon, are used in these examples.

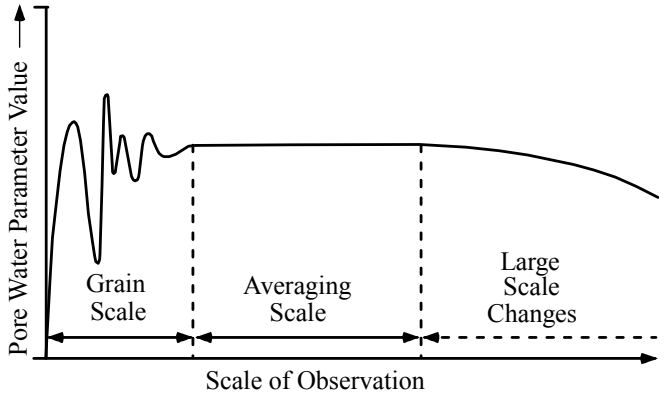

Fig. 3.1 Schematic figure of different observational scales in sediments (based on Boudreau, 1997)

ACF Approach to Scaling Processes

The use of statistical methods to obtain characteristic length scales has a long and rich tradition in oceanography and meteorology. The most common use in meteorology is optimal interpolation, i.e., objective analysis, in which correlation scales are used to objectively map irregularly spaced observations to some type of regular grid. Gandin (1965) is perhaps the seminal work describing this application. In oceanography, Bretherton et al. (1976) describe the use of correlation scales in the design of oceanographic experiments. Sciremammano et al. (1980) present the spatial scales of temperature and flow in Drake Passage using cross-correlation from current measurements of different instruments along a series of mooring lines. Denman and Freeland apply the methodology to inhomogeneous, anisotropic, and non-stationary physical and biological data collected on the continental shelf. Poulain and Niiler (1989) present Lagrangian time and space scales of variability from correlation estimates based on drifter data in the California Current. DiMarco et al. (unpublished manuscript) apply

the methodology to near-surface temperature, salinity, and current velocity data taken along repeated cruise tracks over a continental slope. These examples are but a small subset of the many applications of the methodology presented in this paper.

In physical oceanography, the operation of performing a scales analysis of collected data has essentially become a first-order analysis performed at the same time that basic statistics (record length mean and standard deviation) and power spectra are computed. Most physical oceanographic field programs deploy a scales array, i.e., an array consisting of closely spaced mooring elements, to verify that larger arrays are capturing the dominant modes of variability present during the measurements. These analyses can reveal whether station spacing is too great thereby aliasing small scale processes into the observations without resolving them or too small thereby causing unnecessary redundancy and waste of resources.

Correlation scales can be defined for both temporal and spatial data; the methodology is functionally identical, requiring only a sequence of measurements. Conceptually, spatial correlation can be thought of as the minimum distance that two temporal sequences of simultaneous observations of the same parameter become uncorrelated. Temporal correlation can be thought of as the minimum time one must wait for spatial conditions to become uncorrelated with present conditions. A more rigorous explanation of criteria which constitute uncorrelated sequences will be explored later.

The method employs the basic statistical concept of correlation and the covariance function. Covariance is simply a measure of how two (or more) variables co-vary in sequence. This is usually written as:

$$C_{xy} = \frac{1}{N-1}\sum_{i=1}^{N}(x_i - \bar{x})(y_i - \bar{y}), \tag{3.1}$$

where x and y are sequences of two random variables, N is the number of points in each sequence, x and y are the mean values of the sequence, and C_{xy} is the covariance of the sequences x and y. When C_{xy} is divided by the variance of each sequence, the quantity is known as the correlation coefficient, r. The covariance, C_{xy}, is also known as the zero-lagged covariance. The covariance function is then defined by introducing an offset (or lag) between the two sequences and then recalculating the covariance. The covariance function then is dependent on the magnitude of the offset. The prefixes auto or cross are added to indicate if x and y are identical or different data series. The equation for the covariance function is:

$$C_{xy}(\tau_k) = \frac{1}{N-k}\sum_{i=1}^{N-k}(x_i - \bar{x})(y_{i+k} - \bar{y}),\ k = 1, 2, 3 \ldots M;\ M << N, \tag{3.2}$$

where the dependence on the lag, τ, is shown. The subscript k indicates the number of sampling increments, Δt, such that, $\tau_k = k\,\Delta t$. The covariance function is often normalized: $\rho_{xy} = C_{xy} / \sigma_x \sigma_y$, where σ_x and σ_y are the standard deviation of each sequence. This quantity is known as the normalized auto- (or cross-) covariance function and has maximum and minimum values of +1 and -1. Positive values of ρ indicate the sequences are correlated, while negative values indicate anti-correlation. Note that as k increases, the covariance estimate is based on fewer samples.

This concept is illustrated by considering a simple sinusoidal sequence of constant magnitude and frequency. At zero lag, $k = 0$, the normalized auto-covariance function (NACF) will be the maximum value of +1. If τ is equal to one-half of the period of the sinusoid, then the NACF becomes -1, i.e., anti-correlation. At the lag equal to one-quarter of the period, the NACF is equal to zero, i.e., no correlation. At lags equal to the period of oscillation, the NACF returns to a value of +1. For a sinusoidal sequence, the NACF will simply oscillate from +1 to -1 with the same period as that found in the original sequence.

For realistic geophysical data, the NACF will often approach zero for very large lags. However, measurement costs rarely allow for record lengths to be sufficient for the NACF to approach zero. Therefore, low-frequency oscillations present in the data usually cause the NACF to oscillate around zero for large lags. It should be noted that as k approaches N, the NACF becomes statistically meaningless as fewer points are used in the estimation.

The authors define the scale length as the value of the lag in which the NACF goes from its maximum value of +1 (at zero lag) to zero, i.e., the first zero-crossing. The scale length is a temporal or spatial scale depending on the type of data sequence. This definition of scale length can be considered an upper bound of the true scale (Poulain and Niiler, 1989).

In practice a background sequence is often removed from the data sequence prior to estimating the NACF. This background or reference field generally represents large scale spatial patterns or trends in the data. Its removal allows for the analysis of the

shorter (i.e., larger wave number) energetic spatial variability. Not removing the reference field will usually bias the scales to larger values. The reference field is usually estimated by fitting a polynomial to the original data. The order of polynomial is highly dependent upon the nature of the data set, the inherent characteristics of the system being measured, and the magnitude of the scales that are wished to be resolved. When investigating spatial scales of current dynamics on a continental shelf, Li et al. (1996) compared several different polynomial fits before selecting the quadratic fit to define the reference field. The partitioning of the data into a background and residual field can also be interpreted as separating the measurements into competing or independent mechanisms. The residual field in this sense is then thought to be causes by mechanisms with smaller scales than that responsible for the reference field.

The computer routines used to estimate the NACF have been optimized for speed and efficiency. To this end, the Wiener-Khintchine theorem (Hsu, 1984) will be used to estimate the NACF using the Fast Fourier Transform (FFT). The theorem simply states that the NACF is the Fourier transform of the spectral energy density of that series. This technique is particularly efficient when the number of samples is large, i.e., on the order of 1000s.

Let us now consider the practical estimation of the scale length. It is assumed that the raw data have been examined for statistical outliers, calibration errors, and other problems and have passed quality control and assurance criteria, i.e., the data are suitable for scientific analysis. The raw data are first interpolated to a regular grid (e.g. concentration versus depth). This step is necessary when using the FFT to estimate the

NACF. Usually the number of points in the new sequence is a power of two to further maximize computational efficiency, but is not absolutely necessary. The interval length of the interpolated sequence should be at least as large as the interval length of the original sequence so that sampling resolution is not lost. Next, the reference field is determined. This step is the most subjective part of the analysis.

However, usually a plot of the data will indicate the type of reference field to use. The key is to identify the largest pattern of variability in the data. If the data are evenly distributed around a mean value, then the mean value is the reference field. However, if a more complex pattern is present a higher-order polynomial is required. A rule of thumb is that the ratio of variance in the residual field (raw field minus reference field) to variance in the raw field should exceed 0.10. For ratios less than this value, the scale estimates may be statistically meaningless.

After the reference field is identified and estimated it is then subtracted from the interpolated data to yield the residual field. The NACF of the residual field is then estimated using the FFT. Many mathematical software packages have easily-used built-in FFT subroutines (e.g., MATLAB, IDL, PV-WAVE, etc.). It is noted that the NACF is written as:

$$\rho_{xx} = \frac{1}{\sigma^2} iFFT\left[\left\|FFT[x]\right\|^2\right], \tag{3.3}$$

where σ is the standard deviation of the residual field x and *FFT* and *iFFT* indicate the operation of the FFT and inverse-FFT. Note that the iFFT operation is performed on the square of the absolute value of the FFT of the residual field.

Finally, the scale length is determined by identifying the lag of the first zero-crossing of the NACF (either objectively or visually from plots of the NACF versus lag). It is noteworthy that the first e-folding or significance-level crossing, in addition to the first zero-crossing, of the NACF can also been used to define scale length. However, as stated above, the first zero-crossing represents an upper bound of the true scale length. The e-folding scale is primarily used in meteorology and is the lag in which the NACF crosses e^{-1}, i.e., the natural decay rate. The significance level is the maximum value of the NACF which is indistinguishable from zero based on the effective degrees of freedom of the residual field (Emery and Thomson, 1997). The significance-level crossing, therefore, provides some estimate of the error associated with the zero-crossing scale.

The next step is to repeat the whole procedure outlined above for many independent sequences to create an ensemble of scale estimates. The scales should then be compared to other known parameters and scales and processes known to exist in the system being measured.

Methods for Analytical Data

Voltammetric analysis of pore water components has been used in a wide variety of sediments to analytically quantify fine-scale (0.1 mm) spatio-temporal differences in pore water geochemistry (Brendel and Luther, 1995; Theberge and Luther, 1997; Luther et al. 1998; Bull and Taillefert, 2001; Hebert and Morse, 2003). Solid-state, gold-mercury amalgam (100 μm sensing tip) microelectrodes were used to simultaneously

measure concentrations of dissolved O_2, Mn^{2+}, Fe^{2+}, and ΣH_2S (Brendel and Luther, 1995). The microelectrodes were calibrated against Mn^{2+} standards in seawater, and the pilot ion method was used for Fe^{2+} and ΣH_2S (Brendel and Luther, 1995). Minimum detection limits for each analyte using a DLK-100A electrochemical analyzer from Analytical Instrument Systems Inc. (AIS) were as given in Brendel and Luther (1995). O_2 concentrations dropped below minimum detection limits in the first few millimeters of sediment and Mn^{2+} was generally below its detection limit. Consequently, only Fe^{2+} and H_2S concentrations are reported in this study. Core profiles were obtained at 2-5 mm depth intervals in replicate (for most cases) but may be collected at sub-millimeter depth resolution using a micromanipulator (Velmex).

Data were obtained using anodic stripping voltammetry for dissolved sulfide (ΣH_2S) and iron (Fe^{2+}) at a seagrass site and a reference unvegetated site. The seagrass meadow studied was at Idaho Point in Yaquina Bay, OR, and was sampled in August 2003. It is composed of *Zostera marina*, also commonly referred to as eelgrass. Collection at all sites included use of 14 cm diameter, 40 cm long polycarbonate push-cores to a sediment depth of ~20 cm.

For the seagrass and unvegetated sites, cores of intact plants and adjacent (<10 m) unvegetated cores were taken during the day at low tide and immediately brought to the laboratory, placed in aquaria with *in situ* seawater, and maintained at *in situ* temperature. The lighting was supplied by 1000 watt metal halide bulbs with a measured irradiance (PAR) of around 400 $\mu mol \cdot m^{-2} \cdot s^{-1}$ with a 12/12 h on/off system, and seagrass leaves were allowed to stretch out of the core as they do in nature. For

vertical scales analysis, both the seagrass and unvegetated cores were profiled every four hours for a 24 h period. Three profiles spaced 1.5 cm apart laterally were near-simultaneously (<2 s lag) obtained for each time point. Measurements for each profile were made at 2 mm depth increments down to 50 mm, at which point 5 mm depth increments were made to a total depth of 150 mm (maximum depth of micromanipulator (Velmex controller and micromanipulator)). Scales analysis was performed for all three profiles and averaged for one scale length. For lateral scales analysis, a single electrode was used to profile sediments at the sediment-water interface (0 mm), 50 mm, 100 mm, and 150 mm sediment depth. Profiles were performed every 5 mm horizontally, which was the minimum spacing interval allowed where adjacent profiles would not disturb the sediments, for a total horizontal distance of 75 mm. Core liner diameter (14 cm) limited the capacity of increased sampling. Profiles were not performed within 2 cm of either side of the core liner.

Application of the ACF Method to Pore Water Data with Discussion

In this section, application of the ACF approach to data sets for dissolved Fe^{2+} and ΣH_2S obtained as described in the previous chapter is illustrated. It is important to keep in mind that the purpose here is not to describe the processes that were under study, which are topics of other papers (e.g., Hebert and Morse, 2003; Chapter II), but rather to illustrate major considerations and practical methodology when using the ACF approach to choose sampling intervals. As noted earlier, this involves both quantitative mathematics and some good common sense.

Before applying the ACF method to the data sets, it is useful to consider its utility in a broader context. The "golden rule" is do not use it if you don't need to. If only a few cores are to be studied or plenty of time and money is available, it is probably always best to obtain as much data as possible. In practice, this must always be initially done on a selected set of cores that are believed to be "representative" of the area to be studied. This in itself can be a difficult decision. Although concentrations and distributions may differ among them, if a similar scale length is obtained it will provide a solid guide for further work.

Spatial and temporal variability occur over a broad range of scales reflecting different physical and biogeochemical processes. A rather obvious "first rule" is that processes leading to variability on an incremental size smaller than that observable by the sampling method cannot be determined. For example, the traditional "slice and squeeze" method of obtaining pore waters that is still often about the only practical means of obtaining sufficient volumes of pore water for a variety of analyses (e.g., nutrients, dissolved organic carbon, dissolved inorganic carbon, sulfate, etc.) often requires sediment core intervals on the order of 1 to 4 cm. The changes that occur over several cm to tens of cm and the impact of some macrofaunal processes such a burrowing by shrimp and large bivalves are observable on this scale. Most of the major diagenetic models have consequently been built on fitting model results to data sets of this scale (e.g., Berner, 1974, 1980; van Cappellen and Wang, 1996; Boudreau, 1997, 2000; Eldridge and Morse, 2001). However, while such models and the processes on which they are based have considerable utility, they cannot deal with smaller scale

variability and essentially produce a description of an average composition of what is often a highly heterogeneous system at a smaller scale (e.g., Aller, 1980; Aller et al., 1998).

The microelectrode method, used in the data sets presented here, improves the observable scale by about one to two orders of magnitude. As will be subsequently shown, this reveals an important scale length for the variability of dissolved reduced iron and sulfide on the order of a few millimeters that probably reflects the importance of meiofauna and, in vegetated sediments, small roots in controlling iron and sulfide distributions. Still beyond our analytical observation scale is the ability to determine the importance of the heterogeneous distribution of microorganisms such as iron oxide and sulfate reducing bacteria.

A "second rule" for applying the ACF method is that it should be used only over intervals where change is observable beyond the analytical precision or detection limit of the measuring technique. Including regions where no observable change is occurring leads to considerable fitting difficulties and can badly bias results where the objective is to determine the scale length of the dominant process leading to variability within the interval of change. An example of this is where no Fe^{2+} is observable until a few cm below the sediment-water interface, it then goes through a depth interval of several cm where it varies substantially and at greater depths is below detection limits. It should also be noted that such fitting will commonly be done over different depth intervals for different dissolved components. For example, detectable dissolved Fe^{2+} and H_2S usually

do not extensively coexist over the same depth range, however, their scale lengths in this study were not observably different (Table 3.1).

Closely related to the "second rule" is the most mathematically arbitrary aspect of our approach to the ACF method which is the fitting to the data an equation to describe the large scale changes (background or reference data field). The resulting plot is similar to that which would be produced by the previously cited diagenetic models (Fig. 3.2). Here, a least squares polynomial fit of varying degree has been used. There is no theoretical basis for this and in specific cases other types of fitting equations (e.g. exponential) may be more appropriate. In Fig. 3.2, results show using first through fourth degree polynomial least squares fits to determine the characteristic length for A) total dissolved H_2S versus depth with fits, B) the residual versus depth, and C) value of the normalized ACF versus scale length.

In Table 3.1, the value of the zero crossing are given with sampling times. Average scale lengths were recorded for each time (recall that three electrodes were used for each sampling time) and time-averaged scale lengths with standard deviations and a total scale length for both sediment types was determined. In this case, the second through fourth order fits yield similar zero crossing values of 9.9, 10.6, and 9.8 mm, respectively, indicating that a second order fit is probably adequate for estimating the characteristic length. It should be noted that if, upon visual inspection the more smoothly varying data below 60 cm depth is treated separately, its characteristic length is a bit larger, ~12 mm.

Table 3.1 Scale length (± standard deviation) for different sediment types for dissolved ΣH_2S and Fe^{2+} using polynomial least squares fits of second order of the zero crossing

Site	Sampling Time	Scale length H_2S (mm)	Scale length Fe^{2+}(mm)
Yaquina Bay Oct., 2000			
Seagrass	Morse et al., 2003	9.9	
Unvegetated	Morse et al., 2003	11.7	
Yaquina Bay Aug., 2003			
Seagrass 1	10:00 AM	15.7	BD
	2:00 PM	15.5	BD
	6:00 PM	9.1	10.7
	10:00 PM	13.6	14.0
	2:00 AM	14.4	9.6
	6:00 AM	15.7	8.0
Average scale		**14.0±2.5**	**10.5±2.5**
Unvegetated 1	11:00 AM	4.0	
	3:00 AM	BD	
	7:00 PM	19.5	
	11:00 AM	21.9	
	3:00 AM	14.7	
	7:00 PM	12.9	
Average scale		**15.1±6.9**	
Seagrass 2	2:00 PM	14.3	
	6:00 PM	19.2	
	10:00 PM	BD	
	2:00 AM	9.1	
	6:00 AM	17.2	
	10:00 AM	17.5	
		15.5±4.0	
Unvegetated 2	3:00 PM	9.4	
	7:00 PM	14.2	
	11:00 PM	8.9	
	3:00 AM	10.0	
	7:00 AM	14.0	
	11:00 AM	6.7	
Average scale		**10.5±3.0**	
Total average		**13.8±2.3**	

BD= ΣH_2S was below detection hence the method could not be performed

Further examples are presented by giving depth profiles for dissolved H_2S in mud-dominated estuarine sediments that are from a seagrass meadow and nearby unvegetated area in Yaquina Bay, Oregon (Fig. 3.3). The parameters previously described for Table 3.1 are given for second order polynomial least squares fits for these profiles. Data from the same site three years later indicated that approximately the same scale length was suitable for measurement. This will give us confidence that anyone can adopt this sampling interval for future seagrass profiles for this system at this site.

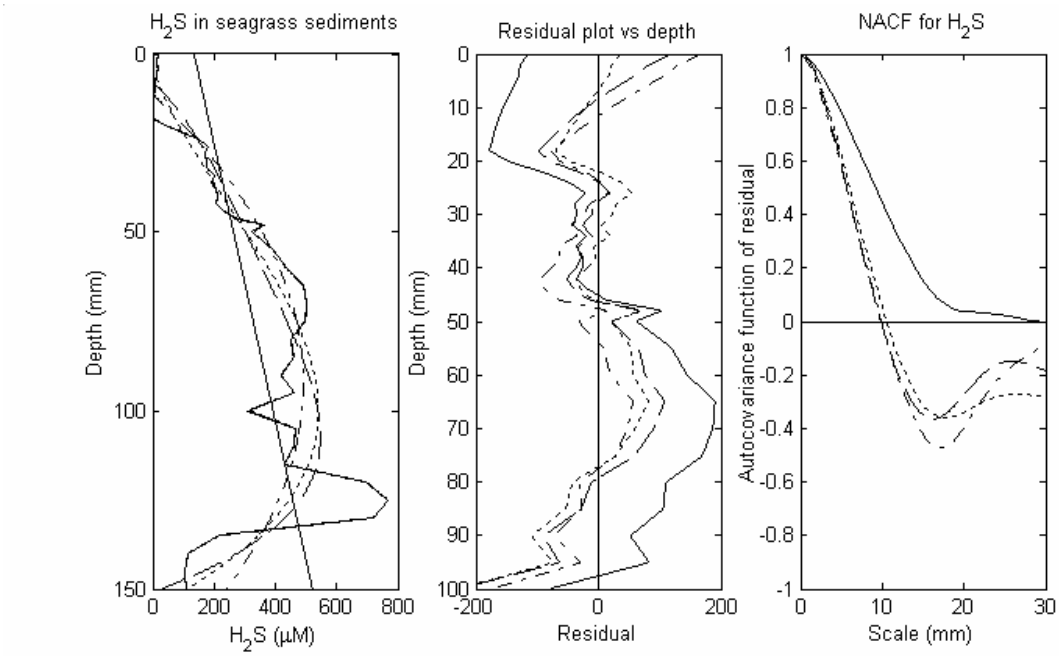

Fig. 3.2 Plots for dissolved H_2S (solid jagged line) with polynomial least squares fits, the ACF residual and the normalized ACF (NACF) versus depth in SG1-3-1, for first (straight solid line), second (dash-dot line), third (dotted line), and fourth (dash-dash line) order fits

The large degree of lateral heterogeneity observed for these systems, as demonstrated by the standard deviations in Fig. 2.4, prompted a closer examination of scale length horizontally. Fig. 3.4 shows the degree of lateral variability associated with seagrass sediments, where a single electrode measured ΣH_2S at 0, 50, 100, and 150 mm sediment depth every 5 mm laterally, and that the same degree of lateral variability is not observed in the unvegetated sediments. However, the surface of the unvegetated sediments does indicate small variability most likely attributed to localized pockets of organic matter degradation from topographical features. Table 3.2 shows the lateral scale lengths that resulted from a second-order polynomial, a first-order polynomial, and a mean fit for the data, and that the percent of variance ascribed by these fits were low <20%). The scale length for 2nd order seagrass fit are near the sampling interval which signifies that the data become completely uncorrelated with 0+1 unit lag shift. It should be noted that the scale lengths are smaller than those associated with vertical sampling intervals. This is important to consider when using diagenetic models that neglect lateral variations or assume homogeneity. These data suggest that there is a pattern of variability associated with lateral processes. The processes that defined our characteristic scale length for lateral variability may be diversity-controlled processes, such as the association of meiofauna with burrow spacing or collection of particulate organic matter in topographical features of the sediment which concentrates sulfate reducing bacteria, or it may be a less likely random distribution of microalgal and/or bacterial aggregates. Small-scale vertical and horizontal distribution of microalgal and/or microbial

assemblages as well as meiofaunal assemblages has been observed by others (Sandulli and Pinckney, 1999, Eckman and Thistle, 1988; Joint et al., 1982; Hewitt et al., 1993).

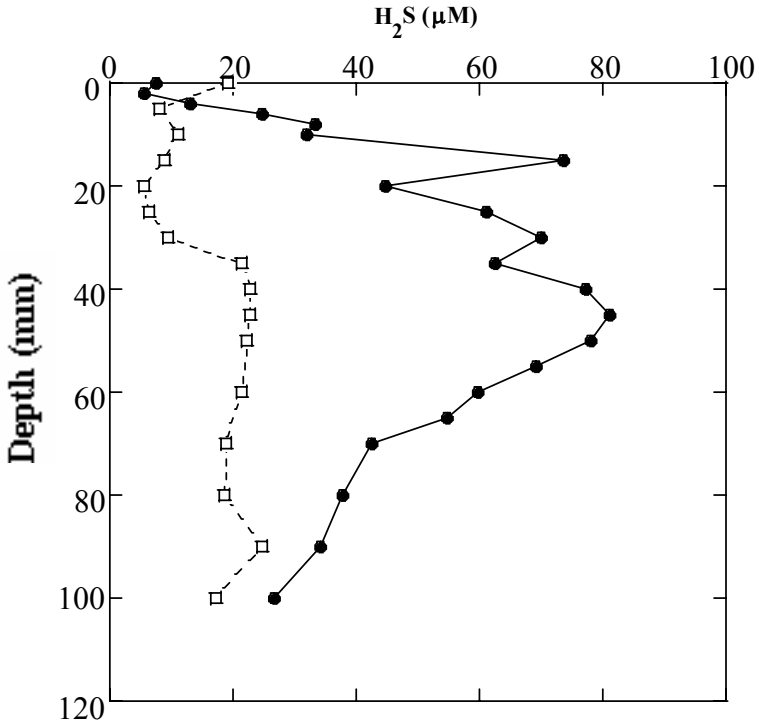

Fig. 3.3 Total dissolved H_2S profiles for Yaquina Bay, Oregon, cores from a seagrass meadow (solid circles) and adjacent unvegetated sediments (open squares) based on data from Hebert and Morse (2003)

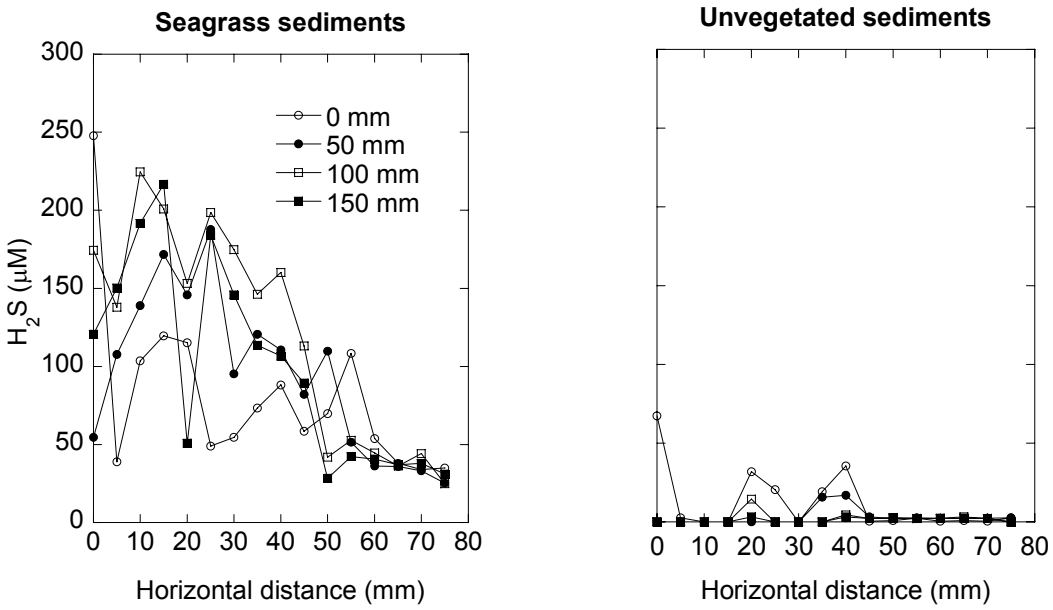

Fig. 3.4 Lateral scale observations of ΣH_2S at four different depths for seagrass and unvegetated sediments

Table 3.2 Lateral scale lengths with 2nd order, 1st order, and mean fit determination

	Seagrass			Unvegetated		
Depth (mm)	2nd	1st	mean	2nd	1st	mean
0	3.91	3.91	4.7	5.04	5.16	5.28
50	5.99	14.72	16.98	7.28	9.37	9.72
100	5.95	8.41	18.03	4.89	5.09	5.09
150	4.29	4.34	17.29	5.58	6.49	12.04

Results of the ACF approach for these seagrass and unvegetated cores yield a considerable range of normalized residuals (0.08 to 0.78) and percent of variance accounted for (26% to 90%) reflecting the major differences in the complexity of the

profile shape and "noisiness" of the data. However, the results for the scale length are more consistent. The range is only from 6.7 to 21.9 mm, with 4.0 as an outlier. Results from the second and third order polynomial fits are statistically not distinguishable. One way of expressing this result is that although the amplitude of signal is quite variable, the frequency falls in a narrow range.

Scale length associated with distance can often be associated with some physical process or characteristic of the system. In sediments, the scale length is often likely to reflect a biogeochemical process. The scale length that has been observed is similar in size to that of common macrofaunal organisms such as polychaete worms (e.g., Aller and Yingst, 1978). It is near agreement with the burrow diameter value of 7.5 mm used by Aller (1977, page 77) in his model for the importance of bioirrigation in controlling sediment chemistry near the sediment-water interface. Although, physically there may be wide variation in the density of infaunal organisms leading to variations in the normalized residuals (something worthy of further investigation), the size range of the dominant organisms (or their burrows) appears to be limited and reasonably predicted by the ACF method for a wide variety of coastal sediments. It should also be noted that the seagrass rhizomes are also in this approximate size range and probably exert an influence in the sediments from the seagrass meadow. Fig. 3.5 illustrates how geochemical gradients are influenced by a shrimp burrow. For burrows that are more vertical, lateral gradients associated with the sphere of influence from the burrow walls can be more variable than the vertical gradients.

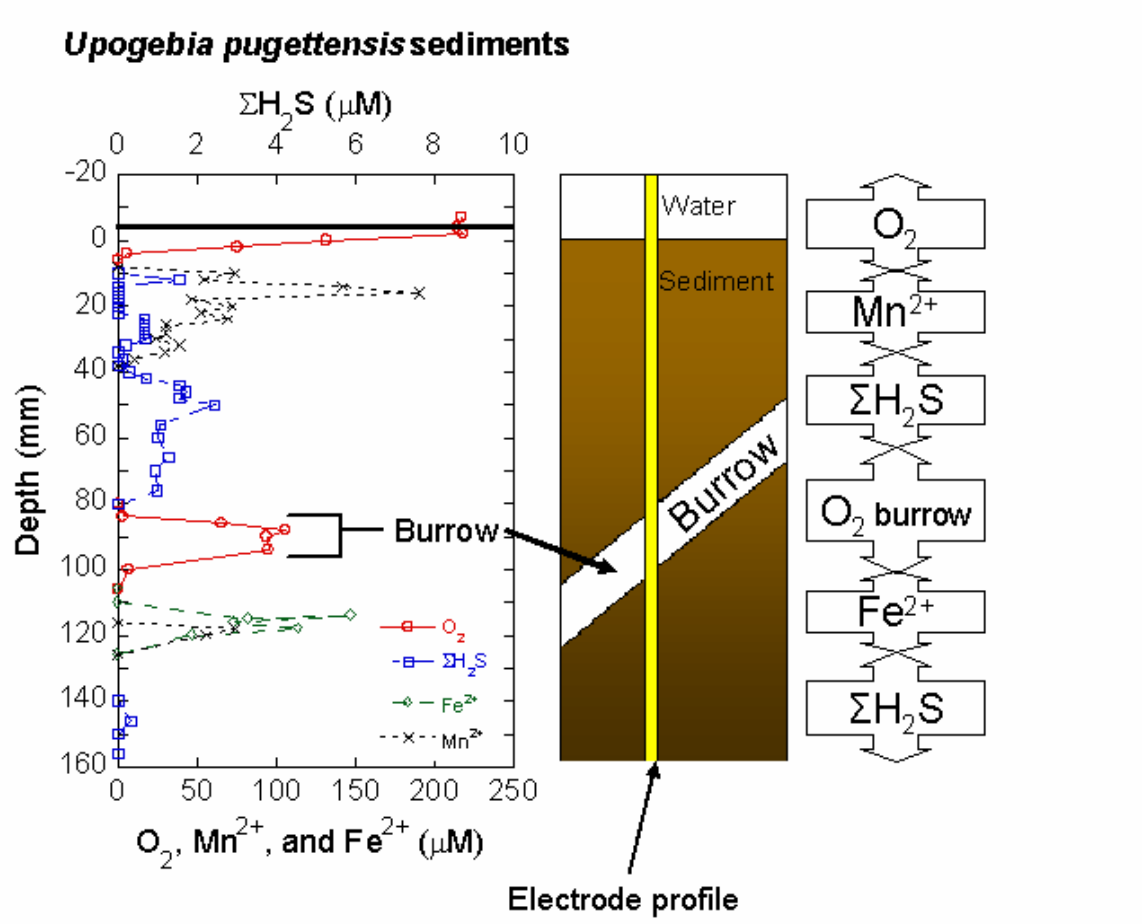

Fig. 3.5 Geochemical gradients associated with a burrow in sediments

Summary

In studies of sedimentary biogeochemistry where large numbers of samples must be analyzed, such as those directed at spatial or temporal change, the ACF method provides a relatively easily applied scaling approach to choosing sample spacing. Results can be used to optimize the sampling interval in time and/or space necessary to minimize the number of samples without losing the dominant source of variability beyond the general large scale process that cause change. The scale length that is obtained usually

reflects the size of the physical or biological process that produces it. This relationship can be used both as a guide for searching for important factors leading to variability or in helping to confirm, as in our examples, expected sources of variability.

CHAPTER IV

A DIAGENETIC MODEL FOR SEDIMENT-SEAGRASS INTERACTIONS*

Introduction

Seagrasses have been shown to alter sedimentary biogeochemical processes both spatially and temporally (Hebert and Morse, 2003; Lee and Dunton, 2000). Important early diagenetic reactions that occur in sedimentary environments may work to the advantage of seagrasses by sequestering toxic sulfides (ΣH_2S) through the precipitation of metastable and stable iron sulfide minerals (e.g., FeS and pyrite, respectively) with Fe^{2+} or by promoting sediment anoxia by releasing ΣH_2S through dissolution of sulfide minerals enabling bioavailability and consequently stressing respiratory demands of belowground tissues. Translocation of photosynthetically produced oxygen from leaves to belowground biomass helps to mitigate the degree of anaerobiosis surrounding roots and rhizomes (Smith et al., 1984; Caffrey and Kemp, 1991). This complicates interpretation of diagenetic processes on shorter time scales. However, geochemical data obtained for light and dark conditions may be used to calibrate and simulate diagenetic models which may provide the framework for describing biogeochemical transformations in seagrass sediments.

---

*Reprinted in part from *Marine Chemistry*, Vol 70, Eldridge and Morse, A diagenetic model for sediment-seagrass interactions, Pages 89-103, (©2000) with permission from Elsevier.

Eldridge and Morse (2000) showed that their seagrass diagenetic model, largely adapted from Boudreau (1996) and Van Cappellen and Wang (1996), when parameterized with root zone fluxes estimated from field surveys of subtropical seagrasses (*Thalassia testudinum*, *Halodule wrightii*, and *Syringodium filiforme*) correlated well with sedimentary geochemical data.

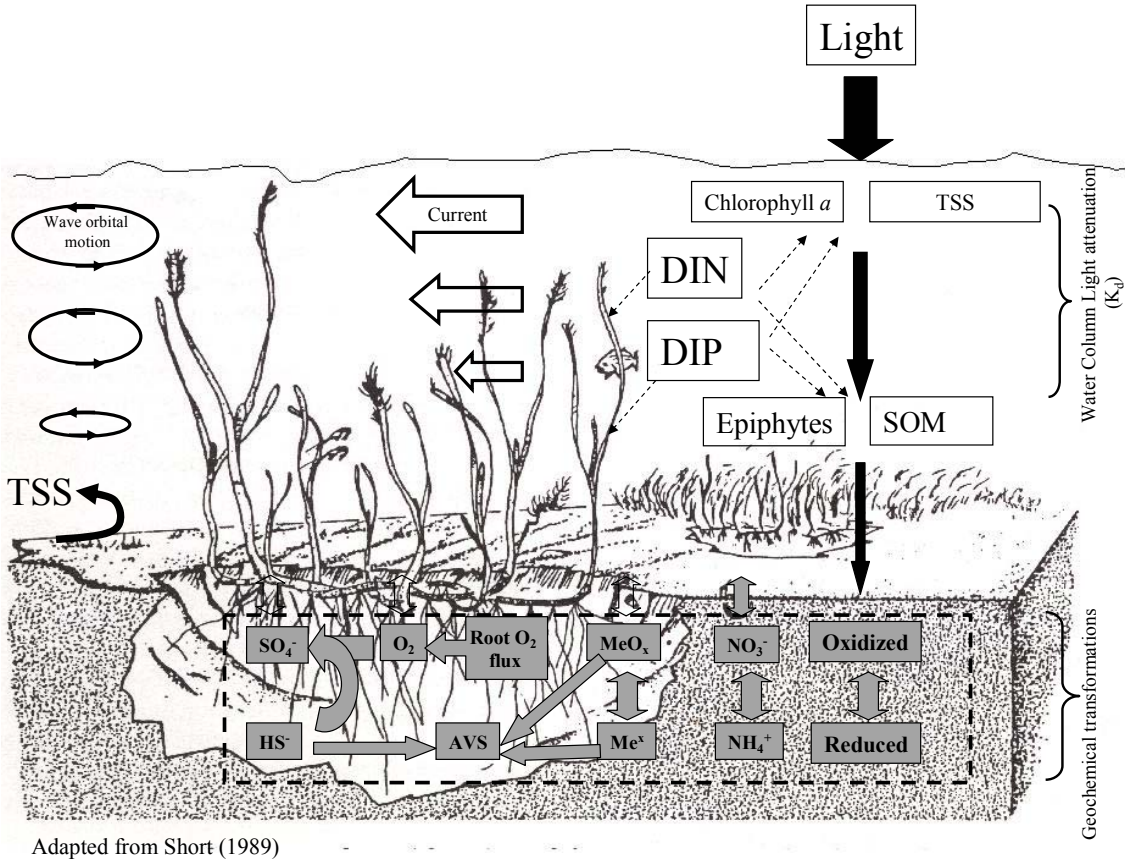

Fig. 4.1 Biomass of seagrass is partitioned into aboveground (water) and belowground components. The above and below ground components are subjected to a different set of physical, biological and geochemical stressors. The present model generally considers the geochemical interactions of the plant with its sediment environment. However we know that the seagrass responses to a much broader set of environmental factors that are lumped in this analysis as fluxes to the sediments

I have conducted similar research in Yaquina Bay, OR, which covers 15.8 km^2 (30 km long), has ~6% of the estuary vegetated with *Zostera marina* contributing ~420 mmol m^{-2} d^{-1} net production (Garber et al., 1992). The chief industries in Yaquina Bay are logging, fisheries, and oyster culture. Most of the nutrients are marine derived as a result of an annual spring summer upwelling. The objective of this modeling effort was to better understand the dynamic relationship between temperate eelgrass beds and their sedimentary environment using a diagenetic model. Model simulations were performed with geochemical data from seagrass sediments over a diel sequence of light and dark cycles.

Light and nutrient constraints limit seagrass growth and recolonization. Sediments may also restrict growth by contamination of toxic materials, such as sulfide, or may be affected by some physical property that slows growth. (Zimmerman *et al*., 1987; Pulich, 1989). Both physical properties, such as consolidation and grain size, and chemical characteristics, including high concentrations of sulfides, ethanol, and metals, may lead to the degradation or stunted growth of seagrass beds. Healthy seagrass plants have the ability to alter their sedimentary environment. For example, photosynthetically produced oxygen and labile DOC can enter the sedimentary environment on diurnal time scales, and seagrass leaf detritus can enhance both the percent concentration and quality of organic matter in the sediments (Fig. 4.1). The nitrogen content and increased lability of seagrass leaf detritus may stimulate bacterial ammonium production through metabolism of the organic matter. This recycled ammonium then becomes available for seagrass growth (Zimmerman *et al*., 1987).

The goal of our geochemical modeling was to produce a quantitative description of the interactions between temperate eelgrass and sediment geochemistry. This allowed us to determine both changes in sediment chemical properties due to seagrass production on diurnal time scales, and to predict with a steady-state model which geochemical constituents were most sensitive to changes in model parameters by performing sensitivity analyses.

Methods

General

Data and observations of general geochemical relationships for sediments in Yaquina Bay presented in Chapter II were used to parameterize a diagenetic model. The model used was similar to that in Eldridge and Morse (2000) which utilized a numerical simulation for vertical transport that borrowed heavily from Boudreau's (1996) general diagenetic model, while the reactions involving organic carbon (OC) mineralization and generation were derived mostly from Van Cappellen and Wang (1996). This diagenetic model differs from the Eldridge and Morse (2000) model in its treatment of sediment interactions with a different species of seagrass and a different climate — temperate *Zostera marina*, however many of the reactions and equations were rewritten in this manuscript for reference. Yaquina Bay sediment geochemistry is linked to seagrass nutrient uptake, dissolved organic carbon (DOC) and CO_2 release, and O_2 transport from the roots to the sediments. The Eldridge and Morse (2000) model represented oxidation of particulate and dissolved organic matter (OM) as coupled reactions in successively deeper sedimentary layers to reduction by oxygen, nitrate, iron, and sulfate with

associated Gibbs free energy, similar to the idealized organic metabolic pathways in biogeochemical textbooks. They maintained these energy relationships by assuming that within each layer of the sediment, populations of bacteria will specialize in using specific oxidants while becoming inhibited by more energetic oxidants (Boudreau, 1996). Eldridge and Morse (2000) formulated a set of equations based on the observed energy relationships and zonation of organic matter degradation pathways (Rabouille and Gaillard 1991; Dhakar and Burgide, 1996; Soetaert *et al*., 1996; and Boudreau, 1997).

Reactions

There are many pathways for organic matter degradation that could be included in this analysis, however for simplicity, only one biogenic reaction for each electron acceptor was used and assumed that each pathway went to completion (CO_2 and water) (Lovley and Phillips, 1989; Kristensen and Blackburn, 1987; Postma and Jakobsen, 1996). Eldridge and Morse (2000) also used Boudreau's (1996) Monod-like hyperbolic feedback for inhibition and general Monod relationships to describe the relationship between growth and substrate concentration. The reaction rates were described by Monod relationships with additional terms for inhibition by competing oxidants (Table 4.1) (Boudreau 1997), however the inhibition effects were lessened between iron oxide reduction and sulfate reduction due to the concomitant Fe^{2+} and ΣH_2S that occurred. K^* are inhibition constants, usually multiples of the Monod half saturation constants (Eldridge and Morse, 2000).

Eldridge and Morse's sediment diagenetic model has 13 compartments covering solid and pore-water organic and inorganic species that are important in the diagenesis of Laguna Madre sediments (Table 4.2), and provides a simplified stoichiometry for the oxidation of OM to reduce the number of species modeled, and number of equations (Table 4.3; EQ. 4.1-4.4). The organic matter species oxidation reactions assume that they are biologically mediated.

Once the reduced products are formed, they can become titrated through reactions with other constituents or transported by diffusion and bioturbation back into upper strata of the sediments to be used in a series of redox reactions (Table 4.3; EQ. 4.5-4.11). Most of the coupled redox reactions considered in other recent diagenetic models were included (Boudreau, 1996; Van Cappellen and Wang, 1996), but Mn compounds were excluded because of their low concentrations at the site in Yaquina Bay, similar to their site in Laguna Madre, and a different feedback for FeS production and loss was used (Table 4.4).

Table 4.1 Coupled Monod feedback and inhibition factors used to preserve the energy relationships among oxidants and organic matter (Boudreau, 1997)

$$rO_2 = \frac{[O_2]}{K_{O_2} + [O_2]}$$

$$rNO_3^- = \frac{[NO_3^-]}{K_{NO_3^-} + [NO_3^-]} \frac{K^*_{O_2}}{K^*_{O_2} + [O_2]}$$

$$rFe^{3+} = \frac{[Fe^{3+}]}{K_{Fe^{3+}} + [Fe^{3+}]} \frac{K^*_{O_2}}{K^*_{O_2} + [O_2]} \frac{K^*_{NO_3^-}}{K^*_{NO_3^-} + [NO_3^-]}$$

$$rSO_4^{2-} = \frac{[SO_4^{2-}]}{K_{SO_4^{2-}} + [SO_4^{2-}]} \frac{K^*_{O_2}}{K^*_{O_2} + [O_2]} \frac{K^*_{NO_3^-}}{K^*_{NO_3^-} + [NO_3^-]} \frac{K^*_{Fe^{3+}}}{K^*_{Fe^{3+}} + [Fe^{3+}]}$$

Table 4.2 Solid and dissolved species found in the sediment diagenesis model. The model assumes an oxidation state of zero for organic material. C:N:P of surface flux is that of seagrass above ground biomass. Root zone flux C:N:P is that of the below ground biomass

Explicit species		
TOC_1	labile total organic carbon	Solid
TOC_r	refractory total organic carbon	Solid
DOC	dissolved organic carbon	Pore water
O_2	oxygen	Pore water
NO_3^-	nitrate	Pore water
NH_4^+	ammonium	Pore water
SO_4^{2-}	sulfate	Pore water
ΣH_2S	total sulfides	Pore water
$Fe(OH)_3$	amorphous	Solid
Fe^{2+}	ferrous	Pore water
AVS	acid volatile sulfides (includes ΣH_2S)	
FeS_2	pyrite	Solid
DIC	dissolved inorganic carbon	Pore water
pH	—	Pore water

Table 4.3 The diagenetic reactions simulated in the model. Equations 1 through 4 are replicated for refractory and labile organic matter. x, y, z are the component of oxidation contributed by CH_2O, NH_3, and H_3PO_4 respectively (from Eldridge and Morse, 2000; adapted from Van Cappellen and Wang (1996)

Organic matter oxidations:

$$(CH_2O)_x(NH_3)_y(H_3PO_4)_z + (x+2y)O_2 + (y+2z)HCO_3^- \xrightarrow{R_1/x} (x+y+2z)CO_2 + yNO_3^- + zHPO_4^{2-} + (x+2y+2z)H_2O \quad (4.1)$$

$$(CH_2O)_x(NH_3)_y(H_3PO_4)_z + \left(\frac{4x+3y}{5}\right)NO_3^- + \xrightarrow{R_2/x} \left(\frac{2x+4y}{5}\right)N_2 + \left(\frac{x-3y+10z}{5}\right)CO_2 + \left(\frac{4x+3y-10z}{5}\right)HCO_3^- + zHPO_4^{2-} + \left(\frac{3x+6y+10z}{5}\right)H_2O \quad (4.2)$$

$$(CH_2O)_x(NH_3)_y(H_3PO_4)_z + 4xFe(OH)_3 + (7x+y-2x)HCO_3^- \xrightarrow{R_{41}/x} 4xFe^{2+} + (8x+y-2z)HCO_3^- + yNH_4^+ + zHPO_4^{2-} + (3x-y+2z)H_2O \quad (4.3)$$

$$(CH_2O)_x(NH_3)_y(H_3PO_4)_z + \left(\frac{x}{2}\right)SO_4^{2-} + (y-2z)CO_2 + (y-2z)H_20 \xrightarrow{R_5/x} \frac{x}{2}H_2S + (x+y-2z)HCO_3^- + yNH_4^+ + zHPO_4^{2-} \quad (4.4)$$

Redox cycles:

$$Fe_2 + \frac{1}{4}O_2 + 2HCO_3^- + \frac{1}{2}H_2O \xrightarrow{R_8} Fe(OH)_3 + 2CO_2 \quad (4.5)$$

$$NH_4^+ + 2O_2 + 2HCO_3^- \xrightarrow{R_{11}} NO_3^- + 2CO_2 + 2H_2O \quad (4.6)$$

$$H_2S + 2O_2 + 2HCO_3^- \xrightarrow{R_{11}} SO_4^{2-} + 2CO_2 + 2H_2O \quad (4.7)$$

$$H_2S + 4CO_2 + 2Fe(OH)3 \xrightarrow{R_{14}} 2Fe^{2+} + S^0 + 4HCO_3^- + 2H_2O \quad (4.8)$$

$$FeS + 2O_2 \xrightarrow{R_5} Fe^{2+} + SO4^{2-} \quad (4.9)$$

$$Fe^{2+} + 2HCO_3^- \xleftarrow{R22, R\_22} FeCO_3 + CO_2 + H_2O \quad (4.10)$$

$$Fe^{2+} + 2HCO_3^- + H2S \xleftarrow{R23, R\_23} FeS + 2CO_2 + 2H_2O \quad (4.11)$$

Alkalinity:

$$CO_3^{2-} + \delta CO_2 + (1-\delta)H_2S \Leftrightarrow (1-\delta)HCO_3^- + (1-\delta)HS^- + H_2O \quad (4.12)$$

$$0 \le \delta \le 1$$

Both alkalinity and DIC are the consequence of equilibrium reactions (Table 4.5, EQ 4.14-4.23) and thus provide a "whole system" estimate of the model accuracy when results are compared to measurements. The distribution of carbonate species is temperature and salinity dependent. When DIC or alkalinity is not known, pH is also required for EQ 4.1 to 4.4 (Morse and Mackenzie, 1990). The model uses the Whitfield and Turners (1986) relationship for salinity and temperature dependence of equilibrium constants and the Stumm and Morgan (1981) closed system ionization fractions. Data in this study included vertical profiles of pH. However, the model has the capacity to model pH using formulations from Van Cappellen and Wang (1996).

Table 4.4 Rate equations used in the reaction scheme (from Eldridge and Morse, 2000; revised from Van Cappellen and Wang, 1996).
$\sum H_2S = [H_2S] + [HS^-]$

$R_1 = k_g\, rO_2$	R_{10}=N.A.	R_{-21}= N.A.
$R_2 = k_g\, rNO_3$	$R_{11}=k11\,[NH_4^+]\,[O_2]$	R_{21}= N.A.
$R_4 = k_g\, rFe$	$R_{12}=k12\,[\sum H_2S]\,[O_2]$	R_{-21}= N.A.
$R_{5=}\, k_g\, rSO_4$	R_{13}= N.A.	R_{22}= N.A.
R_6= N.A.	$R_{14}=k14\,[\sum H_2S]\,[Fe(OH)_3]$	R_{-22}= N.A.
R_7= N.A	$R_{15}=k15\,[FeS]\,[O_2]$	$R_{21}=k23\ \sigma 23\ (\Omega[FeS]_]^{-1})$
$R_8=k8\,[Fe^{2+}]\,[O_2]$	R_{16}= N.A.	$R_{-23}=k\_23\ \sigma 23\,[FeS]\,(1-\Omega_{Mn})$
R_9= N.A.	R_{17}= N.A.	R_{24}= N.A.
	R_21=N.A.	R_{-24}= N.A.

$$\Omega_{FeS} = \frac{\left[Fe^{2+}\right]\left[HS^-\right]}{\frac{\left[H^+\right]}{\left[H^+\right]+K_{H^+}}K'_{FeS}} \qquad \begin{array}{l}\Omega_{FeS}\ \mathrm{f}\ 1:\ \delta_{23}=1, \delta_{-23}=0\\ \Omega_{FeS}\le 1:\ \delta_{23}=0, \delta_{-23}=1\end{array} \qquad (4.13)$$

Table 4.5 Reactions involving each model constituent $\sum R_{C_s}(x)$ (from Eldridge and Morse, 2000; revised from Van Cappellen and Wang, 1996)

$$R_{OM} = -\left(R_1 + R_2 + R_3 + R_4 + R_5\right) \tag{4.14}$$

$$R_{O_2} = \frac{1-\phi}{\phi}\left(\frac{-x+2y}{x}R_1 - \frac{R_7}{2} - 2R_{15}\right) - \left(\frac{R_8}{4} + 2R_{12}\right) \tag{4.15}$$

$$R_{NO_3^-} = \frac{1-\phi}{\phi}\left(\frac{y}{x}R_1 - \frac{4x+3y}{5x}R_2\right) + R_{11} \tag{4.16}$$

$$R_{Fe^{2+}} = \frac{1-\phi}{\phi}\left(4R_4 - 2R_{10} + R_{15} - R_{23} + R_{-23}\right) - R_8 \tag{4.17}$$

$$R_{SO_4^{2-}} = \frac{1-\phi}{\phi}\left(-\frac{R_5}{2}\right) + R_{12} - R_{17} \tag{4.18}$$

$$R_{NH_4^+} = \frac{1-\phi}{\phi}\frac{y}{x}\left(R_3 + R_4 + R_5\right) - R_{11} \tag{4.19}$$

$$R_{Fe(OH)_3} = -4R_4 + \left(\frac{\phi}{1-\phi}\right)R_8 + 2R_{10} - 2R_{14} \tag{4.20}$$

$$R_{FeS} = -R_{15} + R_{23} - R_{-23} \tag{4.21}$$

$$R_{TC} = \frac{1-\phi}{\phi}\left(R_1 + R_2 + R_3 + R_4 + R_5\right) \tag{4.22}$$

$$R_{TS} = \frac{1-\phi}{\phi}\left(\frac{R_5}{2} - R_{13} - R_{14} - R_{23} + R_{-23}\right) - R_{12} \tag{4.23}$$

$$R_{ALK} = \frac{1-\phi}{\phi}\left(\begin{array}{l} -\dfrac{y+2z}{x}R_1 + \dfrac{4x+3y-10z}{5x}R_2 + \dfrac{4x+y-2z}{x}R_3 + \dfrac{8x+y-2z}{x}R_4 \\ \dfrac{x+y-2z}{x}R_5 - 2R_{10} + 2R_{13} + 4R_{14} - R_{23} + R_{-23} \end{array}\right) - 2R_8 - 2R_{11} - 2R_{12} \tag{4.24}$$

Transport processes

The same equations for transport processes were used as in Eldridge and Morse (2000), and are rewritten for reference. Solids (C_s, μmol cm^{-3}_s) and pore water (C_w, μmol cm^{-3}_w) constituents are subject to advective and diffusive transport within the sediments and at the sediment/water interface. Because of compaction, molecular diffusion and irrigation by infaunal filter feeding organisms, solids and pore water constituents are transported in the sediments at different rates. Solid transport is dependent on mixing induced by infaunal organisms (bioturbation, D_b), burial rates (ω), and compaction (EQ. 4.25).

$$\frac{\partial[C]}{\partial t} = \frac{1}{\phi_s}\frac{\partial}{\partial x}\left[\phi_s D_b \frac{\partial[C_s]}{\partial x} - \phi_s \omega[C_s]\right] + \sum R_{C_s}(x) \qquad (4.25)$$

Profiles of porosity (ϕ) are used to determine the amount of compaction with depth. In this analysis, steady-state compaction is assumed (EQ. 26) to simplify both the parameterization of ω and pore water velocity (v,) and to reduce the number of derivatives that need to be calculated (Berner, 1981).

$$\frac{\partial((1-\phi_w)\omega)}{\partial x} = \frac{\partial(\phi_w \vartheta)}{\partial x} = 0 \qquad (4.26)$$

Conversion of organic and inorganic solids occurs through the reactions ($\sum R_{C_s}(x)$) (Table 4.5). Expansion and simplification based on steady-state compaction

results in an equation that can be converted to a finite difference and solved numerically (EQ. 4.27).

$$\frac{\partial[C_s]}{\partial x} = \frac{1}{\phi_s}\left[\left(\frac{\partial \phi_s}{\partial x} D_b + \phi_s \frac{\partial D_b}{\partial x} - \phi_s \omega\right)\frac{\partial[C_s]}{\partial x}\right] + D_b \frac{\partial^2[C_s]}{\partial x^2} + \sum R_{C_s}(x) \qquad (4.27)$$

The pore water transport equation, although similar to that used for solids, has the added complexity of molecular diffusion (D_w), tortuosity (T), and irrigation (α). Molecular diffusion and tortuosity are constant over depth while the other parameters change, requiring additional derivatives in the transport equation (EQ.4.28).

$$\frac{\partial[C_w]}{\partial t} = \frac{1}{\phi}\frac{\partial}{\partial x}\left[\phi\left(D_b + \frac{D_w}{T^2}\right)\frac{\partial[C]}{\partial x} - \phi v[C]\right] - v\frac{\partial[C_w]}{\partial x} + \alpha_{C_w}\left([C_w]_\infty - [C_w]_x\right) + \frac{(1-\phi)}{\phi}\sum R_{C_w}(x) \qquad (4.28)$$

Irrigation in this analysis is assumed to occur through non-local exchange with the water-column or exchange with a benthic boundary layer composed of unconsolidated seagrass leaf litter. Irrigation is therefore a function of the difference between these concentrations and the actual concentration of each constituent in the sediment profile (Berner, 1980) (e.g. third term RHS, EQ. 4.27). The positive sign on the reaction term signifies that the reactions proceed according to Table 4.4. Once again expansion of the equation and simplification based on steady-state compaction provides an equation that can be formulated into a finite difference scheme. This process reduces

the total number of calculation in the model (EQ. 4.29). Units of the parameters in EQ. 4.25 through 4.28 are shown in Table 4.6.

$$\frac{\partial[C]}{\partial t} = \frac{1}{\phi}\left[\left(\frac{\partial\phi}{\partial x}D_b + \phi\frac{\partial D_b}{\partial x} - \phi v\right)\frac{\partial[C]}{\partial x} + \left(\frac{\partial\phi}{\partial x}\frac{D_w}{T} + \phi\frac{D_w}{T^2}\frac{\partial T}{\partial x}\right)\frac{\partial[C]}{\partial x}\right] + \left(D_b + \frac{D_w}{T}\right)\frac{\partial^2[C]}{\partial x^2} + \alpha_{C_w}\left([C_w]_\infty - [C_w]_x\right) + \frac{(1-\phi)}{\phi}\sum R_{C_w}(x) \tag{4.29}$$

A simple linear relationship for $D_b(x)$ (EQ. 4.30) and its derivative (EQ. 4.31) is used (Boudreau, 1997).

$$\begin{aligned} x < x_1 \qquad & D_b(x) = D_b(0), \\ x \geq x_1 \geq x_2 \qquad & D_b(x) = D_b(0)\frac{(x_2 - x)}{(x_2 - x_1)}, \\ x > x_2 \qquad & D_b(x) = 0. \end{aligned} \tag{4.30}$$

Here, the derivative of bioturbation ($DD_B(x)$) is assumed zero to depth x_1 and is constant to x_2 (see Boudreau, 1997).

$$\begin{aligned} x < x_1 \qquad & DD_b(x) = 0., \\ x \geq x_1 \geq x_2 \qquad & DD_b(x) = -\frac{D_b(0)}{(x_2 - x_1)}, \\ x > x_2 \qquad & D_b(x) = 0. \end{aligned} \tag{4.31}$$

Table 4.6 Model parameters

Description	Symbol	Units
Temperature	T	°C
Salinity	S	psu
Pressure	P	atm
Biodiffusion or mixing coefficient	D_b	$\frac{cm^2}{y}$
Depth biodiffusion decreases	$DD_b\downarrow$	cm
Depth biodiffusion goes to zero	$DD_b \rightarrow 0$	cm
Velocity of solid particle burial	ω	$\frac{cm}{y}$
Porosity	ϕ	$\frac{cm_w^3}{cm_b^3}$
Pore water irrigation constant (nonlocal)	$\alpha(i)$	y^{-1}
Tortuosity	θ	dimensionless
Density	ρ	$\frac{g}{cm_s^3}$
Generic solid concentration	C_s	$\frac{\mu mol}{gdw}$
Generic pore water concentration	C_w	μM
Rate constant	k	y^{-1}

Boundary conditions

At the sediment-water interface, two types of boundary conditions have been defined; a flux condition for OM and a concentration boundary for all other constituents. The model incorporates options for switching between concentration and flux boundaries depending on the data available. The flux (F_{cs}) boundary has the form EQ. 4.32:

$$-\phi_s D_b(0)\frac{\partial[C_s]}{\partial x}+\phi_s\omega(0)[C_s]=F_{C_s}, \tag{4.32}$$

while the other constituents are set to a known interface (C_{io}) concentrations (EQ. 4.33)

$$C(0)=C_{io}, \tag{4.33}$$

For all constituents the bottom boundary condition assumes that the diffusive flux has diminished to zero (no gradients) (EQ. 4.34).

$$\frac{\partial[C_i]}{\partial x}=0 \tag{4.34}$$

where *i* is a solid or pore-water constituent (Boudreau, 1996). An alternative option for this bottom condition is a concentration boundary similar to EQ. 4.33 when there is sufficient data available.

Root zone fluxes

Root zone fluxes were estimated from data assimilation for *Zostera marina* in Yaquina Bay (Eldridge and Kaldy, in prep.) and were assumed to only occur in the daytime (Table 4.7). Belowground seagrass uptake of dissolved inorganic nitrogen (DIN) was negligible, but release of O_2, dissolved organic carbon (DOC), and CO_2 are, through molecular diffusion, distributed in the root zone according to a Gaussian probability distribution (Berg, 1983) (EQ. 4.35):

$$P(j,\mu,\sigma) = \frac{1}{2\pi\sigma^2} e^{-\frac{(j-\mu)}{2\sigma^2}}; (1 \geq \text{x} \geq \text{np}) \tag{4.35}$$

where j is the index for each gridpoint, np is the number of gridpoints, μ is the gridpoint in the center of the root zone and 2σ dictates the number of gridpoints over which the flux occurs. In turn, the flux at each grid point is shown by EQ. 4.36:

$$F_i(x) = \frac{P(j,\mu,\sigma)F_T}{\Delta x}\ , \tag{4.36}$$

where F_T is the total flux, i are the constituents transported via the root system, and Δx is the length between each gridpoint. The model allows the user to input any root zone depth or width that is consistent with the total depth of the analysis.

Table 4.7 Root zone fluxes used to parameterize the model

Parameter	Flux (mmol m^{-2} d^{-1})
O_2	178
NH_4^+	2.4
NO_3^-	.5
DOC	20
CO_2	30
POC	2.0

Sensitivity analysis

Parameterization of the model first began by selecting values either detected experimentally and through field observations or obtained from a range of values from the literature. The optimum constant values were chosen by successively running the model and comparing results of the model to the raw data. The model parameters were performed ±50% of the value and changes were measured as normalized root-mean-squared difference (N-RMSD) for each geochemical parameter in the model and in the raw data. The sensitivity index was calculated by measuring the change in N-RMSD relative to the change in the parameter. For a N-RMSD value of 1, there is a 1:1 correspondence in the change in the model performance and the change in each parameter (Eldridge and Sieracki, 1993).

Model Results and Discussion

The objectives of this research were to utilize a sediment-seagrass diagenetic model as a tool for examining important biogeochemical processes in sediments. This model provides the framework for understanding dynamic processes through calibration with raw data from the field and attempts to clarify the realization that submerged macrophytes can affect sediment geochemistry and that sediment geochemistry can affect submerged macrophytes, as we have seen in Chapter II. This section begins with model calibrations with raw data from Chapter II. Recall that sedimentary geochemical data were obtained for seagrass cores taken during the day (light conditions) and at night (dark conditions). A separate set of seagrass cores used for laboratory incubations were obtained at the same site for the determination of dissolved iron and sulfide concentrations using microelectrodes. Model calibrations for these profiles were performed with the data during light conditions (10:00 am) and under dark conditions (6:00 am). The incubation experiments were replicated and are henceforth noted as SG1 and SG2 (see Chapter II for details of experimental procedures). Model calibrations were run for both sediment geochemistry under light conditions and under dark conditions.

Although high levels of organic matter degradation occur in the near-surface sediments as observed by sulfate reduction rates (SRR), the model was unable to produce enough metabolism to satisfy dissolved inorganic carbon (DIC) profiles from organic matter oxidation alone, similar to the output of the model calibrated for *Thalassia testudinum* in Eldridge and Morse (2000), indicating that carbonate mineral

dissolution may contribute DIC to pore waters during early diagenesis (Fig. 4.2). The model overestimated Fe^{2+} compared to the raw data, where Fe^{2+} was below detection at all depths but 2 mm (Fig. 4.3). Because of the large heterogeneity that is known to exist in this system and the relatively good fits to the rest of the data, the model depicts processes occurring in the system well except for the Fe^{2+}.

In comparison to seagrass areas under light conditions, a distinguishing characteristic of seagrass sediments under dark conditions was their higher Fe^{2+} and ΣH_2S concentrations in the pore water of seagrass root zones of which the model was able to capture. The model correlated with the lower boundary condition for refractory OC (Fig. 4.4), and model fits to DIC, NH_4^+, and DOC raw data agreed. Fe^{2+} and ΣH_2S under dark conditions occurred simultaneously in high concentrations near the sediment surface (Fig. 4.5). It was difficult for the steady-state diagenetic model to account for this overlap between iron oxide reduction and sulfate reduction because this phenomenon is not observed in classical sedimentary diagenesis, which the model is built upon. Reasons for possible concomitant Fe^{2+} and ΣH_2S may be due to non steady-state processes, where temporary changes in redox and pH (<6.5 observed) may perhaps promote FeS dissolution of metastable iron sulfide minerals (Schippers and Jørgensen, 2002) and the formation of dissolved FeS clusters. Also, microzones and shifting of zonation in the redox ladder might be a more appropriate explanation (supported by the large spatial variability). Another possible explanation for the observed Fe^{2+} with depth could be due to the enhanced bioirrigation that is well documented for this system, where pumping of pore water by biological activity may act as a transport mechanism. This would require

sufficient biological and/or chemical oxygen demand to effectively remove O_2 from overlying waters to prevent oxidation of transported Fe^{2+}. A third explanation may be that the voltage applied to the microelectrode stripped off Fe^{2+} that was adsorbed onto organic substances giving the false interpretation that it is dissolved. What is clearly demonstrated is that these geochemical components are spatially and temporally heterogeneous which confounds interpretation of diagenetic processes.

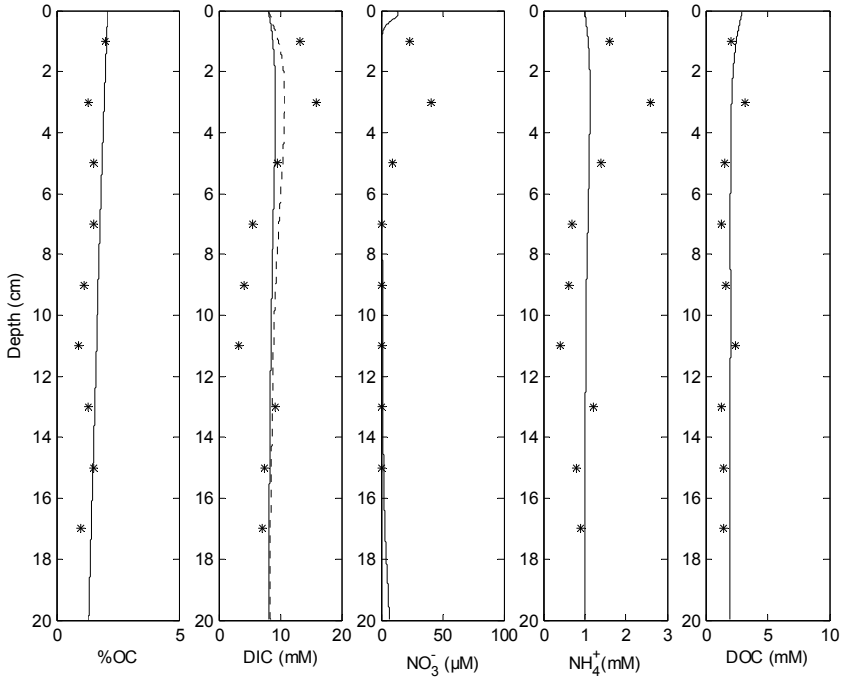

Fig. 4.2 Sediment geochemical profiles (*) with modeled data (solid line) from a seagrass core taken during light. Dashed line represents contribution to DIC from carbonate dissolution

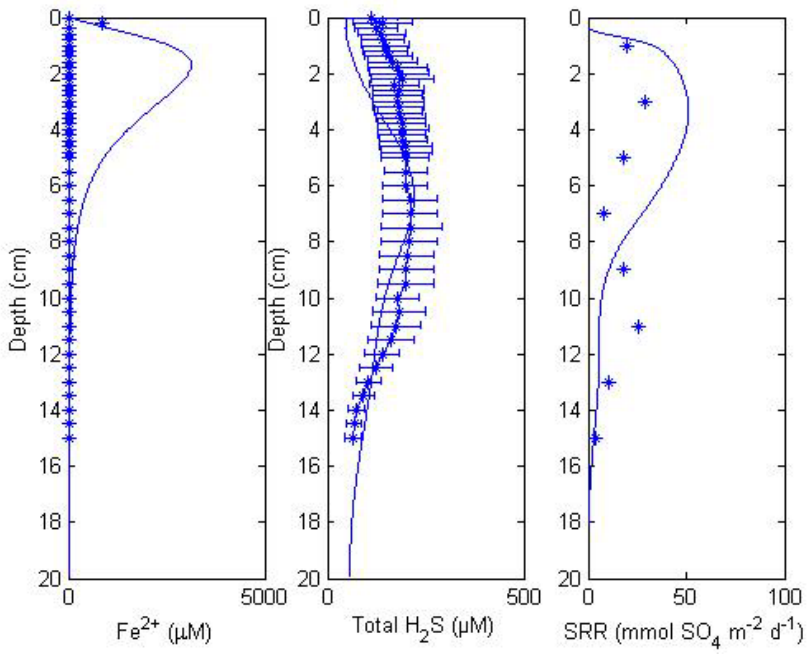

Fig. 4.3 Fe^{2+} and ΣH_2S (*) from seagrass under light conditions with modeled data (solid lines)

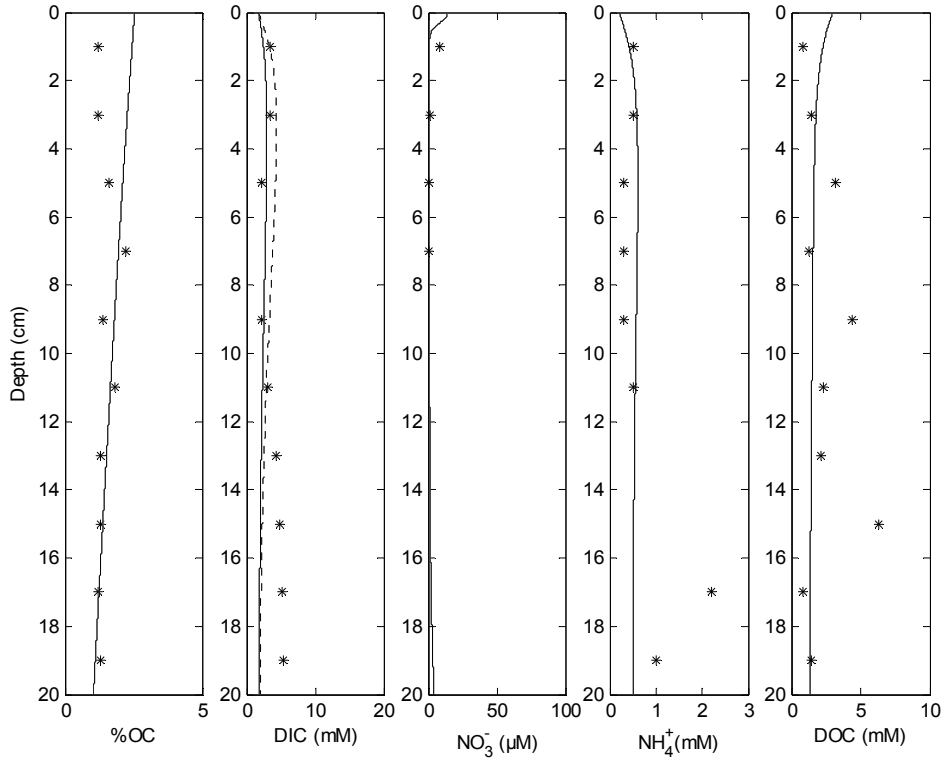

Fig. 4.4 Sediment geochemical profiles (*) with modeled data (solid line) from seagrass under dark conditions. Dashed line represents contribution to DIC from carbonate dissolution

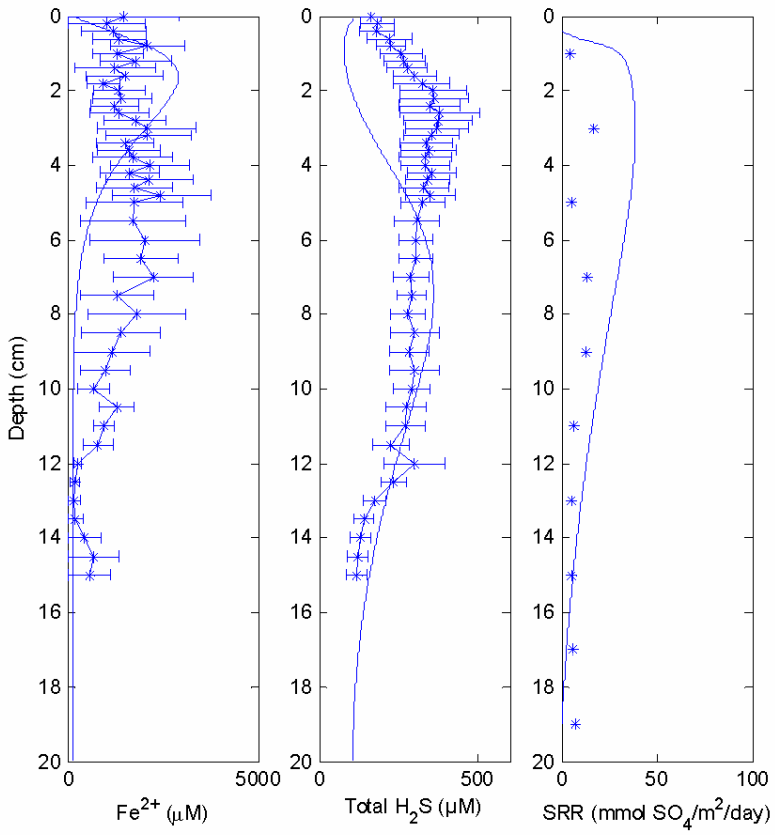

Fig. 4.5 $Fe^{2+}$and ΣH_2S (*) from seagrass under dark conditions with modeled data (solid lines)

Because of the large heterogeneity observed in Chapter II and III between the magnitude of pore water ΣH_2S concentrations of SG1 and SG2, separate model calibrations were performed for light and dark conditions. As mentioned in Chapter II, there was no iron detected in any of the microprofiles of SG2 and ΣH_2S concentrations were an order of magnitude smaller than in SG1. Calibrations for both light and dark revealed good fits for ΣH_2S, however the model output included a zone of iron oxide reduction as observed in idealized sedimentary diagenesis, similar to Fig. 4.3 (Fig. 4.6 and

Fig. 4.7). I feel that these observed raw data profiles are more typical of what has been observed for this system (Claire Reimers, pers. comm.).

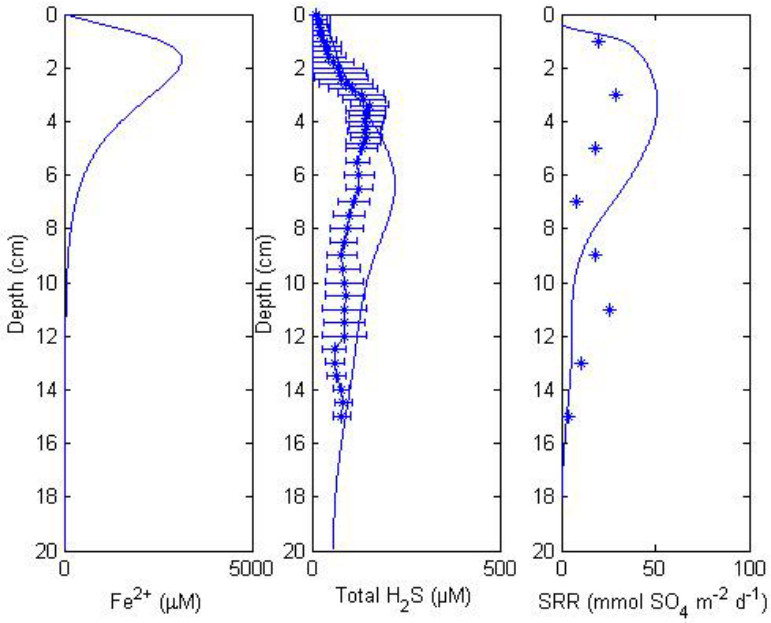

Fig. 4.6 Model simulations with raw data for SG2 light (10:00 am) microprofiles

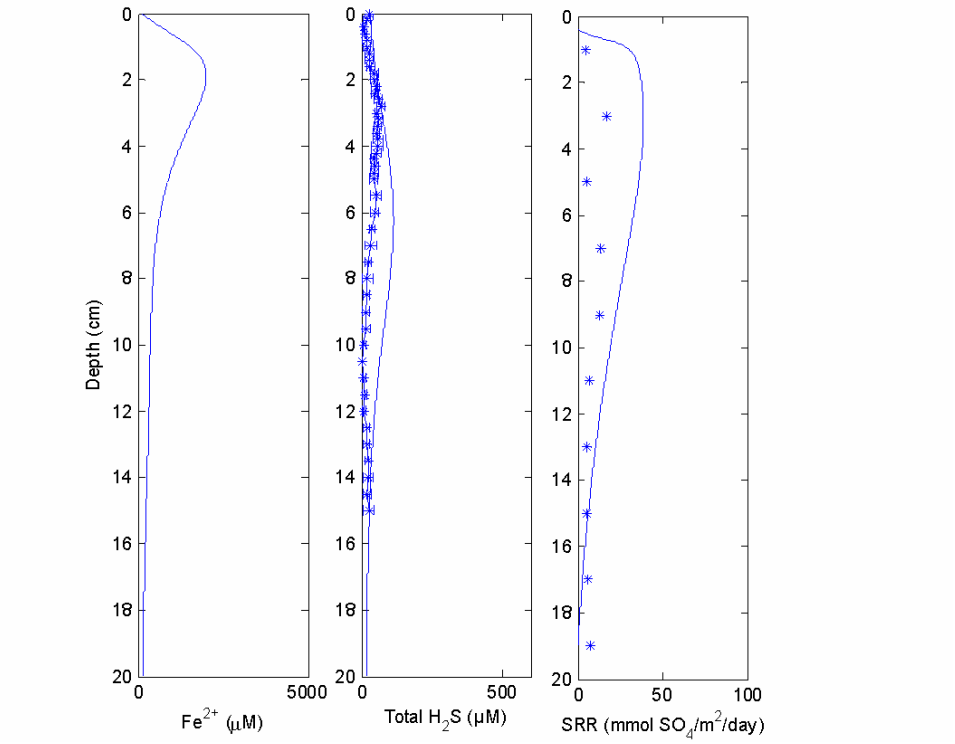

Fig. 4.7 Model simulations with raw data for SG2 dark (6:00 am) microprofiles

A number of free parameters were adjusted to calibrate the model to meet the constraints of the measured geochemical profiles for light and dark seagrass sediments. These included advection, irrigation, and organic matter flux, the last of which has been determined and is known to be quite variable. Several hundred model runs were made in which each model parameter was varied by 50% in the positive and negative direction and a N-RMSD between the model and data were calculated (see methods) (Tables 4.8 and 4.9). I tested the effect of a parameter change on 5 different model outputs including: [TOC], [DIC], [NH_4^+], [DOC], and [H_2S].

Model simulations and sensitivity analyses indicated for both light and dark conditions that ΣH_2S and total organic carbon (TOC) are most sensitive to physical processes (i.e. temperature, advection, biodiffusion, irrigation, and porosity) which may be essential in maintaining non-toxic levels of sulfide by transport of overlying oxic waters and consequently promote healthy conditions for seagrass growth (Table 4.8 and Table 4.9). Changes in labile organic carbon flux demonstrated sensitivity to ΣH_2S for both light and dark sediments, while refractory organic carbon fluxes had effects on TOC. Changes in Fe^{3+} exhibited sensitivity to Fe^{2+} and ΣH_2S for both light and dark conditions where they may decrease through precipitation of iron sulfide minerals or through oxidation of ΣH_2S. In addition, decrease in mean root depth affected ΣH_2S during light conditions, but not in dark conditions (recall that root zone fluxes were shut of at night in the model). This indicates that photosynthetic processes of seagrass during the day may affect ΣH_2S either through input of labile DOC stimulating sulfate reduction or by the introduction of oxygen which oxidizes it.

Table 4.8 Parameter sensitivity analysis for seagrass geochemical data under light conditions

				N-RMSD									
				TOC		DIC		NH4+		DOC		H_2S	
Parameter (p)	Std. case	Max	Min	Max	Min	Max	Min	Max	Min	Max	Min	Max	Min
T	15.0	22.5	7.5	6.73	-0.35	0.06	0.01	0.07	0.04	0.00	0.00	1.25	0.62
S	34.2	51.3	17.1	-0.01	-0.01	0.00	0.00	0.00	0.00	0.00	0.00	0.03	0.04
P	1.0	1.50	0.5	0.00	0.00	0.00	0.00	0.00	0.00	0.00	0.00	0.00	0.00
D_b	125.0	187.5	62.5	-0.45	-7.30	0.02	0.07	-0.02	-0.03	0.00	0.00	0.98	-4.84
$DD_b\downarrow$	20.0	30.0	10	0.00	-29.02	0.00	-0.06	0.00	-0.10	0.00	0.01	0.00	-5.62
$DD_b\rightarrow 0$	20.0	30.0	10	0.00	-0.88	0.00	0.01	0.00	0.06	0.00	0.03	0.00	-1.54
OC_l rate constants	40.0	60.0	20	-0.32	-0.65	-0.03	-0.04	0.01	0.03	0.00	0.00	-0.17	-0.48
OC_r rate constants	0.150	0.230	0.075	-0.83	-3.92	0.00	0.00	0.00	0.00	0.00	0.00	0.06	0.06
DOC rate constants	20.0	30.0	10	0.29	0.30	0.00	0.00	0.00	0.00	-0.01	-0.01	0.06	0.05
K_{FeS}	0.006	0.010	0.00315	-0.01	-0.02	0.00	0.00	0.00	0.00	0.00	0.00	0.01	-0.65
k8	8000	12000	4000	0.01	0.01	0.00	0.00	0.00	0.00	0.00	0.00	-0.04	-0.05
k11	3.0	4.5	1.5	0.01	0.00	0.00	0.00	0.00	0.00	0.00	0.00	0.00	0.00
k12	26000	39000	13000	0.00	0.00	0.00	0.00	0.00	0.00	0.00	0.00	0.00	0.00
k14	8.0	12.0	4.0	-0.02	-0.02	0.00	0.00	0.00	0.00	0.00	0.00	0.10	0.11
k15	3.0	4.5	1.5	0.14	0.22	0.00	0.00	0.00	0.00	0.00	0.00	0.02	0.03
k23	2.0	3.0	1.0	0.01	0.02	0.00	0.00	0.00	0.00	0.00	0.00	0.32	-0.14
k_23	0.0001	0.00015	0.00005	0.00	0.00	0.00	0.00	0.00	0.00	0.00	0.00	0.00	0.00

Table 4.8 Continued

				N-RMSD									
				TOC		DIC		NH4+		DOC		H_2S	
Parameter (p)	Std. case	Max	Min	Max	Min	Max	Min	Max	Min	Max	Min	Max	Min
C:Ps atom (OC_l)	81.37	122.06	40.69	-0.05	-0.11	0.00	0.00	-0.03	-0.10	0.00	0.00	0.00	-0.03
N:Ps atom (OC_l)	8.76	13.14	4.38	0.06	0.08	0.00	0.00	0.05	0.05	0.00	0.00	0.01	0.00
P:Ps atom (OC_l)	1.0	1.5	0.5	0.00	0.00	0.00	0.00	0.00	0.00	0.00	0.00	0.00	0.00
C:Ps atom (OC_r)	81.37	122.06	40.69	-0.11	-0.33	0.00	0.00	0.00	-0.01	0.00	0.00	-0.01	-0.03
N:Ps atom (OC_r)	8.76	13.14	4.38	0.17	0.16	0.00	0.00	0.00	0.00	0.00	0.00	0.01	0.01
P:Ps atom (OC_r)	1.0	1.5	0.5	0.00	0.00	0.00	0.00	0.00	0.00	0.00	0.00	0.00	0.00
C:Ps atom (DOC)	81.37	122.06	40.69	-0.03	-0.07	0.00	0.00	0.00	0.00	0.00	0.00	0.00	-0.01
N:Ps atom (DOC)	8.76	13.14	4.38	0.04	0.04	0.00	0.00	0.00	0.00	0.00	0.00	0.00	0.00
P:Ps atom (DOC)	1.0	1.5	0.5	0.00	0.00	0.00	0.00	0.00	0.00	0.00	0.00	0.00	0.00
kNO_3^-	0.10	0.15	0.05	0.09	0.15	0.00	0.00	0.00	0.00	0.00	0.00	0.03	0.04
$kSO4^{2-}$	8.50	12.75	4.25	0.08	0.09	0.00	0.00	0.00	0.00	0.00	0.00	0.04	0.04
kFe^{3+}	100	150	50	0.02	0.06	0.00	0.01	0.00	0.00	0.00	0.00	-0.35	-0.49

Table 4.8 Continued

				N-RMSD									
				TOC		DIC		NH_4^+		DOC		H_2S	
Parameter (p)	Std. case	Max	Min	Max	Min	Max	Min	Max	Min	Max	Min	Max	Min
α(i)	400	600	200	-0.85	-2.61	0.02	-0.04	-0.05	-0.15	0.01	0.02	-0.19	-2.32
Irrigation depth	20	30	10	0.00	-0.68	0.00	-1.77	0.00	-0.99	0.00	0.20	0.00	-59.39
ω	0.40	0.60	0.20	2.55	-0.11	0.00	0.00	0.01	0.01	0.00	0.00	0.20	0.16
ϕ- surface	0.70	0.84	0.49	1.65	1.03	0.14	0.17	-0.04	-0.07	0.00	0.00	2.72	-2.26
ϕ- asymptotic	0.70	0.88	0.35	8.87	0.63	-0.08	-0.11	-0.03	-0.09	-0.01	0.00	-0.89	-2.73
ϕ- coefficient	0.150	0.230	0.075	0.00	0.00	0.00	0.00	0.00	0.00	0.00	0.00	0.00	0.00
O_2	160	240	80	-0.80	-2.83	0.02	0.02	-0.03	-0.04	0.00	0.00	0.22	-1.51
NO_3^-	12.0	18.0	6.0	-0.10	-0.08	0.00	0.00	0.00	0.00	0.00	0.00	-0.05	-0.07
NH_4^+	1000	1500	500	0.00	0.00	0.00	0.00	0.09	0.08	0.00	0.00	0.00	0.00
SO_4^{2-}	28000	42000	14000	-0.06	-0.16	0.00	0.00	0.00	0.00	0.00	0.00	-0.03	-0.09
$\sum H_2S$	112	168	56	0.00	-0.01	0.00	0.00	0.00	0.00	0.00	0.00	0.77	-0.10
Fe^{3+}	45.0	67.5	22.5	0.01	0.07	-0.01	0.00	0.00	0.00	0.00	0.00	0.94	-2.17
FeS	120	180	60	0.33	0.31	0.00	0.00	0.00	0.00	0.00	0.00	0.04	0.03
DOC	3000	4500	1500	0.00	0.00	0.00	0.00	0.00	0.00	0.22	-0.05	0.00	0.00
DIC	8000	12000	4000	0.00	0.00	1.05	-0.82	0.00	0.00	0.00	0.00	0.00	0.00
benthic boundary DOC	2000	3000	1000	0.29	0.30	0.00	0.00	0.00	0.00	2.19	-0.76	0.06	0.05
benthic boundary NH_4^+	1000	1500	500	0.00	0.00	0.00	0.00	0.87	0.85	0.00	0.00	0.00	0.00
benthic boundary NO_3^-	12.0	18.0	6.0	0.00	0.00	0.00	0.00	0.00	0.00	0.00	0.00	0.00	0.00
OC_l (mmol m^{-2} d^{-1})	50	75	25	0.24	0.45	-0.04	-0.06	0.08	0.07	0.00	0.00	4.24	-1.92
OC_r (mmol m^{-2} d^{-1})	80	120	40	5.84	-1.00	0.00	0.00	0.01	0.01	0.00	0.00	0.45	0.15
mean root depth (cm)	10	15	5	-0.26	-0.07	0.01	-0.02	0.01	0.00	0.00	0.00	0.34	-0.75
root zone width (cm)	5.0	7.5	2.5	0.01	0.03	0.00	-0.01	0.00	0.00	0.00	0.00	-0.01	-0.10

Table 4.9 Sensitivity analysis for seagrass geochemical data under dark conditions

				N-RMSD											
				TOC		DIC		NH_4^+		DOC		Fe^{2+}		H_2S	
Parameter (p)	value	Max	Min	Max	Min	Max	Min	Max	Min	Max	Min	Max	Min	Max	Min
T	15.0	22.5	7.5	0.50	0.29	-0.11	-0.07	0.08	0.07	-0.14	-0.11	0.04	-0.01	0.56	0.24
S	34.2	51.3	17.1	0.00	0.00	0.00	0.00	0.00	0.00	0.00	0.00	0.01	0.01	0.02	0.04
P	1.0	1.5	0.5	0.00	0.00	0.00	0.00	0.00	0.00	0.00	0.00	0.00	0.00	0.00	0.00
D_b	100	150	50	-0.41	-3.76	0.03	0.01	-0.08	-0.12	0.06	0.11	-0.36	-0.32	0.76	-0.76
$DD_b \downarrow$	20	30	10	0.00	-15.8	0.00	0.42	0.00	-0.30	0.00	0.27	0.00	-0.31	0.00	-2.78
$DD_b \rightarrow 0$	20	30	10	0.00	-3.61	0.00	-0.08	0.00	0.10	0.00	-0.12	0.00	0.10	0.00	-0.48
kOC_l	22	33	11	-0.10	-0.23	0.01	-0.02	0.03	0.07	0.00	0.01	0.22	0.32	-0.22	-0.48
kOC_r	0.250	0.380	0.125	-0.20	-0.40	-0.02	-0.02	0.03	0.03	0.02	0.02	0.06	0.07	-0.02	-0.10
kDOC	20	30	10	0.01	0.01	0.00	0.00	0.00	0.00	0.00	0.00	0.00	0.00	-0.01	-0.01
D_b - dissltn	0.050	0.08	0.025	-0.01	-0.10	0.00	0.00	0.00	0.00	0.00	-0.01	0.00	0.00	0.00	0.00
kdissltn.	0.02	0.03	0.01	-0.27	-1.31	0.01	0.03	-0.01	-0.02	-0.05	-0.07	-0.02	-0.04	0.02	-0.01
K_{FeS}	0.006	0.01	0.003	-0.01	-0.02	0.00	0.00	0.00	0.00	0.00	0.00	0.00	-0.01	-0.22	-0.45
k8	8000	12000	4000	0.01	0.01	0.00	0.00	0.00	0.00	0.00	0.00	0.01	0.01	-0.03	-0.03
k11	3.0	4.5	1.5	0.00	0.00	0.00	0.00	0.00	0.00	0.00	0.00	0.00	0.00	0.00	0.00
k12	26000	39000	1300	0.00	0.00	0.00	0.00	0.00	0.00	0.00	0.00	0.00	0.00	0.00	0.00
k14	8	12	4	-0.01	-0.01	0.00	0.00	0.00	0.00	0.00	0.00	0.02	0.02	0.08	0.10
k15	3.0	4.5	1.5	0.02	0.03	0.00	0.00	0.00	0.00	0.00	0.00	0.00	0.01	0.00	0.00
k23	2	3	1	0.01	0.01	0.00	0.00	0.00	0.00	0.00	0.00	0.00	-0.01	0.26	0.35
k_23	$1x10^{-4}$	$1x10^{-5}$	$5x10^{-6}$	0.00	0.00	0.00	0.00	0.00	0.00	0.00	0.00	0.00	0.00	0.00	0.00
C:Ps (OC_l)	81.37	122.06	40.69	0.00	-0.01	0.00	0.00	-0.07	-0.23	0.00	0.00	0.00	-0.02	0.00	0.02
N:Ps (OC_l)	8.76	13.14	4.38	0.00	0.01	0.00	0.00	0.11	0.11	0.00	0.00	0.01	0.01	-0.01	-0.01
P:Ps (OC_l)	1.0	1.5	0.5	0.00	0.00	0.00	0.00	0.00	0.00	0.00	0.00	0.00	0.00	0.00	0.00
C:Ps (OC_r)	81.37	122.06	40.69	-0.01	-0.02	0.00	0.00	-0.01	-0.04	0.00	0.00	0.00	0.00	0.00	0.00
N:Ps (OC_r)	8.76	13.14	4.38	0.01	0.01	0.00	0.00	0.02	0.02	0.00	0.00	0.00	0.00	0.00	0.00
P:Ps (OC_r)	1.0	1.5	0.5	0.00	0.00	0.00	0.00	0.00	0.00	0.00	0.00	0.00	0.00	0.00	0.00
C:Ps (DOC)	81.37	122.06	40.69	0.00	0.00	0.00	0.00	0.00	-0.01	0.00	0.00	0.00	0.00	0.00	0.00
N:Ps (DOC)	8.76	13.14	4.38	0.00	0.00	0.00	0.00	0.00	0.00	0.00	0.00	0.00	0.00	0.00	0.00
P:Ps (DOC)	1.0	1.5	0.5	0.00	0.00	0.00	0.00	0.00	0.00	0.00	0.00	0.00	0.00	0.00	0.00

Table 4.9 Continued

				N-RMSD											
				TOC		DIC		NH_4^+		DOC		Fe^{2+}		H_2S	
Parameter (p)	value	Max	Min	Max	Min	Max	Min	Max	Min	Max	Min	Max	Min	Min	Min
kNO_3^-	0.10	0.15	0.05	0.01	0.01	0.00	0.00	0.00	0.00	0.00	0.00	-0.01	-0.02	0.00	0.00
$kSO4^{2-}$	8.50	12.75	4.25	0.02	0.03	0.00	0.00	-0.01	-0.01	0.00	0.00	0.03	0.03	0.05	0.05
kFe^{3+}	100	150	50	0.00	0.01	0.00	0.00	0.00	0.00	0.00	0.00	-0.19	-0.44	-0.14	-0.16
α(i)	400	600	200	-0.10	0.06	0.08	0.11	-0.10	-0.33	0.07	0.14	-0.18	-0.94	0.22	-1.35
Irrig. depth	20	30	10	0.00	-0.02	0.00	-5.81	0.00	-4.14	0.00	-0.02	0.00	0.02	0.00	-47.51
ω	0.50	0.63	0.25	0.65	0.09	-0.02	-0.03	0.01	0.02	-0.05	-0.07	0.01	0.02	0.02	-0.02
ϕ- surface	0.70	0.84	0.49	1.50	0.82	0.01	-0.01	-0.11	-0.18	-0.03	-0.03	-0.22	-4.13	-1.02	-1.21
ϕ- asymptotic	0.70	0.88	0.35	9.68	-0.34	0.09	0.20	-0.05	-0.18	-0.30	-0.12	0.47	0.14	-1.10	-1.23
ϕ- coefficient	0.150	0.230	0.075	0.00	0.00	0.00	0.00	0.00	0.00	0.00	0.00	0.00	0.00	0.00	0.00
O_2	135.0	202.5	67.5	-0.11	-0.01	0.00	0.01	-0.06	-0.08	0.01	0.00	-0.18	-0.22	0.31	-0.08
NO_3^-	12.0	18.0	6.0	0.00	0.01	0.00	0.00	-0.01	-0.01	0.00	0.00	-0.03	-0.03	0.03	0.02
NH_4^+	200	300	100	0.00	0.00	0.00	0.00	0.03	0.03	0.00	0.00	0.00	0.00	0.00	0.00
SO_4^{2-}	28000	42000	14000	-0.02	-0.05	0.00	0.00	0.01	0.01	0.00	0.00	-0.02	-0.05	-0.03	-0.09
$\sum H_2S$	112	168	56	0.00	0.00	0.00	0.00	0.00	0.00	0.00	0.00	0.00	0.01	-0.05	-0.21
Fe^{3+}	45.0	67.5	22.5	0.00	0.01	0.00	-0.01	-0.01	-0.01	0.00	0.00	0.66	-0.03	0.58	0.67
Fe^{2+}	120	18	60	0.02	0.03	0.00	0.00	0.00	0.00	0.00	0.00	-0.02	-0.02	0.01	-0.01
FeS	160	240	80	0.02	0.03	0.00	0.00	0.00	0.00	0.00	0.00	0.00	0.00	0.00	0.00
DOC	3000	4500	1500	0.00	0.00	0.00	0.00	0.00	0.00	0.06	0.04	0.00	0.00	0.00	0.00
DIC	1700	2550	850	0.00	0.00	-0.46	-0.64	0.00	0.00	0.00	0.00	0.00	0.00	0.00	0.00
DOC_{BB}^*	1000	1500	500	0.01	0.01	0.00	0.00	0.00	0.00	-0.18	-0.27	0.00	0.00	0.00	0.00
$NH_4^+{}_{BB}^*$	500	750	250	0.00	0.00	0.00	0.00	0.84	0.83	0.00	0.00	0.00	0.00	0.00	0.00
$NO_3^-{}_{BB}^*$	12.0	18.0	6.0	0.00	0.00	0.00	0.00	0.00	0.00	0.00	0.00	0.00	0.00	0.00	0.00
OC_l (flux)	50	75	25	0.09	0.11	-0.02	-0.10	0.18	0.16	0.00	0.00	0.50	0.42	0.69	-1.12
OC_r (flux)	135.0	202.5	67.5	2.64	-0.36	-0.03	-0.03	0.04	0.04	-0.09	-0.11	0.07	0.08	0.01	-0.12
root depth	10.0	15.0	5.0	0.00	0.00	0.00	0.00	0.00	0.00	0.00	0.00	0.00	0.00	0.00	0.00
root width	5.0	7.5	2.5	0.00	0.00	0.00	0.00	0.00	0.00	0.00	0.00	0.00	0.00	0.00	0.00

The advantage of comparing raw data to model results is that the model provides a framework for synthesizing biogeochemical processes of seagrass with diagenetic reactions. Eldridge and Kaldy (in prep.) provided the root zone fluxes for *Z. marina* which were used in the model.

Biological processes other than those related to seagrass can have profound effects on the geochemistry of sediments. The most obvious of these effects is that bacteria mediate most geochemical processes of oxidation and reduction. Yet in this analysis, I also had to invoke a high rate of irrigation (ventilation of the sediments) by polychaete worms, shrimp, and molluscs. Wang and Van Cappellen (1996) and Boudreau (1997) have shown that irrigation and bioturbation can provide a significant portion of the oxidants for sedimentary geochemical processes. Irrigating and deposit feeding organisms are found in high concentrations within both bare areas and seagrass bed of Yaquina Bay and are known to be quite active. I used an $\alpha(x)$ of 400 yr^{-1} in Yaquina Bay which is slightly higher than for observed values in other coastal environments (see Boudreau, 1996, p. 142, for discussion). The sensitivity analysis suggests that a tighter coupling between submerged macrophytes and benthic infaunal organisms may exist due to the large changes in sedimentary sulfide with irrigation. Cohabitation of benthic infauna and seagrass may in fact be mutualistic, where organic carbon sources and habitat are provided for infauna and sediment ventilation is offered for seagrass to lower sedimentary sulfide concentrations. The benefit of seagrass as a source of nutrition and refuge to infaunal communities has been demonstrated in numerous studies (Webster et al., 1998; Mattila et al., 1999; Bostrom et al., 2002; etc.).

Fewer studies, however, have demonstrated the benefits that seagrasses derive from the presence and activity of infaunal organisms. Peterson and Heck (2001) found a positive relationship between infaunal nutrient cycling and seagrass productivity. Eldridge et al. (in press) suggest that seagrass derive additional benefits from irrigating infauna through the introduction of oxidants from the water column into the root zone. The additional complement of oxidants in the rhizosphere helps maintain low levels of sulfides and other reduced toxicants.

Summary

The model simulations indicate that physical parameters such as advection, irrigation, and biodiffusion had the largest effect on sulfide concentrations. Other geochemical parameters such as ammonium, DOC, and DIC did not exhibit any changes with increases and decreases in most of the model parameters. The sediment-seagrass diagenetic model presented for *Z. marina* provided the necessary framework for understanding biogeochemical cycling in these sediments. The large changes in sedimentary sulfides with changes in irrigation and biodiffusion indicates that infaunal processes may assist seagrass in sediment ventilation and lower the concentration of sedimentary sulfides. Because of the large spatial heterogeneities in these sediments, increased modeling efforts, both steady-state and dynamic, are necessary to fully describe the most important biogeochemical processes.

CHAPTER V

CONCLUSIONS

The results of this dissertation contribute to our knowledge of biogeochemical processes in seagrass sediments in several ways. Sedimentary geochemical changes in the solids (TRS) for seagrass sediments implies that dissolution of sulfide minerals is possible with changes in redox from photosynthetic and/or physical processes (infaunal activity) that occur on diurnal time scales. The dissolution of sulfide minerals may introduce toxic sulfides back into dissolved phases thus exacerbating the degree of anaerobiosis. The increase in sulfides will decrease the photosynthetic maximum for *Z. marina* which will ultimately affect the amount of oxygen that is translocated to the sediments (Goodman et al., 1995; Holmer and Bondgaard, 2001). More sulfides will accumulate until seagrass mortality results. The daytime reduction in pyrite-Fe in seagrass sediments agreed well with the increase in the dissolved sulfide phase also observed during light cycles. Not only does the dissolution of sulfide minerals enhance sediment anoxia, but trace metals that are adsorbed or co-precipitated with such sulfide minerals may be released into pore waters enabling bioavailability. Scant trace metal data on spatial and temporal scales exists with respect to seagrass processes, where much of the literature revolves around water column contamination and leaf uptake. However, in light of these results, spatial and diurnal changes of toxic trace metals in sediments that were once believed to be buried in solid form needs consideration. The utility in understanding such processes may lead to sedimentary biomarkers or bioindicators of

seagrass and consequently ecosystem health. The CBI suggested in Chapter II is a first approach at ascribing a numerical indicator for seagrass ecosystem health. This has important applications to ecosystem managers where previously only light attenuation and water column nutrient stressors were under consideration. Because increased organic matter load to the sediments that can occur in eutrophic systems may result in increased sediment anoxia and cause more reducing conditions to persist, a sediment stressor application should also be evaluated. An improved CBI may be formulated when relative oxygen translocation rates are better quantified, the relationship between aboveground biomass and translocation rates are understood, and seagrass species-specific sulfide toxicity tolerances are determined. The development of a CBI will address belowground seagrass processes that are equally important compared to aboveground/water column processes when determining seagrass health.

Another benefit of this research was the application of the autocovariance function to sediments for determining the appropriate length of scale for dissolved sedimentary geochemical parameters (e.g., ΣH_2S and Fe^{2+}). The large degree of heterogeneity for these sediments were accounted for on smaller scales. The advantage of microelectrodes in this study made possible the observation of sedimentary geochemical changes at high sampling resolution (<2 mm). This higher sampling resolution is necessary to account for as much of the variability as possible, at which point scales analysis can be performed. However, extrapolation of microprofiles to larger sampling intervals, such as those for determining other geochemical parameters, made interpretation of temporal variability from spatial variability difficult.

The scales analysis yielded results similar to those from the same site three years prior and that the dominant source of depth variability could be captured at 1.0-1.5 cm sampling intervals. This has benefits with regard to future sampling efforts, where costly analyses and limitation of instrumentation makes higher sampling resolution difficult. Lateral scale lengths were smaller than vertical scale lengths indicating that sediment complexity was intensified in horizontal dimensions compared to vertical dimensions. This was supported by the observed heterogeniety from seagrass roots and rhizomes that can quickly change redox conditions and that infaunal organisms creating burrows may also affect redox through bioirrigation and bioturbation. A cylinder of influence that radiates from burrows and/or seagrass roots may have enhanced effects on scale processes in horizontal directions.

Finally, this research was able to sample and measure a wider range of sedimentary geochemical parameters simultaneously, where many other studies have fallen short. The combination of many analytes concurrently obtained allowed for the determination of geochemical interactions. Most diagenetic models require large input variables for accurately fitting data. By sampling a larger range of geochemical parameters I am able to determine which analytes are most important to sample in the future and determine which ones are most sensitive to changes in model parameters. The model presented in this dissertation predicted, by use of normalized root-mean squared differences, that ΣH_2S and TOC were most sensitive to changes in physical characteristics. This result suggests that benthic infaunal processes such as bioirrigation and bioturbation may play an important role in maintaining non-lethal levels of sulfides

to seagrass. Through the concept of sediment ventilation (infaunal pumping of overlying oxic waters to sediment depths) seagrass health and propagation may be tightly coupled with infaunal biomass as seen in other studies (Webster et al., 1998; Mattila et al., 1999; Bostrom et al., 2002; etc.).

Because of seagrass importance in food web ecology and as habitat source, understanding the relationship between sedimentary geochemical processes and seagrass processes is crucial in determining health and distribution. This multi-analyte approach to examining geochemical interactions on various time and space scales is highly recommended when investigating seagrass productivity and vitality.

REFERENCES

Agawin N. S. R. and Duarte C. M. (2002) Evidence of direct particle trapping by a tropical seagrass meadow. *Estuaries* **25**, 1205-1209.

Aller R. C. (1978) Experimental studies of changes produced by deposit feeders on pore water, sediment, and overlying water chemistry. *Amer. J. Sci.* **278**, 1185-1234.

Aller R.C. and Yingst J.Y. (1978) Biogeochemistry of tube-dwellings: A study of the sedimentary polychaete *Amphitrite ornata* (Leidy). *J. Mar. Res.* **36**, 201-254.

Aller R. C. (1980) Quantifying solute distributions in the bioturbated zone of marine sediments by defining an average microenvironment. *Geochim. et Cosmochim. Acta* **44**, 1955-1965.

Aller R.C., Hall O.J., Rude P.D. and Aller J.Y. (1998) Biogeochemical heterogeneity and suboxic diagenesis in hemipelagic sediments of the Panama Basin. *Deep-Sea Res.* I. **45**, 133-165.

Bagarinao T. (1992) Sulfide as an environmental factor and toxicant: Tolerance and adaptations in aquatic organisms. *Aquatic Toxicology* **24**, 21-62.

Berg H. C. (1984) *Random Walks in Biology*. Princeton University Press. Princeton, NJ, pp. 1-142.

Berner R. A. (1964) An idealized model of dissolved sulfate distribution in recent sediments. *Geochim. Cosmochim. Acta* **28**, 1497-1503.

Berner R. A. (1974) Kinetic models for the early diagenesis of nitrogen, sulfur, phosphorus and silicon in anoxic marine sediments. In *The Sea V* (ed. E.D. Goldberg), pp. 427-450. John Wiley & Sons, New York.

Berner R. A. (1980) *Early Diagenesis*. Princeton University Press, Princeton, NJ.

Berner R. A. (1981) Authigenic mineral formation resulting from organic matter decomposition in modern sediments. *Fortschr. Miner*. **59**, 117-135.

Berner R. A. (1982) Burial of organic carbon and pyrite sulfur in the modern ocean: Its geochemical and environmental significance. *American Journal of Science* **282**, 451-473.

Blaabjerg V. and Finster K. (1998) Sulphate reduction associated with roots and rhizomes of the marine macrophyte *Zostera marina*. *Aquatic Microbial Ecology* **15**, 311-314.

Blaabjerg V., Mouritsen K. N., and Finster K. (1998) Diel cycles of sulphate reduction rates in sediments of a *Zostera marina* bed (Denmark). *Aquatic Microbial Ecology* **15**, 97-102.

Boschker H. T. S., Wielemaker A., Schaub B. E. M., and Holmer M. (2000) Limited coupling of macrophyte production and bacterial carbon cycling in the sediments of *Zostera* spp. meadows. *Marine Ecology Progress Series* **203**, 181-189.

Bostrom C., Bonsdorff E., Kangas P., and Norkko A. (2002) Long-term changes of brackish-water eelgrass (*Zostera marina* L.) community indicate effects of coastal eutrophication. *Estuarine, Coastal and Shelf Science* **55**, 795-804.

Boudreau B. P. (1984) On the equivalence of nonlocal and radial-diffusion models for porewater irrigation models for porewater irrigation. *J. Mar. Res.***42,** 731-735.

Boudreau B. P. and Canfield D. E. (1988) A provisional diagenetic model for pH in anoxic porewaters: Application to the FOAM Site. *J. Mar. Res*.

Boudreau B. P. (1991) Modelling the sulfide-oxygen reaction and associated pH gradients in porewater. *Geochimica et Cosmochimica Acta* **55**, 145-159.

Boudreau B. P. (1996) A method-of-lines code for carbon and nutrient diagenesis in aquatic sediments. *Computers & Geosciences* **22,** 479-496.

Boudreau B.P. (1997) *Diagenetic Models and Implementation*. Spring-Verlag, New York.

Boudreau B.P. (2000) The mathematics of early diagenesis: From worms to waves. *Rev. Geophys*. **38**, 389-416.

Brendel P. J. (1995) Development of a mercury thin film voltammetric microelectrode for the determination of biogeochemically important redox species in porewaters of marine and freshwater sediments, Ph.D. Dissertation. Univ. Delaware.

Brendel P. J. and Luther G. W. III (1995) Development of a gold amalgam voltammetric microelectrode for the determination of dissolved Fe, Mn, O_2, and S(-II) in porewaters of marine and freshwater sediments. *Environ. Sci. Technol.* **29**, 751-761.

Bretherton F.P., Davis R.E. and Fandry C.B. (1976) A technique for objective analysis and design of oceanographic experiments applied to MODE-73. *Deep-Sea Research* **23**, 559-582.

Brinkhuis B. H., Penello W. F., and Churchill A. C. (1980) Cadmium and manganese flux in eelgrass Zostera marina II. Metal uptake by leaf and root-rhizome tissues. *Marine Biology* **58**, 187-196.

Brix H., Lyngby J. E., and Schierup H.-H. (1983) Eelgrass (*Zostera marina* L.) as an indicator organism of trace metals in the Limfjord, Denmark. *Marine Environmental Research* **8**, 165-181.

Bull D.C. and Taillefert M. (2001) Seasonal and topographic variations in porewaters of a southeastern USA salt marsh plants: Mechanism and rate of formation. *Limnol. Oceanogr.* **13**, 1-8.

Canfield D. E., Raiswell R., Westrich J. T., Reaves J. T., and Berner R. A. (1986) The use of chromium reduction in the analysis of reduced inorganic sulfur in sediments and shales. *Chem. Geol*. **54**, 149-155.

Carlson P. R., Jr., Yarbro L. A., and Barber T. R. (1994) Relationship of sediment sulfide to mortality of *Thalassia testudinum* in Florida Bay. *Bulletin of Marine Science* **54**(3), 733-746.

Connell E. L., Colmer T. D., and Walker D. I. (1999) Radial oxygen loss from intact roots of Halophila ovalis as a function of distance behind the root tip and shoot illumination**.** ***Aquatic Botany*** **63,** 219-228.

Cooper D.C. and Morse J.W. (1996) The chemistry of Offatts Bayou, Texas: A seasonally highly sulfidic basin. *Estuaries* **19**, 595-611.

Cornwell J. C. and Morse J. W. (1987) The characterization of iron sulfide minerals in anoxic marine sediments. *Marine Chemistry* **22**, 193-206.

Dayton P.K., Tenger M.J., Parnell P.E. and Edwards P.B. (1992) Temporal and spatial patterns of disturbance and recovery in a kelp forest. *Ecol. Monogr.* **62**, 421-445.

Denman K. L. and Freeland H. J. (1985) Correlation scales, objective mapping and a statistical test of geostrophy over the continental shelf. *J. Mar. Res.* **43**, 517-539.

Dennison W. C. (1987) Effects of light on seagrass photosynthesis, growth and depth distribution. *Aquatic Botany* **27**, 15-26.

Dhakar S. P. and Burgide D. J. (1996) A coupled, non-linear, steady state model for early diagenetic processes in pelagic sediments. *American J. of Science* **296**, 296-330.

DiMarco S. F., Nowlin W. D. Jr. and Reid R. O. (Unpublished manuscript) Horizontal spatial scales of hydrographic data and current velocity in the Northeast Gulf of Mexico.

Dickson, A.G. and Goyet, C. (Editors) (1994) *Handbook of Methods for the Analysis of the Various Parameters of the Carbon Dioxide System in Seawater*. Department of Energy.

Duarte C. M. and Chiscano C. L. (1999) Seagrass biomass and production: A reassessment. *Aquatic Botany* **65**, 159-174.

Eckman J. E. and Thistle D. (1988) Small-scale spatial pattern in meiobenthos in the San Diego Trough. *Deep-Sea Research* **35**(9), 1565-1578.

Eldridge P. M. and Sieracki M. E. (1993) Biological and hydrodynamic regulation of the microbial food web in a periodically mixed estuary. *Limnol. Oceanogr.* **38**, 1666-1679.

Eldridge P.M. and Morse J.W. (2000) A diagenetic model for sediment-seagrass interactions. *Mar. Chem.* **70**, 89-104.

Eldridge P. M. and Johnson M. G. (2004) *Seagrass-Sediment Interactions*, pp. 1-14. US Environmental Protection Agency.

Emery W. J., and Thomson R. E. (1997) *Data Analysis Methods in Physical Oceanography*. Pergamon, New York.

Erskine J. M. and Koch M. S. (2000) Sulfide effects on Thalassia testudinum carbon balance and adenylate energy charge. *Aquatic Botany* **67**, 275-285.

Faraday W. E. and Churchill A. C. (1979) Uptake of cadmium by the eelgrass *Zostera marina*. *Marine Biology* **53**, 293-298.

Fonseca M. S. (1996) Scale dependence in the study of seagrass systems. *Seagrass Biology: Proceedings of an International Workshop.* Rottnest Island, Western Australia. pp. 95-104.

Fourqurean J. W. and Cai Y. (2001) Arsenic and phosphorous in seagrass leaves from the Gulf of Mexico. *Aquatic Botany* **71**, 247-258.

Gandin L.S. (1965) *Objective Analysis of Meteorological Fields*. Translated from the Russian. Israel Program for Scientific Translations, Jerusalem.

Garber J. H., Collins J. L., Jr., and Davis M. W. (1992) Impact of estuarine benthic algal production on dissolved nutrients and water quality in the Yaquina River Estuary, Oregon, pp. 1-58. Oregon State University and Mark O. Hatfield Marine Science Center.

Goodman J. L., Moore K. A., and Dennison W. C. (1995) Photosynthetic responses of eelgrass (*Zostera marina* L.) to light and sediment sulfide in a shallow barrier island lagoon. *Aquatic Botany* **50**, 37-47.

Hammerstrom K., Sheridan P., and McMahan G. (1998) Potential for seagrass restoration in Galveston Bay, Texas. *Texas Journal of Science* **50**(1), 35-50.

Hannson I. (1973) A new set of pH-scales and standard buffers for seawater. *Deep-Sea Research* **20**, 479-491.

Hansen J. W., Udy J. W., Perry C. J., Dennison W. C., and Lomstein B. A. (2000) Effect of the seagrass *Zostera capricorni* on sediment microbial processes. *Marine Ecology Progress Series* **199**, 83-96.

Harper M.P., Davison W. and Tych W. (1999) One-dimensional views of three-dimensional sediments. *Environ. Sci. Technol.* **33**, 2611-2616.

Hebert A. B. and Morse J. W. (2003) Microscale effects of light on H_2S and Fe^{2+} in vegetated (*Zostera marina*) sediments. *Mar. Chem.* **81**, 1-9.

Hemminga M. A. (1998) The root/rhizome system of seagrasses: An asset and a burden. *Journal of Sea Research* **39**, 183-196.

Hemminga M. A. and Duarte C. M. (2000) *Seagrass Ecology*. Cambridge University Press.

Hewitt J. E., McBride G. B., Pridmore R. D., and Thrush S. F. (1993) Patchy distributions: Optimizing sampling size. *Environmental Monitoring and Assessment* **27**, 95-105.

Holmer M. and Nielsen S. L. (1997) Sediment sulfur dynamics related to biomass-density patterns in *Zostera marina* (eelgrass) beds. *Marine Ecology Progress Series* **146**, 163-171.

Holmer M. and Bondgaard E. J. (2001) Photosynthetic and growth response of eelgrass to low oxygen and high sulfide during hypoxic events. *Aquatic Botany* **70**, 29-38.

Holmer M., Andersen F. O., Nielsen S. L., and Boschker H. T. S. (2001) The importance of mineralization based on sulfate reduction for nutrient regeneration in tropical seagrass sediments. *Aquatic Botany* **71**, 1-17.

Holmer M. and Laursen L. (2002) Effect of shading of *Zostera marina* (eelgrass) on sulfur cycling in sediments with contrasting organic matter and sulfide pools. *Journal of Experimental Marine Biology and Ecology* **270**, 25-37.

Hsu H.P. (1984) *Applied Fourier Analysis*. Hartcourt, Brace, Jovanovich, San Diego, CA.

Huerta-Diaz M. and Morse J. W. (1992) Pyritization of trace metals in anoxic marine sediments. *Geochimica et Cosmochimica Acta* **56**, 2681-2702.

Joint I. R., Gee J. M., and Warwick R. M. (1982) Determination of fine-scale vertical distribution of microbes and meiofauna in an intertidal sediment. *Marine Biology* **72**, 157-164.

Jørgensen B. B. (1978) A comparison of methods for the quantification of bacterial sulfate reduction in coastal marine sediments: Measurement with radiotracer techniques. *Geomicrobiology Journal* **1**, 11-28.

Jumars P. A. (1976) Deep-Sea species diversity: Does it have a characteristic scale? *Journal of Marine Research* **34**(2), 217-246.

Koch E. W. (2001) Beyond light: Physical, geological, and geochemical parameters as possible submersed aquatic vegetation habitat requirements. *Estuaries* **266**, 1-17.

Koch M. S. and Erskine J. M. (2001) Sulfide as a phytotoxin to the tropical seagrass *Thalassia testudinum*: Interactions with light, salinity and temperature. *Journal of Experimental Marine Biology and Ecology* **266**, 81-95.

Koenig B., Holst G., Glud R.N. and Kuehl M. (2001) Imaging of oxygen distribution at benthic interfaces: A brief review. In *Organism-Sediment Interactions* (eds., J.Y. Aller, S.A Woodin and R.C. Aller) pp. 63-72. University of South Carolina Press, Columbia, SC.

Kristensen E. and Blackburn T. H. (1987) The fate of organic carbon and nitrogen in experimental marine sediments: Influences of bioturbation and anoxia. *J. Mar. Res* **45**, 23-257.

Kulm L. D. (1965) Sediments of Yaquina Bay, Oregon. Ph.D. Dissertation, Oregon State University.

Lavigne C., Juniper S.K. and Silberberg N. (1997) Spatio-temporal variability in benthic microbial activity and particle flux in the Laurentian Trough. *Deep-Sea Res.* I. **44**, 1793-1813.

Lee K.-S. and Dunton K. H. (2000) Diurnal changes in pore water sulfide concentrations in seagrass *Thalassia testudinum* beds: The effects of seagrasses on sulfide dynamics. *Journal of Experimental Marine Biology and Ecology* **25**, 201-214.

Li Y., Nowlin W. D. Jr. and Reid R. O. (1996) Spatial-scale analysis of hydrographic data over the Texas-Louisiana continental shelf. *J. Geophys. Res.* **101**, 20595-20605.

Lin S. and Morse J. W. (1991) Sulfate reduction and iron sulfide mineral formation in Gulf of Mexico anoxic sediments. *American Journal of Science* **291**, 55-89.

Lovely D.R. and Phillips E. J. P. (1989) Requirements for a microbial consortium to completely oxidise glucose in Re(III)-reducing sediments. *Appl. Environ. Microbiol*. **54**, 3234-3236.

Luther G.W. III., Brendel P. J., Lewis B. L., Sunby B., Lefrançois L., Silverberg N. and Nuzzio, D. (1998) Simultaneous measurement of O_2, Mn, Fe, I^-, and S(-II) in marine pore waters with a solid-state voltammetric microelectrode. *Limnol. Oceanogr.* **43**, 325-333.

Luther G. W., III, Glazer B. T., Hohmann L., Popp J. I., Taillefert M., Rozan T. R., Brendel P. J., Theberge S. M., and Nuzzio D. B. (2001) Sulfur speciation monitored *in situ* with solid state gold amalgam voltammetric microelectrodes: Polysulfides as a special case in sediments, microbial mats and hydrothermal vent waters. *Journal of Environmental Monitoring* **3**, 61-66.

Lyngby J. E. and Brix H. (1982) Seasonal and environmental variation in cadmium, copper, lead and zinc concentrations in eelgrass (Zostera marina L.) in the Limfjord, Denmark. *Aquatic Botany* **14**, 59-74.

Madureira M. J., Vale C., and Simoes Goncalves M. L. (1997) Effect of plants on sulphur geochemistry in the Tagus salt-marshes sediments. *Marine Chemistry* **58**, 27-37.

Mannio A. and Montagna P.A. (1997) Small-scale spatial variation of macrobenthic community structure. *Estuaries* **20**, 159-173.

Mattila J., Chaplin G., Eilers M. R., Heck K. L., O'Neal J. P., and Valentine J. F. (1999) Spatial and diurnal distribution of invertebrate and fish fauna of a *Zostera marina* bed and nearby unvegetated sediments in Damariscotta River, Maine (USA). *Journal of Sea Research* **41**, 321-332.

Moriarty D. J. W., Iverson R. L., and Pollard P. C. (1986) Exudation of organic carbon by the seagrass Halodule wrightii aschers. and its effect on bacterial growth in the sediment. *Journal of Experimental Marine Biology and Ecology* **96**(2), 115-126.

Morse J. W. and Emeis K. C. (1990) Controls on C/S ratios in hemipelagic upwelling sediments. *American Journal of Science* **290**, 1117-1135.

Morse J. W. and Mackenzie F. T. (1990) *Geochemistry of Sediment Carbonates*. Elsevier, Amsterdam pp.707.

Morse J. W. (1991) Oxidation kinetics of sedimentary pyrite in seawater. *Geochimica et Cosmochimica Acta* **55**, 3665-3667.

Morse J. W. (1994) Interactions of trace metals with authigenic sulfide minerals: Implications for their bioavailability. *Marine Chemistry* **46**, 1-6.

Morse J. W. and Berner R. A. (1995) What determines sedimentary C/S ratios? *Geochimica et Cosmochimica Acta* **59**(6), 1073-1077.

Perez M., Duarte C. M., Romero J., Sand-Jensen K., and Alcoverro T. (1994) Growth plasticity in Cymodocea nodosa stands: The importance of nutrient supply. *Aquatic Botany* **47**, 249-264.

Peterson B. J. and Heck K. L. (2001) Positive interactions between suspension-feeding bivalves and seagrass-a facultative mutualism. *Marine Ecology Progress Series* **213**, 143-155.

Postma D. and Jakobsen R. (1996) Redox zonation: Equilibrium constraints on the Fe(III)/SO_4^-reduction interface. *Geochimica et Cosmochimica Acta* **60**, 3169-3175.

Poulain P.-M. and P. P. Niiler (1989) Statistical analysis of the surface circulation of the California Current system using satellite-tracker drifters. *J. Phys. Oceanogr.* **19**, 1588-1603.

Pulich W. M., Jr. (1989) Effects of rhizosphere macronutrients and sulfide levels on the growth physiology of *Halodule wrightii* Aschers. and *Ruppia maritima* L. s.l. *Journal of Experimental Marine Biology and Ecology* **127**, 69-80.

Rabouille C. and Galiiard J. (1991) Towards the edge: Early diagenetic explanation. A model depicting the early diagenesis of organic matter, O_2, NO_3, Mn, and PO_4. *Geochimica et Cosmochimica* **55**, 2511-2525.

Raiswell R. and Berner R. A. (1985) Pyrite formation in euxinic and semi-euxinic sediments. *American Journal of Science* **285**, 710-724.

Raiswell R., Canfield D. E., and Berner R. A. (1994) A comparison of iron extraction methods for the determination of the degree of pyritization and the recognition of iron-limited pyrite formations. *Chem. Geol*. **111,** 101-110.

Reeburgh W. (1967) An improved interstitial water sampler. *Limnol. Oceanogr*. **12**, 163-165.

Ritter C. and Montagna P.A. (1999). Seasonal hypoxia and models of benthic response in a Texas bay. *Estuaries.* **22**, 7-20.

Sandulli R. and Pinckney J. L. (1999) Patch sizes and spatial patterns of meibenthic copepods and benthic microalgae in sandy sediments: A microscale approach. *Journal of Sea Research* **41**, 179-187.

Schippers A. and Jørgensen B. B. (2002) Biogeochemistry of pyrite and iron sulfide oxidation in marine sediments. *Geochimica et Cosmochimica Acta* **66**(1), 85-92.

Sciremammano F., Pillsbury R. D., Nowlin W. D. Jr. and Whitworth T. (1980) Spatial scales of temperature and flow in Drake Passage. *J. Geophys. Research* **85**, 4015-4028.

Short F. T. (1987) Effects of sediment nutrients on seagrasses: Literature review and mesocosm experiment. *Aquatic Botany* **27**, 41-57.

Shuttleworth S.M., Davison W. and Hamilton-Taylor J. (1999) Two-dimensional and fine structure in the concentrations of iron and manganese in sediment pore-waters. *Environ. Sci. Technol.* **33**, 4169-4175.

Smith R. D., Dennison W. C., and Alberte R. S. (1984) Role of seagrass photosynthesis in root aerobic processes. *Plant Physiology* **74**, 1055-1058.

Soetaert K., Herman P.M.J., and Middleberg J.J. (1997) A model of early diagenetic processes from the shelf to abyssal depths. *Geochimica et Cosmochimica Acta* **57**, 1473-1488.

Strickland J. D. H. and Parsons T. R. (1972) *A Practical Handbook of Seawater Analysis*. Fisheries Research Board of Canada.

Stumm W and Morgan J.J. (1981). *Aquatic Chemistry*. 2nd ED. Wiley-Interscience.p.1-780.

Terrados J., Duarte C. M., Kamp-Nielson L., Agawin N. S. R., Gacia E., Lacap D., Fortes M. D., Borum J., Lubanski M., and Greve T. (1999) Are seagrass growth and survival constrained by the reducing conditions of the sediment? *Aquatic Botany* **65**, 175-197.

Terrados J., Duarte, Carlos M. (2000) Experimental evidence of reduced particle resuspension within a seagrass (*Posidonia oceanica* L.) meadow. *Journal of Experimental Marine Biology and Ecology* **243**, 45-53.

Theberge S. M. and Luther G. W. III (1997) Determination of the electrochemical properties of a soluble aqueous FeS species present in sulfidic solutions. *Aquatic Geochemistry* **3**, 191-211.

Van Cappellen P. and Wang, Y. (1996) Cycling of iron and manganese in surface sediments: A general theory for the coupled transport and reaction of carbon, oxygen, nitrogen, sulfur, iron, and manganese. *Amer. Jour. Sci.* **296**, 197-242.

Wang Y. and Van Cappellen P. (1996) A multicomponent reactive transport model of early diagenesis: Application to redox cycling in coastal marine sediments. *Geochimica et Cosmochimica Acta* **60**(16), 2993-3014.

Ward T. J. (1987) Temporal variation of metals in the seagrass *Posidonia australis* and its potential as a sentinel accumulator near a lead smelter. *Marine Biology* **95**, 315-321.

Webster P. J., Rowden A. A., and Atrill M. J. (1998) Effect of shoot density on the infaunal macro-invertebrate community within a *Zostera marina* seagrass bed. *Estuarine, Coastal and Shelf Science* **47**, 351-357.

Whilatch R.B., Lohrer A.M. and Thrush S.F. (2001) Scale-dependent recovery of the benthos: Effects of larval and post-larval life stages. In *Organism-Sediment Interactions* (eds., J.Y. Aller, S.A Woodin and R.C. Aller) pp. 181-198. University of South Carolina Press, Columbia, SC.

Whitfield M. and Turner D. R. (1986) The carbon dioxide system in estuaries— and inorganic perspective. *Science of the Total Environment* **49**, 235-255.

Wu J. (1999) Hierarchy and scaling: Extrapolating information along a scaling ladder. *Can. J. Remote Sens*. **25**, 367-380.

Wu J. and Qi Y. (2000) Dealing with scale in landscape analysis: An overview. *Geogr. Info. Sci*. **6**, 1-7.

Wu J., Jelinski D.E., Luck Y. and Tueller P.T. (2000) Multiscale analysis of landscape heterogeneity: Scale variance and pattern metrics. *Geogr. Info. Sci.* **6**, 1-19.

Zajac R.N. (2001) Organism-sediment relations at multiple spatial scales: Implications for community structure and successional dynamics. In *Organism-Sediment Interactions* (eds., J.Y. Aller, S.A Woodin and R.C. Aller) pp. 119-140. University of South Carolina Press, Columbia, SC.

Ziegler S. and Benner R. (1999) Dissolved organic carbon cycling in a subtropical seagrass-dominated lagoon. *Marine Ecology Progress Series* **180**, 149-160.

Ziegler S. and Benner R. (2000) Effects of solar radiation on dissolved organic matter cycling in a subtropical seagrass meadow. *Limnol. Oceanogr.* **45**(2), 257-266.

Zimmerman R. C., Smith R.D., and Alberte R. S. (1987) Is Growth of eelgrass nitrogen limited? A numerical simulation of the effects of light and nitrogen on the growth dynamics of *Zostera marina*. *Mar. Ecol. Prog. Ser*. **41**, 167-176.

APPENDIX I

SCALE CODE

```
%Andrew B. Hebert
%Texas A&M University
%Department of Oceanography
%Scale Code for seagrass data
%2-21-04

clear;

%load data matrix file
load sg16dat.dat;

%save raw data into vectors
%Let all rows of column one = Depth
depth=sg16dat(:,1);
%Let all rows of column 2 = sulfide concentrations
h2s=sg16dat(:,2);

%plot raw data
figure(1)
subplot(1,3,1);
plot(h2s,depth, 'k-');
axis ij;%reverses y-axis so depth is decreasing
xlabel('H_2S (\muM)');
ylabel('Depth (mm)');
title('H_2S in seagrass sediments')
hold on;
meanraw=mean(h2s);

%interpolate over regular depth grid
newz=(depth(46)-depth(1))./511
xi=depth(1)-([0:1:511]./511).*(depth(1)-depth(46));
interpdata=interp1(depth,h2s,xi);
plot(interpdata,xi,'k-');
axis([0 500 0 150]);

%polyfit data using least squares 2nd order polynomial
[P,S]=polyfit(xi,interpdata,2);
y2=polyval(P,xi);
plot(y2,xi,'k-');

%remove polynomial fit to obtain residuals
resid=interpdata-y2;
subplot(1,3,2);
plot(resid,xi, 'k-');
```

```
hold on;
plot(0,[0:0.05:150],'k-');
title('Residual plot vs depth');
xlabel('Residual'),ylabel('Depth (mm)');
axis ij;
axis([-100 100 0 100]);
mavr=mean(abs(resid));
nmean=mavr./meanraw

%calculate percent of variance (pov)
pov=(std(resid).^2)./(std(interpdata).^2).*100

%calculate and plot autocovariance fn
acv=real(fft(abs(ifft(resid-mean(resid))).^2));
nacv=acv./acv(1);
figure (1)
subplot(1,3,3);
plot(((0:511).*newz),nacv,'k-')
hold on;
plot([0:0.05:256], 0,'k-');
xlabel('Scale (mm)')
ylabel('Autocovariance function of residual');
title('NACF for H_2S');
axis([0 30 -1 1]);

%find the first zero crossing
scale=((0:511).*newz);
zerox=min(find(nacv<=0));
zeroxing=scale(zerox)
```

APPENDIX II

KLUWER LETTER OF PERMISSION

Kluwer Academic Publishers B.V.
Van Godewijckstraat 30
P.O. Box 17
3300 AA Dordrecht
The Netherlands
T +31 (0) 78 65 76 000
F +31 (0) 78 65 76 254
I www.wkap.nl
E services@wkap.nl

Mr. Andrew Brian Hebert
Texas A&M University
3146 TAMU
College of Geosciences; Dept of Oceanography
O&M Bldg, Room 502; COLLEGE STATION
TX 77843-3146; USA

03/03/2004

Re: Aquatic Geochemistry 9 (2003): 41-57

Dear Mr. Hebert,

With reference to your request (copy herewith) to reprint material on which Kluwer Academic Publishers control the copyright, our permission is granted, free of charge, for the use indicated in your enquiry.

This permission

- allows you non-exclusive reproduction rights throughout the World.
- includes use in an electronic form; for the use indicated in your inquiry (microfilmed by ProQuest Information and Learning Company/ thesis electronically submitted to Texas A&M University electronically to be available through on-line sources)
- requires a full credit (Kluwer Academic Publishers book/journal title, volume, year of publication, page, chapter/article title, name(s) of author(s), figure number(s), original copyright notice) to the publication in which the material was originally published, by adding: with kind permission of Kluwer Academic Publishers.

Material may not be republished until at least one year after our publication date.

Permission free of charge on this occasion does not prejudice any rights we might have to charge for reproduction of our copyrighted material in the future.

This permission letter replaces the permission letter, dated February 19th, 2004.

Sincerely yours,

Ingrid de Boer (Ms)
Rights and Permissions

Fa.xnr.: +31-78-6576744
E-mail: Ingrid.deboer@wkap.nl

PS.PLEASE BE CERTAIN TO INCLUDE OUR REFERENCE IN ALL CORRESPONDENCE

APPENDIX III

ELSEVIER LETTER OF PERMISSION

28 May 2004 Our ref: HW/smc/May 2004.jl345

Mr Andrew Hebert
Hebert@ocean.tamu.edu
Dear Mr Hebert

MARINE CHEMISTRY, Vol 70, No 1-3, 2000, Pages 89-103, Eldridge and Morse, "A diagenetic model for …"

As per your letter dated 19 April 2004, we hereby grant you permission to reprint the aforementioned material at no charge **in your thesis, in print and on the Texas A&M University web site** subject to the following conditions:

1. If any part of the material to be used (for example, figures) has appeared in our publication with credit or acknowledgement to another source, permission must also be sought from that source. If such permission is not obtained then that material may not be included in your publication/copies.

2. Suitable acknowledgment to the source must be made, either as a footnote or in a reference list at the end of your publication, as follows:

   "Reprinted from Publication title, Vol number, Author(s), Title of article, Pages No., Copyright (Year), with permission from Elsevier".

3. Reproduction of this material is confined to the purpose for which permission is hereby given.

4. This permission is granted for non-exclusive world **English** rights only. For other languages please reapply separately for each one required. Permission excludes use in an electronic form other than as specified above.

5. This includes permission for UMI to supply single copies, on demand, of the complete thesis. Should your thesis be published commercially, please reapply for permission.

Yours sincerely

Helen Wilson
Rights Manager

APPENDIX IV

BIOGEOCHEMISTRY OF SEAGRASS SEDIMENTS UTILIZING *IN SITU* TECHNIQUES

Microelectrode profiling

A new, *in situ* microprofiler was designed throughout this research so that various types of sediment could be characterized *in situ* using a submerged lander, Benthic Automated Microelectrode System (BAMS) (Fig. A1). BAMS has the capability of sub-millimeter scale resolution in three dimensions with an operating depth in the water column of up to 30 m. This new technique provided an opportunity to sample sediments without the disturbance that traditional methods of sediment analyses such as peepers, sippers, and coring have. Three motors powered by a Velmex step-motor controller (VP9000 series) housed in water tight containers and micro-manipulating slides allowed the three-dimensional determination of dissolved O_2, Mn^{2+}, Fe^{2+}, and ΣH_2S using a gold-mercury amalgam voltammetric microelectrode (Brendel and Luther, 1995). An external cell with amplifier was used with a cable (top end, Fig. A1) to send current detected by the working, reference, and counter electrode (bottom end, Fig. A1) to a DLK-100A electrochemical analyzer (Analytical Instrument Systems) that was connected to a laptop computer on a boat.

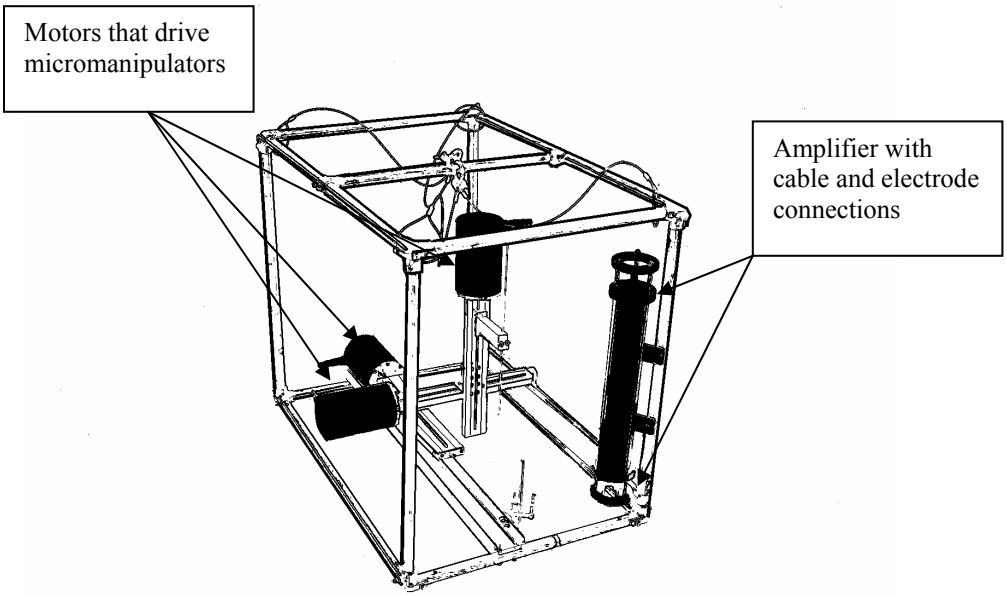

Fig. A.1 BAMS *in situ* microprofiler (dimensions: 0.95 m long x 0.65 m wide x 0.80 m tall)

APPENDIX V

GEOCHEMISTRY

Seagrass 1

SG1-1 10:00 am	Trode 1		Trode 2		Trode 3			
depth (mm)	H2S uM	Fe (uM)	H2S uM	Fe (uM)	H2S uM	Fe (uM)	**Ave H2S (uM)**	**Ave Fe**
0.0	236.2	0.0	86.3	0.0	16.3	0.0	112.9	0.0
2.0	291.1	0.0	89.5	857.8	40.8	0.0	140.5	285.9
4.0	229.8	0.0	79.8	0.0	59.4	0.0	123.0	0.0
6.0	261.8	0.0	87.3	0.0	64.9	0.0	138.0	0.0
8.0	249.0	0.0	91.9	0.0	80.4	0.0	140.5	0.0
10.0	268.1	0.0	86.8	0.0	88.1	0.0	147.7	0.0
12.0	260.5	0.0	93.2	0.0	90.1	0.0	147.9	0.0
14.0	275.8	0.0	93.1	0.0	99.2	0.0	156.0	0.0
16.0	291.1	0.0	99.7	0.0	102.3	0.0	164.4	0.0
18.0	330.7	0.0	100.4	0.0	101.8	0.0	177.6	0.0
20.0	330.7	0.0	98.3	0.0	116.1	0.0	181.7	0.0
22.0	348.6	0.0	103.8	0.0	116.8	0.0	189.7	0.0
24.0	295.0	0.0	106.5	0.0	110.7	0.0	170.7	0.0
26.0	312.8	0.0	108.0	0.0	121.4	0.0	180.8	0.0
28.0	303.9	0.0	114.9	0.0	118.1	0.0	179.0	0.0
30.0	308.4	0.0	112.2	0.0	121.4	0.0	180.7	0.0
32.0	312.8	0.0	114.0	0.0	119.6	0.0	182.2	0.0
34.0	303.9	0.0	121.2	0.0	118.4	0.0	181.1	0.0
36.0	312.8	0.0	127.6	0.0	121.8	0.0	187.4	0.0
38.0	312.8	0.0	133.7	0.0	123.2	0.0	189.9	0.0
40.0	321.8	0.0	133.8	0.0	121.4	0.0	192.3	0.0
42.0	312.8	0.0	133.3	0.0	124.5	0.0	190.2	0.0
44.0	312.8	0.0	135.2	0.0	128.6	0.0	192.2	0.0
46.0	330.7	0.0	138.3	0.0	129.1	0.0	199.4	0.0
48.0	330.7	0.0	141.1	0.0	128.6	0.0	200.1	0.0
50.0	321.8	0.0	143.6	0.0	130.6	0.0	198.7	0.0
55.0	312.8	0.0	142.1	0.0	144.4	0.0	199.8	0.0
60.0	311.6	0.0	146.7	0.0	136.5	0.0	198.3	0.0
65.0	350.9	0.0	150.5	0.0	131.0	0.0	210.8	0.0
70.0	348.6	0.0	149.0	0.0	133.7	0.0	210.4	0.0
75.0	370.7	0.0	141.1	0.0	131.0	0.0	214.3	0.0
80.0	352.8	0.0	143.6	0.0	127.6	0.0	208.0	0.0
85.0	343.0	0.0	138.3	0.0	127.6	0.0	202.9	0.0
90.0	343.0	0.0	135.2	0.0	126.0	0.0	201.4	0.0
95.0	343.0	0.0	130.4	0.0	124.5	0.0	199.3	0.0
100.0	286.0	0.0	125.8	0.0	119.5	0.0	177.1	0.0
105.0	316.1	0.0	116.1	0.0	118.4	0.0	183.5	0.0
110.0	298.3	0.0	111.5	0.0	108.0	0.0	172.6	0.0
115.0	279.6	0.0	101.1	0.0	106.9	0.0	162.5	0.0
120.0	229.8	0.0	93.6	0.0	95.4	0.0	139.6	0.0
125.0	206.9	0.0	70.9	0.0	90.0	0.0	122.6	0.0
130.0	168.5	0.0	60.5	0.0	85.7	0.0	104.9	0.0
135.0	145.6	0.0	56.7	0.0	75.0	0.0	92.4	0.0
140.0	114.9	0.0	45.8	0.0	60.7	0.0	73.8	0.0
145.0	107.3	0.0	39.5	0.0	56.8	0.0	67.8	0.0
150.0	107.3	0.0	37.3	0.0	50.8	0.0	65.1	0.0

Seagrass 1

SG1-2 2:00 pm

	Trode 1		Trode 2		Trode 3			
depth (mm)	H2S uM	Fe (uM)	H2S uM	Fe (uM)	H2S uM	Fe (uM)	**Ave H2S (uM)**	**Ave Fe**
0.0	88.1	0.0	121.0	0.0	7.3	0.0	72.1	0.0
2.0	85.5	0.0	109.6	0.0	24.8	0.0	73.3	0.0
4.0	90.7	0.0	126.3	0.0	82.6	0.0	99.8	0.0
6.0	87.2	0.0	146.8	0.0	118.0	0.0	117.3	0.0
8.0	89.8	0.0	157.1	0.0	154.0	0.0	133.6	0.0
10.0	98.1	0.0	174.2	0.0	178.0	0.0	150.1	0.0
12.0	108.8	0.0	177.5	0.0	206.8	0.0	164.4	0.0
14.0	115.7	0.0	190.8	0.0	220.6	0.0	175.7	0.0
16.0	127.4	0.0	199.4	0.0	221.4	0.0	182.8	0.0
18.0	140.2	0.0	208.4	0.0	234.2	0.0	194.3	0.0
20.0	166.2	0.0	241.3	0.0	263.7	0.0	223.7	0.0
22.0	167.3	0.0	249.8	0.0	279.6	0.0	232.2	0.0
24.0	170.1	0.0	242.3	0.0	262.3	0.0	224.9	0.0
26.0	166.0	0.0	250.9	0.0	262.5	0.0	226.5	0.0
28.0	172.4	0.0	249.0	0.0	272.7	0.0	231.4	0.0
30.0	168.3	0.0	252.3	0.0	291.1	0.0	237.2	0.0
32.0	166.0	0.0	242.3	0.0	244.5	0.0	217.6	0.0
34.0	168.3	0.0	249.2	0.0	241.3	0.0	219.6	0.0
36.0	171.9	0.0	258.2	0.0	260.7	0.0	230.3	0.0
38.0	170.1	0.0	252.6	0.0	245.9	0.0	222.9	0.0
40.0	190.5	0.0	257.9	0.0	245.9	0.0	231.4	0.0
42.0	180.0	0.0	257.4	0.0	250.5	0.0	229.3	0.0
44.0	176.2	0.0	249.0	0.0	251.5	0.0	225.6	0.0
46.0	180.5	0.0	238.1	0.0	241.1	0.0	219.9	0.0
48.0	180.3	0.0	234.9	0.0	237.0	0.0	217.4	0.0
50.0	184.4	0.0	225.2	0.0	234.9	0.0	214.9	0.0
55.0	190.8	0.0	220.6	0.0	234.9	0.0	215.4	0.0
60.0	180.0	0.0	221.9	0.0	224.0	0.0	208.6	0.0
65.0	181.6	0.0	211.4	0.0	224.0	0.0	205.7	0.0
70.0	178.2	0.0	203.5	0.0	210.9	0.0	197.6	0.0
75.0	174.7	0.0	188.2	0.0	200.7	0.0	187.9	0.0
80.0	174.2	0.0	124.5	0.0	188.5	0.0	162.4	0.0
85.0	170.8	0.0	144.0	0.0	166.0	0.0	160.3	0.0
90.0	165.5	0.0	126.4	0.0	157.1	0.0	149.6	0.0
95.0	153.0	0.0	154.0	0.0	121.8	0.0	142.9	0.0
100.0	140.2	0.0	132.8	0.0	107.3	0.0	126.7	0.0
105.0	130.2	0.0	178.1	0.0	84.5	0.0	131.0	0.0
110.0	125.6	0.0	124.1	0.0	67.2	0.0	105.6	0.0
115.0	117.2	0.0	113.9	0.0	59.2	0.0	96.8	0.0
120.0	106.0	0.0	116.8	0.0	54.1	0.0	92.3	0.0
125.0	91.2	0.0	108.0	0.0	46.7	0.0	82.0	0.0
130.0	87.0	0.0	112.9	0.0	46.2	0.0	82.0	0.0
135.0	81.6	0.0	91.4	0.0	58.6	0.0	77.2	0.0
140.0	67.3	0.0	90.4	0.0	46.5	0.0	68.1	0.0
145.0	60.5	0.0	89.6	0.0	43.7	0.0	64.6	0.0
150.0	54.4	0.0	94.0	0.0	52.1	0.0	66.8	0.0

Seagrass 1

SG1-3 6:00 pm

	Trode 1		Trode 2		Trode 3			
depth (mm)	H2S uM	Fe (uM)	H2S uM	Fe (uM)	H2S uM	Fe (uM)	**Ave H2S (uM)**	**Ave Fe**
0.0	19.9	0.0	788.3	0.0	397.4	0.0	401.9	0.0
2.0	11.8	0.0	521.5	0.0	350.4	0.0	294.5	0.0
4.0	16.2	0.0	490.6	0.0	407.5	0.0	304.7	0.0
6.0	11.6	0.0	482.1	0.0	410.1	0.0	301.3	0.0
8.0	7.7	0.0	506.6	0.0	440.2	0.0	318.1	0.0
10.0	5.2	0.0	470.2	0.0	430.6	0.0	302.0	0.0
12.0	3.1	0.0	520.2	0.0	439.9	0.0	321.1	0.0
14.0	2.2	0.0	455.0	0.0	449.0	77.9	302.1	26.0
16.0	3.1	0.0	498.1	0.0	494.3	1918.5	331.8	639.5
18.0	2.6	0.0	442.4	496.7	426.2	1269.6	290.4	588.8
20.0	38.4	0.0	444.7	1198.7	474.7	957.9	319.3	718.9
22.0	100.5	0.0	521.9	1140.5	590.8	3174.9	404.4	1438.5
24.0	149.0	0.0	499.4	1624.3	633.7	1698.9	427.4	1107.7
26.0	180.8	0.0	485.7	921.4	605.0	1653.7	423.8	858.4
28.0	168.6	0.0	442.4	923.4	608.3	1434.2	406.4	785.9
30.0	177.0	0.0	457.4	1143.6	599.6	5193.0	411.3	2112.2
32.0	175.1	0.0	462.6	1834.7	603.9	1583.9	413.9	1139.5
34.0	202.7	0.0	453.0	1378.3	597.8	2167.0	417.9	1181.8
36.0	191.4	0.0	460.7	1319.4	597.0	1494.3	416.4	937.9
38.0	208.3	0.0	471.6	2061.2	608.3	3398.4	429.4	1819.9
40.0	211.4	0.0	462.1	2277.3	605.7	5073.6	426.4	2450.3
42.0	207.6	0.0	463.2	2696.0	585.2	7061.5	418.6	3252.5
44.0	230.6	0.0	459.0	2511.6	600.9	3201.8	430.2	1904.5
46.0	265.1	0.0	453.9	2580.9	596.5	6334.6	438.5	2971.8
48.0	362.6	0.0	455.5	2742.6	560.4	5739.4	459.5	2827.3
50.0	325.0	0.0	475.2	3230.5	570.4	4954.0	456.9	2728.1
55.0	395.8	0.0	424.5	2883.8	562.1	6379.6	460.8	3087.8
60.0	433.6	0.0	416.2	2736.8	559.6	1843.1	469.8	1526.6
65.0	492.7	0.0	393.1	2409.0	559.2	3932.0	481.7	2113.6
70.0	502.3	0.0	386.9	2755.2	560.6	5256.8	483.3	2670.6
75.0	498.3	0.0	383.2	2156.8	528.5	6236.9	470.0	2797.9
80.0	450.7	0.0	354.8	2208.3	541.5	2054.5	449.0	1420.9
85.0	459.4	0.0	372.5	1501.0	513.5	3016.7	448.5	1505.9
90.0	418.8	0.0	340.3	1486.4	524.2	1637.4	427.8	1041.3
95.0	462.6	0.0	295.6	2696.8	451.6	2412.2	403.3	1703.0
100.0	310.6	0.0	300.0	3397.7	411.8	2161.5	340.8	1853.1
105.0	464.6	0.0	258.9	2963.1	405.4	1910.5	376.3	1624.6
110.0	461.2	0.0	242.1	1293.1	353.3	1546.2	352.2	946.4
115.0	428.8	0.0	265.6	2172.6	239.9	3338.8	311.4	1837.1
120.0	695.7	0.0	409.6	890.8	206.6	3727.8	437.3	1539.5
125.0	769.0	0.0	637.3	0.0	276.9	4116.9	561.1	1372.3
130.0	721.0	0.0	534.2	0.0	334.4	457.5	529.8	152.5
135.0	217.5	0.0	149.8	0.0	125.8	271.5	164.4	90.5
140.0	116.6	0.0	138.5	0.0	110.0	46.3	121.7	15.4
145.0	103.1	0.0	130.6	0.0	99.6	0.0	111.1	0.0
150.0	108.8	0.0	129.7	0.0	88.6	0.0	109.1	0.0

Seagrass 1

SG1-4

10:00 pm	Trode 1		Trode 2		Trode 3			
depth (mm)	H2S uM	Fe (uM)	H2S uM	Fe (uM)	H2S uM	Fe (uM)	**Ave H2S (uM)**	**Ave Fe**
0.0	162.0	0.0	87.4	0.0	23.2	0.0	90.9	0.0
2.0	73.0	0.0	60.3	283.2	15.4	0.0	49.6	94.4
4.0	122.3	0.0	77.0	166.3	55.2	0.0	84.8	55.4
6.0	100.4	0.0	68.2	194.2	125.8	0.0	98.1	64.7
8.0	109.7	0.0	80.9	130.0	194.3	0.0	128.3	43.3
10.0	135.9	0.0	80.0	314.4	203.2	0.0	139.7	104.8
12.0	134.6	0.0	91.8	671.8	183.0	0.0	136.5	223.9
14.0	109.7	0.0	91.3	636.3	187.8	0.0	129.6	212.1
16.0	176.9	0.0	95.8	549.5	225.3	377.6	166.0	309.0
18.0	123.2	0.0	109.6	563.6	243.5	240.4	158.8	268.0
20.0	111.5	0.0	106.1	2852.5	296.6	830.2	171.4	1227.6
22.0	185.6	0.0	145.5	598.8	328.0	1123.5	219.7	574.1
24.0	180.4	0.0	149.8	677.3	356.8	2160.9	229.0	946.0
26.0	153.0	0.0	183.9	886.9	394.8	334.1	243.9	407.0
28.0	138.0	0.0	222.8	817.4	457.8	1016.8	272.9	611.4
30.0	159.4	0.0	240.6	1130.7	514.4	1184.3	304.8	771.7
32.0	130.6	0.0	246.3	1591.7	553.5	740.8	310.1	777.5
34.0	142.9	0.0	241.0	2036.6	545.4	4570.3	309.8	2202.3
36.0	120.2	0.0	245.9	2749.4	548.9	3224.2	305.0	1991.2
38.0	106.2	0.0	243.4	2906.7	628.5	1817.4	326.1	1574.7
40.0	171.8	0.0	233.7	5340.9	593.6	2818.2	333.1	2719.7
42.0	150.7	0.0	241.1	4449.0	658.6	2342.6	350.1	2263.9
44.0	124.9	0.0	251.8	8427.7	641.1	2333.6	339.3	3587.1
46.0	132.4	0.0	249.3	4892.6	520.1	7618.2	300.6	4170.3
48.0	142.4	0.0	247.6	5754.2	654.6	3146.6	348.2	2966.9
50.0	164.2	0.0	262.4	5677.3	684.8	4643.1	370.5	3440.1
55.0	162.0	0.0	284.4	4358.8	670.4	1071.0	372.3	1809.9
60.0	194.3	0.0	284.9	2339.4	669.2	2719.7	382.8	1686.4
65.0	168.6	0.0	277.9	2061.5	663.1	3976.9	369.8	2012.8
70.0	160.3	0.0	268.2	2502.8	643.7	5651.8	357.4	2718.2
75.0	128.0	0.0	268.2	2080.0	630.3	6581.1	342.2	2887.0
80.0	123.2	0.0	257.8	2061.4	605.7	7246.7	328.9	3102.7
85.0	142.8	0.0	252.6	791.2	636.3	8164.1	343.9	2985.1
90.0	135.4	0.0	252.4	36.3	580.0	2365.5	322.6	800.6
95.0	122.3	0.0	227.5	4806.4	507.5	10066.2	285.7	4957.6
100.0	131.0	0.0	231.6	1663.1	532.3	6073.5	298.3	2578.9
105.0	125.3	0.0	226.3	1680.3	523.6	4664.0	291.8	2114.8
110.0	108.7	0.0	209.6	1664.0	467.0	2112.3	261.8	1258.8
115.0	94.8	0.0	193.2	2940.6	396.5	1080.0	228.2	1340.2
120.0	83.9	0.0	170.9	5402.0	332.6	1306.0	195.8	2236.0
125.0	86.1	0.0	148.3	5502.0	279.2	1303.4	171.2	2268.5
130.0	81.3	0.0	166.9	4106.2	225.8	1394.8	158.0	1833.7
135.0	117.5	0.0	148.1	1792.6	118.4	3276.4	128.0	1689.7
140.0	287.4	0.0	146.8	941.8	135.4	3393.5	189.9	1445.1
145.0	189.7	0.0	135.6	338.4	128.8	65.9	151.4	134.8
150.0	153.8	0.0	118.0	289.8	84.4	129.3	118.7	139.7

Seagrass 1

SG1-5 2:00 am

	Trode 1		Trode 2		Trode 3			
depth (mm)	H2S uM	Fe (uM)	H2S uM	Fe (uM)	H2S uM	Fe (uM)	**Ave H2S (uM)**	**Ave Fe**
0.0	44.5	0.0	228.8	0.0	496.5	0.0	256.6	0.0
2.0	37.6	0.0	223.6	548.2	652.0	0.0	304.4	182.7
4.0	31.0	0.0	212.5	1396.2	610.3	0.0	284.6	465.4
6.0	27.1	0.0	204.1	1039.9	721.0	0.0	317.4	346.6
8.0	43.7	0.0	202.7	2022.6	691.5	0.0	312.7	674.2
10.0	64.7	0.0	198.7	2401.1	758.4	0.0	340.6	800.4
12.0	84.0	0.0	197.5	2541.5	694.8	690.1	325.4	1077.2
14.0	98.7	0.0	174.1	4238.4	701.1	1162.7	324.6	1800.3
16.0	103.1	0.0	177.9	1976.9	652.4	966.1	311.1	981.0
18.0	120.6	0.0	169.5	2313.5	653.8	835.1	314.6	1049.5
20.0	173.4	0.0	166.5	3349.8	623.6	930.7	321.2	1426.8
22.0	174.9	0.0	172.2	1878.4	613.1	851.6	320.1	910.0
24.0	173.4	0.0	162.3	2514.5	595.6	978.9	310.5	1164.5
26.0	172.4	0.0	185.6	2164.7	562.9	1326.3	307.0	1163.7
28.0	180.0	0.0	174.5	3130.0	583.0	1154.4	312.5	1428.1
30.0	212.7	0.0	227.6	699.5	582.1	960.0	340.8	553.2
32.0	224.5	0.0	242.6	391.9	587.1	812.9	351.4	401.6
34.0	208.1	0.0	238.1	1870.7	596.5	1106.1	347.6	992.2
36.0	174.3	0.0	245.2	187.9	595.2	1790.2	338.2	659.4
38.0	167.4	0.0	251.6	726.1	580.8	1502.5	333.3	742.9
40.0	172.1	0.0	276.2	304.2	587.8	1948.2	345.3	750.8
42.0	182.2	0.0	257.4	3450.0	567.4	2748.7	335.6	2066.2
44.0	203.1	0.0	290.5	505.8	571.1	2043.3	354.9	849.7
46.0	179.0	0.0	275.2	3487.8	550.6	3040.9	334.9	2176.2
48.0	197.4	0.0	291.3	3583.9	552.9	2933.8	347.2	2172.6
50.0	194.8	0.0	309.2	127.0	541.0	3227.1	348.3	1118.0
55.0	196.1	0.0	316.2	49.0	505.7	3215.2	339.3	1088.1
60.0	185.2	0.0	311.4	81.2	487.4	1852.6	328.0	644.6
65.0	159.9	0.0	285.7	4676.3	483.9	2105.3	309.8	2260.5
70.0	180.5	0.0	295.3	106.3	470.7	2393.6	315.5	833.3
75.0	185.3	0.0	283.1	0.0	453.8	2005.9	307.4	668.6
80.0	165.5	3431.0	274.0	0.0	451.5	2443.0	297.0	1958.0
85.0	161.6	3885.3	269.9	0.0	429.7	3352.5	287.1	2412.6
90.0	138.5	5190.2	242.0	0.0	372.6	2582.3	251.0	2590.9
95.0	114.9	4303.5	226.1	0.0	314.9	2749.8	218.7	2351.1
100.0	153.7	0.0	195.3	0.0	211.8	2424.5	186.9	808.2
105.0	362.0	0.0	280.0	0.0	261.6	2099.3	301.2	699.8
110.0	239.8	0.0	187.4	0.0	187.4	74.0	204.9	24.7
115.0	163.8	0.0	162.4	2421.4	128.4	0.0	151.5	807.1
120.0	153.0	2258.8	160.4	2463.9	85.2	341.3	132.9	1688.0
125.0	130.2	3741.9	142.8	1913.9	59.8	417.1	111.0	2024.3
130.0	105.8	3010.7	120.7	1467.4	55.6	0.0	94.0	1492.7
135.0	82.2	3463.4	107.9	1236.8	53.4	0.0	81.1	1566.7
140.0	66.9	3011.5	95.8	723.2	50.3	0.0	71.0	1244.9
145.0	57.3	2796.9	83.6	778.9	49.9	0.0	63.6	1192.0
150.0	53.3	2482.2	80.8	728.3	48.0	0.0	60.7	1070.2

Seagrass 1

SG1-6 6:00 am

	Trode 1		Trode 2		Trode 3			
depth (mm)	H2S uM	Fe (uM)	H2S uM	Fe (uM)	H2S uM	Fe (uM)	**Ave H2S (uM)**	**Ave Fe**
0.0	122.7	4347.5	140.8	0.0	226.9	0.0	163.5	1449.2
2.0	142.6	3021.8	118.7	0.0	292.6	0.0	184.6	1007.3
4.0	154.8	2874.1	103.4	232.9	287.3	508.8	181.9	1205.3
6.0	167.4	2722.9	134.1	294.2	363.0	1008.5	221.5	1341.9
8.0	162.5	2605.6	196.9	241.3	314.0	3440.8	224.5	2095.9
10.0	170.3	2595.2	214.1	362.9	391.6	964.6	258.6	1307.6
12.0	183.5	3582.4	227.6	432.7	395.2	1300.6	268.8	1771.9
14.0	180.8	3320.6	254.4	319.1	397.9	75.0	277.7	1238.2
16.0	206.2	3497.5	266.0	814.4	433.7	150.4	302.0	1487.4
18.0	202.2	1403.4	269.5	1292.4	498.3	63.7	323.3	919.8
20.0	218.0	2356.1	291.4	1582.8	569.6	64.5	359.7	1334.5
22.0	215.3	2741.5	296.1	1417.5	574.0	65.3	361.8	1408.1
24.0	205.7	2051.1	303.2	1613.9	534.6	0.0	347.8	1221.7
26.0	201.7	2668.6	311.2	1342.8	628.4	0.0	380.4	1337.1
28.0	223.3	3355.0	314.8	1315.3	583.4	621.6	373.8	1764.0
30.0	225.8	4498.6	319.7	1662.9	563.9	59.6	369.8	2073.7
32.0	229.7	3843.6	314.0	2423.2	517.6	0.0	353.8	2088.9
34.0	204.4	2161.7	318.6	2352.3	486.9	0.0	336.6	1504.7
36.0	204.8	2002.8	326.7	2765.5	503.5	0.0	345.0	1589.4
38.0	200.9	1298.9	316.7	3701.6	486.9	93.1	334.8	1697.9
40.0	209.6	2250.5	317.0	3900.0	475.3	303.7	334.0	2151.4
42.0	232.9	2197.1	334.6	2599.6	495.7	62.4	354.4	1619.7
44.0	228.6	2499.2	324.1	3911.8	469.9	0.0	340.9	2137.0
46.0	193.5	1711.4	328.4	3470.8	468.2	0.0	330.0	1727.4
48.0	230.6	2884.6	323.3	4431.7	493.8	0.0	349.2	2438.8
50.0	211.9	998.1	317.1	4228.1	448.5	0.0	325.8	1742.1
55.0	178.2	716.0	323.2	4405.0	421.4	0.0	307.6	1707.0
60.0	203.6	1263.3	318.5	4821.7	390.8	0.0	304.3	2028.3
65.0	200.0	1288.4	323.1	3806.8	385.2	617.6	302.8	1904.3
70.0	186.0	1974.5	307.0	4169.7	373.4	580.0	288.8	2241.4
75.0	206.6	659.0	312.2	3210.2	356.9	0.0	291.9	1289.7
80.0	180.4	1030.0	291.3	4329.3	365.7	102.5	279.1	1820.6
85.0	170.9	466.7	297.8	3463.6	434.4	250.6	301.1	1393.6
90.0	180.9	181.7	278.7	3175.2	396.1	118.7	285.2	1158.5
95.0	174.3	540.1	282.5	2251.4	443.5	142.8	300.1	978.1
100.0	193.5	425.8	285.6	1465.7	394.5	124.2	291.2	671.9
105.0	176.9	1141.3	252.2	2127.1	390.4	571.0	273.1	1279.8
110.0	175.1	977.3	251.1	1414.9	385.2	439.7	270.5	944.0
115.0	119.3	1525.6	241.1	641.9	317.5	205.8	226.0	791.1
120.0	203.0	498.2	205.7	139.5	488.3	140.6	299.0	259.5
125.0	180.4	137.4	212.7	388.2	312.7	12.1	235.3	179.2
130.0	207.6	504.7	212.7	0.0	105.2	0.0	175.2	168.2
135.0	157.7	588.9	187.4	0.0	79.6	0.0	141.6	196.3
140.0	146.7	1319.0	177.8	0.0	67.7	0.0	130.7	439.7
145.0	139.3	2013.5	167.9	0.0	58.1	0.0	121.8	671.2
150.0	134.9	1688.8	162.2	0.0	52.9	0.0	116.7	562.9

Seagrass 2

SG2-1 2:00 pm	Trode 1		Trode 2		Trode 3		Trode 4		Trode 5		
depth (mm)	H2S uM	Fe (uM)	H2S uM	Fe (uM)	H2S uM	Fe (uM)	H2S uM	Fe (uM)	H2S uM	Fe (uM)	**Ave H2S (uM)**
0.0	0.0	0.0	23.1	0.0	21.6	0.0	16.6	0.0	0.0	0.0	12.3
2.0	0.0	0.0	50.3	0.0	7.9	0.0	0.0	0.0	0.0	0.0	11.6
4.0	0.0	0.0	46.3	0.0	6.1	0.0	0.0	0.0	0.0	0.0	10.5
6.0	0.0	0.0	51.2	0.0	4.5	0.0	0.0	0.0	0.0	0.0	11.1
8.0	16.7	0.0	66.4	0.0	3.6	0.0	0.0	0.0	0.0	0.0	17.3
10.0	49.4	0.0	86.1	0.0	0.0	0.0	0.0	0.0	0.0	0.0	27.1
12.0	71.8	0.0	77.9	0.0	0.0	0.0	0.0	0.0	0.0	0.0	29.9
14.0	73.1	0.0	91.7	0.0	0.0	0.0	0.0	0.0	0.0	0.0	33.0
16.0	80.6	0.0	107.4	0.0	0.0	0.0	0.0	0.0	0.0	0.0	37.6
18.0	125.0	0.0	121.0	0.0	0.0	0.0	0.0	0.0	0.0	0.0	49.2
20.0	98.9	0.0	120.6	0.0	0.0	0.0	0.0	0.0	0.0	0.0	43.9
22.0	126.0	0.0	137.2	0.0	4.6	0.0	0.0	0.0	0.0	0.0	53.6
24.0	130.3	0.0	146.4	0.0	9.2	0.0	0.0	0.0	0.0	0.0	57.2
26.0	144.7	0.0	154.8	0.0	10.2	0.0	0.0	0.0	0.0	0.0	61.9
28.0	155.2	0.0	143.7	0.0	7.7	0.0	0.0	0.0	0.0	0.0	61.3
30.0	144.7	0.0	152.0	0.0	15.7	0.0	0.0	0.0	0.0	0.0	62.5
32.0	157.8	0.0	135.8	0.0	16.2	0.0	0.0	0.0	0.0	0.0	62.0
34.0	148.2	0.0	144.1	0.0	6.9	0.0	0.0	0.0	0.0	0.0	59.8
36.0	141.2	0.0	132.3	0.0	22.8	0.0	0.0	0.0	0.0	0.0	59.3
38.0	137.8	0.0	135.0	0.0	24.0	0.0	0.0	0.0	0.0	0.0	59.4
40.0	148.2	0.0	128.5	0.0	14.0	0.0	0.0	0.0	0.0	0.0	58.1
42.0	111.4	0.0	118.8	0.0	16.2	0.0	0.0	0.0	0.0	0.0	49.3
44.0	90.6	0.0	112.2	0.0	10.6	0.0	0.0	0.0	0.0	0.0	42.7
46.0	82.3	0.0	115.4	0.0	7.4	0.0	0.0	0.0	0.0	0.0	41.0
48.0	80.1	0.0	113.2	0.0	10.6	0.0	0.0	0.0	0.0	0.0	40.8
50.0	89.9	0.0	110.2	0.0	0.0	0.0	0.0	0.0	0.0	0.0	40.0
55.0	75.7	0.0	94.3	0.0	0.0	0.0	0.0	0.0	0.0	0.0	34.0
60.0	70.2	0.0	86.0	0.0	0.0	0.0	0.0	0.0	0.0	0.0	31.2
65.0	53.3	0.0	82.6	0.0	0.0	0.0	0.0	0.0	0.0	0.0	27.2
70.0	49.9	0.0	74.7	0.0	0.0	0.0	0.0	0.0	0.0	0.0	24.9
75.0	63.5	0.0	58.6	0.0	0.0	0.0	0.0	0.0	0.0	0.0	24.4
80.0	49.0	0.0	52.8	0.0	0.0	0.0	0.0	0.0	0.0	0.0	20.4
85.0	58.3	0.0	29.3	0.0	0.0	0.0	0.0	0.0	0.0	0.0	17.5
90.0	52.2	0.0	33.2	0.0	0.0	0.0	0.0	0.0	0.0	0.0	17.1
95.0	67.5	0.0	19.2	0.0	0.0	0.0	0.0	0.0	0.0	0.0	17.3
100.0	73.6	0.0	34.9	0.0	0.0	0.0	0.0	0.0	0.0	0.0	21.7
105.0	80.5	0.0	48.5	0.0	75.1	0.0	99.2	0.0	0.0	0.0	60.7
110.0	135.2	0.0	47.6	0.0	97.8	0.0	87.8	0.0	0.0	0.0	73.7
115.0	117.3	0.0	35.8	0.0	60.3	0.0	65.6	0.0	0.0	0.0	55.8
120.0	114.7	0.0	21.9	0.0	43.3	0.0	58.6	0.0	0.0	0.0	47.7
125.0	118.5	0.0	29.3	0.0	32.8	0.0	53.3	0.0	0.0	0.0	46.8
130.0	112.4	0.0	43.3	0.0	24.6	0.0	54.6	0.0	0.0	0.0	47.0
135.0	120.6	0.0	55.5	0.0	19.7	0.0	52.0	0.0	0.0	0.0	49.6
140.0	118.7	0.0	82.1	0.0	21.8	0.0	53.8	0.0	0.0	0.0	55.3
145.0	131.2	0.0	80.4	0.0	29.3	0.0	55.5	0.0	0.0	0.0	59.3
150.0	127.4	0.0	87.8	0.0	36.7	0.0	60.3	0.0	0.0	0.0	62.4

Seagrass 2

SG2-2 6:00 pm

	Trode 1		Trode 2		Trode 3		
depth (mm)	H2S uM	Fe (uM)	H2S uM	Fe (uM)	H2S uM	Fe (uM)	**Ave H2S (uM)**
0.0	60.0	0.0	55.1	0.0	19.7	0.0	44.9
2.0	29.0	0.0	62.2	0.0	1.3	0.0	30.8
4.0	0.0	0.0	74.3	0.0	0.0	0.0	24.8
6.0	0.0	0.0	83.9	0.0	0.0	0.0	28.0
8.0	9.2	0.0	94.8	0.0	0.0	0.0	34.7
10.0	19.2	0.0	117.6	0.0	0.0	0.0	45.6
12.0	119.7	0.0	0.9	0.0	0.0	0.0	40.2
14.0	206.4	0.0	186.1	0.0	0.0	0.0	130.8
16.0	142.5	0.0	170.7	0.0	0.0	0.0	104.4
18.0	134.3	0.0	172.7	0.0	0.0	0.0	102.3
20.0	146.6	0.0	166.8	0.0	0.0	0.0	104.5
22.0	143.8	0.0	167.4	0.0	0.0	0.0	103.7
24.0	123.8	0.0	177.3	0.0	0.0	0.0	100.4
26.0	137.5	0.0	144.7	0.0	0.0	0.0	94.1
28.0	135.9	0.0	160.1	0.0	0.0	0.0	98.6
30.0	153.1	0.0	142.4	0.0	0.0	0.0	98.5
32.0	145.8	0.0	159.0	0.0	0.0	0.0	101.6
34.0	145.6	0.0	217.9	0.0	0.0	0.0	121.2
36.0	141.7	0.0	180.9	0.0	0.0	0.0	107.5
38.0	137.3	0.0	161.7	0.0	0.0	0.0	99.7
40.0	132.9	0.0	160.1	0.0	0.0	0.0	97.7
42.0	122.8	0.0	152.2	0.0	0.0	0.0	91.7
44.0	115.0	0.0	136.7	0.0	0.0	0.0	83.9
46.0	119.4	0.0	129.4	0.0	0.0	0.0	82.9
48.0	137.4	0.0	122.3	0.0	0.0	0.0	86.6
50.0	126.9	0.0	129.3	0.0	0.0	0.0	85.4
55.0	119.0	0.0	119.2	0.0	0.0	0.0	79.4
60.0	100.2	0.0	115.8	0.0	0.0	0.0	72.0
65.0	82.2	0.0	109.3	0.0	0.0	0.0	63.8
70.0	69.2	0.0	102.8	0.0	0.0	0.0	57.3
75.0	53.3	0.0	86.6	0.0	0.0	0.0	46.6
80.0	42.5	0.0	81.4	0.0	0.0	0.0	41.3
85.0	23.7	0.0	76.6	0.0	0.0	0.0	33.4
90.0	19.2	0.0	64.3	0.0	0.0	0.0	27.8
95.0	11.5	0.0	45.4	0.0	0.0	0.0	19.0
100.0	10.2	0.0	77.8	0.0	24.1	0.0	37.4
105.0	36.0	0.0	102.2	0.0	26.2	0.0	54.8
110.0	43.8	0.0	83.5	0.0	21.5	0.0	49.6
115.0	38.5	0.0	93.9	0.0	9.7	0.0	47.4
120.0	41.2	0.0	75.7	0.0	14.4	0.0	43.8
125.0	31.9	0.0	85.3	0.0	9.2	0.0	42.1
130.0	46.8	0.0	128.0	0.0	14.6	0.0	63.1
135.0	32.8	0.0	94.4	0.0	11.4	0.0	46.2
140.0	42.0	0.0	102.6	0.0	8.4	0.0	51.0
145.0	48.9	0.0	110.6	0.0	8.3	0.0	55.9
150.0	90.9	0.0	123.2	0.0	8.3	0.0	74.1

Seagrass 2

SG2-3 10:00 pm

	Trode 1		Trode 2		Trode 3		
depth (mm)	H2S uM	Fe (uM)	H2S uM	Fe (uM)	H2S uM	Fe (uM)	**Ave H2S (uM)**
0.0	16.3	0.0	0.0	0.0	0.0	FeS	5.4
2.0	28.4	0.0	19.7	0.0	0.0	FeS	16.0
4.0	0.0	0.0	0.0	0.0	0.0	FeS	0.0
6.0	0.0	0.0	0.0	0.0	0.0	FeS	0.0
8.0	0.0	0.0	0.0	0.0	0.0	FeS	0.0
10.0	0.0	0.0	0.0	0.0	0.0	FeS	0.0
12.0	0.0	0.0	0.0	0.0	0.0	FeS	0.0
14.0	0.0	0.0	0.0	0.0	0.0	FeS	0.0
16.0	0.0	0.0	0.0	0.0	0.0	FeS	0.0
18.0	0.0	0.0	0.0	0.0	0.0	FeS	0.0
20.0	0.0	0.0	0.0	0.0	0.0	FeS	0.0
22.0	0.0	0.0	0.0	0.0	0.0	FeS	0.0
24.0	0.0	0.0	0.0	0.0	0.0	FeS	0.0
26.0	0.0	0.0	0.0	0.0	0.0	FeS	0.0
28.0	0.0	0.0	0.0	0.0	0.0	FeS	0.0
30.0	0.0	0.0	0.0	0.0	0.0	FeS	0.0
32.0	0.0	0.0	0.0	0.0	0.0	FeS	0.0
34.0	0.0	0.0	0.0	0.0	0.0	FeS	0.0
36.0	0.0	0.0	0.0	0.0	0.0	FeS	0.0
38.0	0.0	0.0	0.0	0.0	0.0	FeS	0.0
40.0	0.0	0.0	0.0	0.0	0.0	FeS	0.0
42.0	0.0	0.0	0.0	0.0	0.0	FeS	0.0
44.0	0.0	0.0	0.0	0.0	0.0	FeS	0.0
46.0	0.0	0.0	0.0	0.0	0.0	FeS	0.0
48.0	0.0	0.0	0.0	0.0	0.0	FeS	0.0
50.0	0.0	0.0	0.0	0.0	0.0	FeS	0.0
55.0	0.0	0.0	0.0	0.0	0.0	FeS	0.0
60.0	0.0	0.0	0.0	0.0	0.0	FeS	0.0
65.0	0.0	0.0	0.0	0.0	0.0	FeS	0.0
70.0	0.0	0.0	0.0	0.0	0.0	FeS	0.0
75.0	0.0	0.0	0.0	0.0	0.0	FeS	0.0
80.0	0.0	0.0	0.0	0.0	0.0	FeS	0.0
85.0	0.0	0.0	0.0	0.0	0.0	FeS	0.0
90.0	0.0	0.0	0.0	0.0	0.0	FeS	0.0
95.0	0.0	0.0	0.0	0.0	0.0	FeS	0.0
100.0	0.0	0.0	0.0	0.0	0.0	FeS	0.0
105.0	0.0	0.0	0.0	0.0	0.0	FeS	0.0
110.0	0.0	0.0	0.0	0.0	0.0	FeS	0.0
115.0	0.0	0.0	0.0	0.0	0.0	FeS	0.0
120.0	0.0	0.0	0.0	0.0	0.0	FeS	0.0
125.0	0.0	0.0	0.0	0.0	0.0	FeS	0.0
130.0	0.0	0.0	0.0	0.0	0.0	FeS	0.0
135.0	0.0	0.0	0.0	0.0	0.0	FeS	0.0
140.0	0.0	0.0	0.0	0.0	0.0	FeS	0.0
145.0	0.0	0.0	0.0	0.0	0.0	FeS	0.0
150.0	0.0	0.0	0.0	0.0	0.0	FeS	0.0

Seagrass 2

SG2-4

2:00 am	Trode 1		Trode 2		Trode 3		
depth (mm)	H2S uM	Fe (uM)	H2S uM	Fe (uM)	H2S uM	Fe (uM)	**Ave H2S (uM)**
0.0	31.9	0.0	24.0	FeS	0.0	0.0	18.7
2.0	0.0	0.0	4.6	FeS	0.0	0.0	1.5
4.0	0.0	0.0	0.0	FeS	0.0	0.0	0.0
6.0	0.0	0.0	0.0	FeS	0.0	0.0	0.0
8.0	0.0	0.0	0.0	FeS	0.0	0.0	0.0
10.0	0.0	0.0	8.4	FeS	0.0	0.0	2.8
12.0	0.0	0.0	3.1	FeS	0.0	0.0	1.0
14.0	0.0	0.0	8.8	FeS	27.6	0.0	12.1
16.0	0.0	0.0	15.8	FeS	42.4	0.0	19.4
18.0	0.0	0.0	4.8	FeS	43.8	0.0	16.2
20.0	0.0	0.0	16.7	FeS	66.9	0.0	27.9
22.0	0.0	0.0	8.7	FeS	69.1	0.0	26.0
24.0	0.0	0.0	0.0	FeS	70.4	0.0	23.5
26.0	11.9	0.0	0.0	FeS	70.4	0.0	27.4
28.0	0.0	0.0	0.0	FeS	71.7	0.0	23.9
30.0	0.0	0.0	0.0	FeS	57.7	0.0	19.2
32.0	0.0	0.0	0.0	FeS	65.2	0.0	21.7
34.0	0.0	0.0	0.0	FeS	50.3	0.0	16.8
36.0	0.0	0.0	0.0	FeS	72.6	0.0	24.2
38.0	0.0	0.0	0.0	FeS	59.9	0.0	20.0
40.0	0.0	0.0	0.0	FeS	64.2	0.0	21.4
42.0	0.0	0.0	0.0	FeS	70.8	0.0	23.6
44.0	0.0	0.0	0.0	FeS	60.5	0.0	20.2
46.0	0.0	0.0	0.0	FeS	53.8	0.0	17.9
48.0	0.0	0.0	0.0	FeS	48.6	0.0	16.2
50.0	0.0	0.0	0.0	FeS	58.1	0.0	19.4
55.0	0.0	0.0	0.0	FeS	57.2	0.0	19.1
60.0	0.0	0.0	0.0	FeS	46.4	0.0	15.5
65.0	0.0	0.0	0.0	FeS	57.8	0.0	19.3
70.0	0.0	0.0	0.0	FeS	56.9	0.0	19.0
75.0	0.0	0.0	0.0	FeS	49.4	0.0	16.5
80.0	0.0	0.0	0.0	FeS	40.7	0.0	13.6
85.0	0.0	0.0	0.0	FeS	57.7	0.0	19.2
90.0	0.0	0.0	0.0	FeS	61.6	0.0	20.5
95.0	0.0	0.0	0.0	FeS	87.0	0.0	29.0
100.0	0.0	0.0	0.0	FeS	80.0	0.0	26.7
105.0	0.0	0.0	0.0	FeS	64.2	0.0	21.4
110.0	0.0	0.0	0.0	FeS	72.8	0.0	24.3
115.0	0.0	0.0	0.0	FeS	57.5	0.0	19.2
120.0	0.0	0.0	0.0	FeS	53.6	0.0	17.9
125.0	0.0	0.0	0.0	FeS	38.3	0.0	12.8
130.0	0.0	0.0	0.0	FeS	46.0	0.0	15.3
135.0	0.0	0.0	0.0	FeS	38.3	0.0	12.8
140.0	0.0	0.0	0.0	FeS	58.5	0.0	19.5
145.0	0.0	0.0	0.0	FeS	26.8	0.0	8.9
150.0	0.0	0.0	0.0	FeS	85.6	0.0	28.5

Seagrass 2

SG2-5 6:00

am	Trode 1		Trode 2		Trode 3		
depth (mm)	H2S uM	Fe (uM)	H2S uM	Fe (uM)	H2S uM	Fe (uM)	**Ave H2S (uM)**
0.0	0.0	0.0	51.6	0.0	26.3	0.0	26.0
2.0	0.0	0.0	42.0	0.0	10.0	0.0	17.3
4.0	0.0	0.0	17.9	0.0	0.0	0.0	6.0
6.0	0.0	0.0	28.9	0.0	0.0	0.0	9.6
8.0	0.0	0.0	50.5	0.0	0.0	0.0	16.8
10.0	0.0	0.0	45.6	0.0	11.2	0.0	18.9
12.0	0.0	0.0	60.5	0.0	18.8	0.0	26.4
14.0	0.0	0.0	45.5	0.0	29.3	0.0	24.9
16.0	12.0	0.0	31.9	0.0	34.9	0.0	26.3
18.0	14.5	0.0	68.2	0.0	53.3	0.0	45.3
20.0	24.5	0.0	42.9	0.0	64.7	0.0	44.0
22.0	27.2	0.0	46.8	0.0	77.3	0.0	50.4
24.0	30.1	0.0	39.8	0.0	66.8	0.0	45.6
26.0	38.5	0.0	52.0	0.0	83.9	0.0	58.1
28.0	42.1	0.0	68.9	0.0	88.2	0.0	66.4
30.0	49.6	0.0	46.0	0.0	55.5	0.0	50.4
32.0	36.8	0.0	86.2	0.0	58.2	0.0	60.4
34.0	32.0	0.0	66.5	0.0	72.1	0.0	56.9
36.0	25.8	0.0	69.1	0.0	56.4	0.0	50.4
38.0	23.2	0.0	91.9	0.0	57.7	0.0	57.6
40.0	19.3	0.0	93.1	0.0	53.3	0.0	55.2
42.0	24.6	0.0	80.4	0.0	46.7	0.0	50.6
44.0	23.3	0.0	59.0	0.0	44.6	0.0	42.3
46.0	21.8	0.0	62.1	0.0	55.0	0.0	46.3
48.0	18.9	0.0	68.3	0.0	46.8	0.0	44.7
50.0	19.3	0.0	70.0	0.0	38.5	0.0	42.6
55.0	17.9	0.0	84.8	0.0	48.5	0.0	50.4
60.0	21.4	0.0	75.6	0.0	41.2	0.0	46.1
65.0	16.7	0.0	53.0	0.0	36.3	0.0	35.3
70.0	0.0	0.0	72.2	0.0	23.6	0.0	31.9
75.0	20.5	0.0	44.3	0.0	0.0	0.0	21.6
80.0	0.0	0.0	60.8	0.0	0.0	0.0	20.3
85.0	14.9	0.0	37.6	0.0	0.0	0.0	17.5
90.0	0.0	0.0	42.9	0.0	0.0	0.0	14.3
95.0	0.0	0.0	44.6	0.0	0.0	0.0	14.9
100.0	0.0	0.0	24.5	0.0	0.0	0.0	8.2
105.0	0.0	0.0	3.8	0.0	0.0	0.0	1.3
110.0	0.0	0.0	20.6	0.0	0.0	0.0	6.9
115.0	0.0	0.0	30.7	0.0	0.0	0.0	10.2
120.0	0.0	0.0	22.0	0.0	0.0	0.0	7.3
125.0	0.0	0.0	31.1	0.0	19.8	0.0	16.9
130.0	0.0	0.0	34.7	0.0	16.2	0.0	17.0
135.0	0.0	0.0	44.7	0.0	20.5	0.0	21.7
140.0	0.0	0.0	56.5	0.0	17.5	0.0	24.7
145.0	0.0	0.0	47.7	0.0	12.0	0.0	19.9
150.0	0.0	0.0	59.9	0.0	15.5	0.0	25.1

Seagrass 2

SG2-6 10:00 am

	Trode 1		Trode 2		Trode 3		
depth (mm)	H2S uM	Fe (uM)	H2S uM	Fe (uM)	H2S uM	Fe (uM)	**Ave H2S (uM)**
0.0	9.6	0.0	22.7	0.0	0.0	0.0	10.8
2.0	62.8	0.0	0.0	0.0	0.0	0.0	20.9
4.0	62.9	0.0	0.0	0.0	0.0	0.0	21.0
6.0	66.7	0.0	0.0	0.0	0.0	0.0	22.2
8.0	72.2	0.0	0.0	0.0	0.0	0.0	24.1
10.0	97.6	0.0	0.0	0.0	0.0	0.0	32.5
12.0	117.1	0.0	0.0	0.0	0.0	0.0	39.0
14.0	115.8	0.0	0.0	0.0	0.0	0.0	38.6
16.0	132.8	0.0	0.0	0.0	0.0	0.0	44.3
18.0	163.0	0.0	7.5	0.0	0.0	0.0	56.8
20.0	202.0	0.0	2.3	0.0	0.0	0.0	68.1
22.0	219.2	0.0	4.6	0.0	0.0	0.0	74.6
24.0	217.1	0.0	16.2	0.0	0.0	0.0	77.7
26.0	236.3	0.0	15.8	0.0	21.4	0.0	91.2
28.0	230.6	0.0	13.5	0.0	83.2	0.0	109.1
30.0	240.6	0.0	39.3	0.0	110.9	0.0	130.3
32.0	237.1	0.0	41.1	0.0	132.8	0.0	137.0
34.0	248.9	0.0	79.2	0.0	131.5	0.0	153.2
36.0	239.5	0.0	52.5	0.0	137.4	0.0	143.1
38.0	237.7	0.0	70.3	0.0	132.4	0.0	146.8
40.0	235.9	0.0	62.5	0.0	129.7	0.0	142.7
42.0	226.3	0.0	70.8	0.0	134.1	0.0	143.7
44.0	222.4	0.0	71.2	0.0	125.4	0.0	139.7
46.0	223.2	0.0	76.0	0.0	136.7	0.0	145.3
48.0	216.7	0.0	59.8	0.0	133.3	0.0	136.6
50.0	206.2	0.0	62.2	0.0	123.6	0.0	130.7
55.0	181.3	0.0	69.9	0.0	112.8	0.0	121.3
60.0	199.6	0.0	64.6	0.0	113.6	0.0	126.0
65.0	195.2	0.0	73.8	0.0	107.5	0.0	125.5
70.0	189.7	0.0	49.4	0.0	97.9	0.0	112.3
75.0	181.2	0.0	39.4	0.0	81.8	0.0	100.8
80.0	175.1	0.0	27.1	0.0	76.9	0.0	93.0
85.0	153.8	0.0	33.6	0.0	68.2	0.0	85.2
90.0	149.8	0.0	18.4	0.0	71.2	0.0	79.8
95.0	168.1	0.0	16.3	0.0	65.5	0.0	83.3
100.0	181.7	0.0	16.6	0.0	56.4	0.0	84.9
105.0	194.8	0.0	29.3	0.0	45.0	0.0	89.7
110.0	204.4	0.0	20.2	0.0	36.8	0.0	87.1
115.0	197.0	0.0	33.7	0.0	31.0	0.0	87.2
120.0	203.2	0.0	29.8	0.0	24.5	0.0	85.8
125.0	122.8	0.0	32.4	0.0	21.4	0.0	58.8
130.0	110.5	0.0	44.6	0.0	29.7	0.0	61.6
135.0	114.8	0.0	32.8	0.0	43.3	0.0	63.7
140.0	120.1	0.0	44.2	0.0	68.2	0.0	77.5
145.0	127.1	0.0	42.9	0.0	81.3	0.0	83.8
150.0	118.8	0.0	40.2	0.0	79.6	0.0	79.5

Unvegetated 1

B1-1 10:00 am	Trode 1		Trode 2		Trode 3		
depth (mm)	H2S uM	Fe (uM)	H2S uM	Fe (uM)	H2S uM	Fe (uM)	**Average H2S**
0.0	30.6	0.0	0.0	0.0	0.0	0.0	10.2
2.0	7.3	0.0	0.0	0.0	0.0	0.0	2.4
4.0	8.0	0.0	0.0	0.0	0.0	0.0	2.7
6.0	0.0	0.0	0.0	0.0	0.0	0.0	0.0
8.0	3.5	0.0	0.0	0.0	0.0	0.0	1.2
10.0	0.0	0.0	0.0	0.0	0.0	0.0	0.0
12.0	13.9	0.0	0.0	0.0	0.0	0.0	4.6
14.0	8.2	0.0	0.0	0.0	0.0	0.0	2.7
16.0	0.0	0.0	0.0	0.0	0.0	0.0	0.0
18.0	9.1	0.0	0.0	0.0	0.0	0.0	3.0
20.0	7.9	0.0	0.0	0.0	0.0	0.0	2.6
22.0	0.0	0.0	0.0	0.0	0.0	0.0	0.0
24.0	0.0	0.0	0.0	0.0	0.0	0.0	0.0
26.0	0.0	0.0	0.0	0.0	0.0	0.0	0.0
28.0	0.0	0.0	0.0	0.0	0.0	0.0	0.0
30.0	0.0	0.0	0.0	0.0	0.0	0.0	0.0
32.0	0.0	0.0	0.0	0.0	0.0	0.0	0.0
34.0	0.0	0.0	0.0	0.0	0.0	0.0	0.0
36.0	0.0	0.0	0.0	0.0	0.0	0.0	0.0
38.0	0.0	0.0	0.0	0.0	0.0	0.0	0.0
40.0	0.0	0.0	0.0	0.0	0.0	0.0	0.0
42.0	0.0	0.0	0.0	0.0	0.0	0.0	0.0
44.0	0.0	0.0	0.0	0.0	0.0	0.0	0.0
46.0	0.0	0.0	0.0	0.0	0.0	0.0	0.0
48.0	0.0	0.0	0.0	0.0	0.0	0.0	0.0
50.0	0.0	0.0	0.0	0.0	0.0	0.0	0.0
55.0	0.0	0.0	0.0	0.0	0.0	0.0	0.0
60.0	0.0	0.0	0.0	0.0	0.0	0.0	0.0
65.0	0.0	0.0	0.0	0.0	0.0	0.0	0.0
70.0	0.0	0.0	0.0	0.0	0.0	0.0	0.0
75.0	0.0	0.0	0.0	0.0	0.0	0.0	0.0
80.0	0.0	0.0	0.0	0.0	0.0	0.0	0.0
85.0	0.0	0.0	0.0	0.0	0.0	0.0	0.0
90.0	0.0	0.0	0.0	0.0	0.0	0.0	0.0
95.0	NAN	0.0	0.0	0.0	NAN	0.0	0.0
100.0	NAN	0.0	0.0	0.0	NAN	0.0	0.0
105.0	NAN	0.0	0.0	0.0	NAN	0.0	0.0
110.0	NAN	0.0	0.0	0.0	NAN	0.0	0.0
115.0	NAN	0.0	0.0	0.0	NAN	0.0	0.0
120.0	NAN	0.0	0.0	0.0	NAN	0.0	0.0
125.0	NAN	0.0	0.0	0.0	NAN	0.0	0.0
130.0	NAN	0.0	0.0	0.0	NAN	0.0	0.0
135.0	NAN	0.0	0.0	0.0	NAN	0.0	0.0
140.0	NAN	0.0	0.0	0.0	NAN	0.0	0.0
145.0	NAN	0.0	NAN	0.0	NAN	0.0	0.0
150.0	NAN	0.0	NAN	0.0	NAN	0.0	0.0

Unvegetated 1

B1-2 2:00 pm

	Trode 1		Trode 2		Trode 3		
depth (mm)	H2S uM	Fe (uM)	H2S uM	Fe (uM)	H2S uM	Fe (uM)	**Average H2S**
0.0	0.0	0.0	0.0	0.0	0.0	0.0	0.0
2.0	0.0	0.0	0.0	0.0	0.0	0.0	0.0
4.0	0.0	0.0	0.0	0.0	0.0	0.0	0.0
6.0	0.0	0.0	0.0	0.0	0.0	0.0	0.0
8.0	1.8	0.0	0.0	0.0	0.0	0.0	0.6
10.0	0.0	0.0	0.0	0.0	8.8	0.0	2.9
12.0	0.0	0.0	0.0	0.0	0.0	0.0	0.0
14.0	0.0	0.0	0.0	0.0	0.0	0.0	0.0
16.0	0.0	0.0	0.0	0.0	0.0	0.0	0.0
18.0	0.0	0.0	0.0	0.0	0.0	0.0	0.0
20.0	0.0	0.0	0.0	0.0	0.0	0.0	0.0
22.0	0.0	0.0	0.0	0.0	0.0	0.0	0.0
24.0	0.0	0.0	0.0	0.0	0.0	0.0	0.0
26.0	0.0	0.0	0.0	0.0	0.0	0.0	0.0
28.0	6.2	0.0	5.2	0.0	0.0	0.0	3.8
30.0	0.0	0.0	0.0	0.0	0.0	0.0	0.0
32.0	0.0	0.0	0.0	0.0	0.0	0.0	0.0
34.0	4.6	0.0	0.0	0.0	0.0	0.0	1.5
36.0	6.9	0.0	0.0	0.0	0.0	0.0	2.3
38.0	6.4	0.0	0.0	0.0	0.0	0.0	2.1
40.0	6.9	0.0	0.0	0.0	0.0	0.0	2.3
42.0	0.0	0.0	0.0	0.0	0.0	0.0	0.0
44.0	0.0	0.0	0.0	0.0	0.0	0.0	0.0
46.0	0.0	0.0	0.0	0.0	0.0	0.0	0.0
48.0	0.0	0.0	0.0	0.0	0.0	0.0	0.0
50.0	0.0	0.0	0.0	0.0	0.0	0.0	0.0
55.0	3.0	0.0	0.0	0.0	0.0	0.0	1.0
60.0	0.0	0.0	0.0	0.0	0.0	0.0	0.0
65.0	0.0	0.0	6.6	0.0	0.0	0.0	2.2
70.0	0.0	0.0	5.2	0.0	0.0	0.0	1.7
75.0	0.0	0.0	0.0	0.0	0.0	0.0	0.0
80.0	0.0	0.0	0.0	0.0	0.0	0.0	0.0
85.0	0.0	0.0	0.0	0.0	0.0	0.0	0.0
90.0	0.0	0.0	0.0	0.0	0.0	0.0	0.0
95.0	0.0	0.0	2.9	0.0	0.0	0.0	1.0
100.0	0.0	0.0	1.6	0.0	0.0	0.0	0.5
105.0	0.0	0.0	0.0	0.0	0.0	0.0	0.0
110.0	0.0	0.0	0.0	0.0	0.0	0.0	0.0
115.0	0.0	0.0	0.0	0.0	0.0	0.0	0.0
120.0	0.0	0.0	0.0	0.0	0.0	0.0	0.0
125.0	0.0	0.0	0.0	0.0	0.0	0.0	0.0
130.0	0.0	0.0	0.0	0.0	0.0	0.0	0.0
135.0	0.0	0.0	0.0	0.0	0.0	19.9	0.0
140.0	0.0	0.0	0.0	0.0	0.0	20.8	0.0
145.0	0.0	0.0	0.0	0.0	0.0	39.8	0.0
150.0	0.0	0.0	0.0	0.0	0.0	62.3	0.0

Unvegetated 1

B1-3 6:00 pm	Trode 1		Trode 2		Trode 3		
depth (mm)	H2S uM	Fe (uM)	H2S uM	Fe (uM)	H2S uM	Fe (uM)	**Average H2S**
0.0	0.0	0.0	0.0	0.0	22.9	0.0	7.6
2.0	0.0	0.0	0.0	0.0	7.9	0.0	2.6
4.0	0.0	0.0	0.0	0.0	5.6	0.0	1.9
6.0	0.0	0.0	0.0	0.0	8.4	0.0	2.8
8.0	0.0	0.0	0.0	0.0	0.0	0.0	0.0
10.0	0.0	0.0	0.0	0.0	0.0	0.0	0.0
12.0	0.0	0.0	0.0	0.0	0.0	0.0	0.0
14.0	0.0	0.0	0.0	0.0	0.0	0.0	0.0
16.0	0.0	0.0	0.0	0.0	0.0	0.0	0.0
18.0	0.0	0.0	0.0	0.0	0.0	0.0	0.0
20.0	0.0	0.0	0.0	0.0	0.0	0.0	0.0
22.0	0.0	0.0	0.0	53.4	0.0	0.0	0.0
24.0	0.0	0.0	0.0	207.6	0.0	0.0	0.0
26.0	0.0	0.0	0.0	0.0	0.0	0.0	0.0
28.0	0.0	0.0	0.0	0.0	0.0	0.0	0.0
30.0	0.0	0.0	0.0	0.0	0.0	0.0	0.0
32.0	0.0	0.0	0.0	19.2	0.0	0.0	0.0
34.0	0.0	0.0	0.0	13.3	0.0	0.0	0.0
36.0	0.0	0.0	0.0	32.7	0.0	0.0	0.0
38.0	0.0	0.0	0.0	38.2	0.0	0.0	0.0
40.0	0.0	0.0	0.0	0.0	0.0	0.0	0.0
42.0	0.0	0.0	3.1	0.0	0.0	0.0	1.0
44.0	0.0	0.0	3.5	0.0	0.0	0.0	1.2
46.0	0.0	0.0	3.0	0.0	0.0	0.0	1.0
48.0	0.0	0.0	6.1	0.0	0.0	0.0	2.0
50.0	0.0	0.0	7.9	0.0	0.0	0.0	2.6
55.0	0.0	0.0	6.9	0.0	0.0	0.0	2.3
60.0	0.0	0.0	6.4	0.0	0.0	0.0	2.1
65.0	0.0	0.0	6.4	0.0	0.0	0.0	2.1
70.0	0.0	0.0	8.5	0.0	0.0	0.0	2.8
75.0	0.0	0.0	13.3	0.0	0.0	0.0	4.4
80.0	0.0	0.0	22.5	0.0	0.0	0.0	7.5
85.0	2.6	0.0	29.4	0.0	0.0	0.0	10.7
90.0	4.0	0.0	39.1	0.0	0.0	0.0	14.4
95.0	7.3	0.0	44.8	0.0	3.3	0.0	18.4
100.0	6.9	0.0	51.2	0.0	6.8	241.4	21.6
105.0	10.2	0.0	59.7	0.0	10.3	431.5	26.7
110.0	9.1	0.0	66.3	0.0	13.5	882.2	29.6
115.0	16.3	0.0	100.6	0.0	14.5	788.4	43.8
120.0	15.8	0.0	75.5	0.0	17.2	657.2	36.2
125.0	15.3	0.0	86.5	0.0	16.6	541.7	39.5
130.0	17.1	0.0	83.7	0.0	17.5	528.6	39.4
135.0	21.1	0.0	86.8	0.0	20.1	754.7	42.7
140.0	18.5	0.0	86.6	0.0	19.6	1052.2	41.6
145.0	15.0	0.0	105.8	0.0	18.1	732.7	46.3
150.0	18.9	0.0	85.0	0.0	16.9	497.9	40.2

Unvegetated 1

B1-4

10:00 pm	Trode 1		Trode 2		Trode 3		
depth (mm)	H2S uM	Fe (uM)	H2S uM	Fe (uM)	H2S uM	Fe (uM)	**Average H2S**
0.0	0.0	0.0	0.0	0.0	0.0	0.0	0.0
2.0	0.0	0.0	0.0	0.0	0.0	0.0	0.0
4.0	0.0	0.0	0.0	0.0	0.0	0.0	0.0
6.0	0.0	0.0	0.0	0.0	0.0	0.0	0.0
8.0	0.0	0.0	0.0	0.0	0.0	0.0	0.0
10.0	0.0	0.0	0.0	0.0	0.0	0.0	0.0
12.0	0.0	0.0	0.0	0.0	0.0	0.0	0.0
14.0	0.0	0.0	0.0	0.0	0.0	0.0	0.0
16.0	0.0	0.0	0.0	0.0	0.0	0.0	0.0
18.0	0.0	0.0	0.0	0.0	0.0	0.0	0.0
20.0	0.0	0.0	0.0	0.0	0.0	0.0	0.0
22.0	0.0	0.0	0.0	0.0	0.0	0.0	0.0
24.0	0.0	0.0	0.0	0.0	0.0	0.0	0.0
26.0	0.0	0.0	0.0	0.0	0.0	0.0	0.0
28.0	0.0	0.0	0.0	0.0	0.0	0.0	0.0
30.0	0.0	0.0	0.0	0.0	0.0	0.0	0.0
32.0	0.0	0.0	0.0	0.0	0.0	0.0	0.0
34.0	0.0	0.0	0.0	0.0	0.0	0.0	0.0
36.0	0.0	0.0	0.0	0.0	0.0	0.0	0.0
38.0	0.0	0.0	0.0	0.0	0.0	0.0	0.0
40.0	0.0	0.0	0.0	0.0	0.0	0.0	0.0
42.0	0.0	0.0	0.0	0.0	0.0	0.0	0.0
44.0	0.0	0.0	7.1	0.0	0.0	0.0	2.4
46.0	0.0	0.0	11.8	0.0	0.0	0.0	3.9
48.0	0.0	0.0	11.6	0.0	0.0	0.0	3.9
50.0	0.0	0.0	12.6	0.0	0.0	0.0	4.2
55.0	2.3	0.0	7.5	0.0	0.0	0.0	3.3
60.0	3.4	0.0	6.0	0.0	0.0	0.0	3.1
65.0	3.2	0.0	5.2	0.0	2.4	0.0	3.6
70.0	5.8	0.0	5.9	0.0	0.0	0.0	3.9
75.0	11.0	0.0	6.8	0.0	3.4	0.0	7.1
80.0	17.1	0.0	8.2	0.0	4.6	0.0	10.0
85.0	23.4	0.0	9.5	0.0	6.5	0.0	13.1
90.0	28.1	0.0	10.6	0.0	8.2	0.0	15.6
95.0	28.4	0.0	12.4	0.0	9.5	0.0	16.8
100.0	37.6	0.0	14.3	0.0	10.4	0.0	20.8
105.0	39.5	0.0	15.4	0.0	10.1	0.0	21.7
110.0	39.3	0.0	16.1	0.0	10.5	0.0	22.0
115.0	46.3	0.0	16.3	0.0	10.7	0.0	24.4
120.0	49.6	0.0	18.0	0.0	10.7	0.0	26.1
125.0	49.6	0.0	18.7	0.0	10.2	0.0	26.2
130.0	48.7	0.0	20.3	0.0	9.9	0.0	26.3
135.0	46.9	0.0	19.9	0.0	9.5	0.0	25.4
140.0	47.5	0.0	20.1	0.0	9.1	0.0	25.6
145.0	47.4	0.0	18.5	0.0	7.3	0.0	24.4
150.0	43.0	0.0	17.3	0.0	8.5	0.0	22.9

Unvegetated 1

B1-5 2:00 am

	Trode 1		Trode 2		Trode 3		
depth (mm)	H2S uM	Fe (uM)	H2S uM	Fe (uM)	H2S uM	Fe (uM)	**Average H2S**
0.0	0.0	0.0	0.0	0.0	0.0	0.0	0.0
2.0	0.0	0.0	0.0	0.0	0.0	0.0	0.0
4.0	0.0	0.0	0.0	0.0	0.0	0.0	0.0
6.0	0.0	0.0	0.0	0.0	0.0	0.0	0.0
8.0	0.0	0.0	0.0	0.0	0.0	0.0	0.0
10.0	0.0	0.0	0.0	0.0	0.0	0.0	0.0
12.0	0.0	0.0	0.0	0.0	0.0	0.0	0.0
14.0	0.0	0.0	0.0	0.0	0.0	0.0	0.0
16.0	0.0	0.0	4.7	0.0	0.0	0.0	1.6
18.0	0.0	0.0	3.8	0.0	0.0	0.0	1.3
20.0	0.0	0.0	2.0	0.0	0.0	0.0	0.7
22.0	0.0	0.0	0.0	0.0	0.0	0.0	0.0
24.0	0.0	0.0	0.0	0.0	0.0	0.0	0.0
26.0	0.0	0.0	0.0	0.0	0.0	0.0	0.0
28.0	0.0	0.0	0.0	0.0	0.0	0.0	0.0
30.0	0.0	0.0	0.0	0.0	0.0	0.0	0.0
32.0	0.0	0.0	0.0	0.0	0.0	0.0	0.0
34.0	0.0	0.0	0.0	0.0	0.0	0.0	0.0
36.0	0.0	0.0	0.0	0.0	0.0	0.0	0.0
38.0	0.0	0.0	0.0	0.0	0.0	0.0	0.0
40.0	0.0	0.0	0.0	0.0	0.0	0.0	0.0
42.0	0.0	0.0	0.0	0.0	0.0	0.0	0.0
44.0	0.0	0.0	0.0	0.0	0.0	0.0	0.0
46.0	0.0	0.0	0.0	0.0	0.0	0.0	0.0
48.0	0.0	0.0	9.0	0.0	0.0	0.0	3.0
50.0	0.0	0.0	8.3	0.0	0.0	0.0	2.8
55.0	0.0	0.0	5.9	0.0	0.0	0.0	2.0
60.0	0.0	0.0	5.5	0.0	0.0	0.0	1.8
65.0	0.0	0.0	6.7	0.0	0.0	0.0	2.2
70.0	0.0	0.0	4.6	0.0	0.0	0.0	1.5
75.0	0.0	0.0	3.8	0.0	0.0	0.0	1.3
80.0	0.0	0.0	3.7	0.0	0.0	0.0	1.2
85.0	0.0	0.0	4.3	0.0	1.9	0.0	2.1
90.0	0.0	0.0	4.2	0.0	0.5	0.0	1.6
95.0	0.0	0.0	4.5	0.0	0.0	0.0	1.5
100.0	0.0	0.0	4.1	0.0	0.0	0.0	1.4
105.0	0.0	0.0	8.5	0.0	0.8	0.0	3.1
110.0	0.0	0.0	8.8	0.0	0.9	0.0	3.2
115.0	0.0	0.0	9.4	0.0	1.1	0.0	3.5
120.0	0.0	0.0	9.9	0.0	1.0	0.0	3.6
125.0	0.0	0.0	11.2	0.0	0.8	0.0	4.0
130.0	0.0	0.0	12.1	0.0	0.9	0.0	4.3
135.0	0.0	0.0	12.3	0.0	0.6	0.0	4.3
140.0	0.0	0.0	13.4	0.0	0.7	0.0	4.7
145.0	0.0	0.0	13.4	0.0	0.6	0.0	4.6
150.0	0.0	0.0	13.0	0.0	0.8	0.0	4.6

Unvegetated 1

B1-6 6:00 am

	Trode 1		Trode 2		Trode 3		
depth (mm)	H2S uM	Fe (uM)	H2S uM	Fe (uM)	H2S uM	Fe (uM)	**Average H2S**
0.0	0.0	0.0	4.5	0.0	0.0	0.0	1.5
2.0	0.0	0.0	0.0	0.0	0.0	0.0	0.0
4.0	0.0	0.0	0.0	0.0	0.0	0.0	0.0
6.0	0.0	0.0	4.2	0.0	0.0	0.0	1.4
8.0	0.0	0.0	4.0	0.0	0.0	0.0	1.3
10.0	0.0	0.0	2.8	0.0	0.0	0.0	0.9
12.0	0.0	0.0	5.1	0.0	0.0	0.0	1.7
14.0	0.0	0.0	4.7	0.0	9.9	0.0	4.9
16.0	0.0	0.0	0.0	0.0	17.3	0.0	5.8
18.0	0.0	0.0	0.0	0.0	19.0	0.0	6.3
20.0	0.0	0.0	0.0	0.0	10.2	0.0	3.4
22.0	0.0	0.0	0.0	84.8	15.2	0.0	5.1
24.0	0.0	0.0	0.0	198.3	9.3	0.0	3.1
26.0	0.0	0.0	5.6	624.7	9.8	0.0	5.1
28.0	0.0	0.0	8.2	536.4	9.0	0.0	5.7
30.0	0.0	0.0	4.8	913.5	4.3	0.0	3.1
32.0	0.0	0.0	9.4	301.1	4.1	0.0	4.5
34.0	0.0	0.0	7.2	385.5	0.0	0.0	2.4
36.0	0.0	0.0	5.9	431.9	0.0	0.0	2.0
38.0	0.0	0.0	9.1	540.4	6.2	0.0	5.1
40.0	0.0	0.0	6.4	453.0	8.6	0.0	5.0
42.0	0.0	0.0	4.3	367.5	6.0	0.0	3.4
44.0	0.0	0.0	3.5	525.6	2.4	0.0	2.0
46.0	0.0	0.0	12.7	550.2	0.0	0.0	4.2
48.0	0.0	0.0	11.6	403.2	0.0	0.0	3.9
50.0	0.0	0.0	14.5	352.0	0.0	0.0	4.8
55.0	0.0	0.0	19.2	99.1	0.0	0.0	6.4
60.0	0.0	0.0	16.0	373.2	0.0	0.0	5.3
65.0	2.1	0.0	6.9	365.0	0.0	0.0	3.0
70.0	2.9	0.0	4.9	335.6	0.0	0.0	2.6
75.0	0.0	0.0	5.4	252.6	0.0	0.0	1.8
80.0	0.5	0.0	5.1	170.1	0.0	0.0	1.9
85.0	1.4	0.0	6.0	217.2	5.4	0.0	4.3
90.0	1.9	0.0	8.0	100.7	24.4	0.0	11.5
95.0	1.3	0.0	8.1	141.8	35.0	0.0	14.8
100.0	3.2	0.0	7.3	67.2	33.6	0.0	14.7
105.0	5.0	0.0	11.3	0.0	39.8	0.0	18.7
110.0	6.0	0.0	11.4	31.6	35.0	0.0	17.5
115.0	6.4	0.0	12.4	165.2	34.0	0.0	17.6
120.0	5.7	0.0	25.5	75.5	34.9	0.0	22.0
125.0	7.0	0.0	43.4	0.0	34.6	0.0	28.4
130.0	17.6	0.0	40.4	140.1	32.7	0.0	30.2
135.0	7.6	0.0	32.1	510.8	33.4	0.0	24.4
140.0	8.0	0.0	27.8	168.5	31.5	0.0	22.4
145.0	7.1	0.0	25.3	44.0	30.1	0.0	20.8
150.0	9.0	0.0	24.2	207.3	29.6	0.0	20.9

Unvegetated 2

B2-1 3:00 pm	Trode 1		Trode 2		Trode 3		
depth (mm)	H2S uM	Fe (uM)	H2S uM	Fe (uM)	H2S uM	Fe (uM)	**Average H2S**
0.0	0.0	0.0	0.0	0.0	0.0	0.0	0.0
2.0	0.0	0.0	0.0	0.0	0.0	0.0	0.0
4.0	0.0	0.0	0.0	0.0	0.0	0.0	0.0
6.0	0.0	0.0	0.0	0.0	0.0	0.0	0.0
8.0	4.2	0.0	0.0	0.0	0.0	0.0	1.4
10.0	8.4	0.0	0.0	0.0	0.0	0.0	2.8
12.0	25.8	0.0	0.0	0.0	16.6	0.0	14.1
14.0	28.9	0.0	0.0	0.0	31.0	0.0	20.0
16.0	30.6	0.0	0.0	0.0	87.8	0.0	39.5
18.0	36.8	0.0	0.0	0.0	102.2	0.0	46.3
20.0	51.6	0.0	0.0	0.0	108.7	0.0	53.4
22.0	53.3	0.0	0.0	0.0	115.3	0.0	56.2
24.0	56.0	0.0	0.0	0.0	128.4	0.0	61.5
26.0	58.3	0.0	0.0	0.0	155.0	0.0	71.1
28.0	55.9	0.0	0.0	0.0	128.0	0.0	61.3
30.0	50.3	0.0	0.0	0.0	129.7	0.0	60.0
32.0	60.8	0.0	0.0	0.0	143.7	0.0	68.2
34.0	66.5	0.0	0.0	0.0	115.8	0.0	60.8
36.0	81.4	0.0	0.0	0.0	200.9	0.0	94.1
38.0	67.7	0.0	18.4	0.0	175.6	0.0	87.2
40.0	84.4	0.0	24.9	0.0	188.2	0.0	99.2
42.0	73.8	0.0	25.3	0.0	165.4	0.0	88.2
44.0	78.2	0.0	19.2	0.0	189.5	0.0	95.7
46.0	78.3	0.0	20.1	0.0	201.4	0.0	100.0
48.0	80.5	0.0	27.1	0.0	175.2	0.0	94.3
50.0	75.6	0.0	27.5	0.0	195.3	0.0	99.5
55.0	77.0	0.0	27.1	0.0	168.6	0.0	90.9
60.0	82.5	0.0	27.5	0.0	170.8	0.0	93.6
65.0	75.6	0.0	34.5	0.0	181.2	0.0	97.1
70.0	134.5	0.0	33.2	0.0	168.6	0.0	112.1
75.0	111.4	0.0	46.7	0.0	165.9	0.0	108.0
80.0	159.8	0.0	42.4	0.0	162.1	0.0	121.4
85.0	160.4	0.0	43.2	0.0	162.1	0.0	121.9
90.0	125.3	0.0	48.0	0.0	144.6	0.0	106.0
95.0	117.5	0.0	60.3	0.0	166.8	0.0	114.9
100.0	114.9	0.0	61.2	0.0	197.4	0.0	124.5
105.0	104.8	0.0	60.3	0.0	189.1	0.0	118.1
110.0	110.5	0.0	65.9	0.0	160.3	0.0	112.3
115.0	99.1	0.0	70.3	0.0	191.7	0.0	120.4
120.0	110.1	0.0	72.1	0.0	186.5	0.0	122.9
125.0	114.4	0.0	72.5	0.0	169.0	0.0	118.7
130.0	117.9	0.0	66.4	0.0	170.8	0.0	118.4
135.0	NAN	0.0	NAN	0.0	NAN	0.0	135.2
140.0	NAN	0.0	NAN	0.0	NAN	0.0	135.2
145.0	NAN	0.0	NAN	0.0	NAN	0.0	135.2
150.0	231.9	0.0	94.0	0.0	130.3	0.0	152.0

Unvegetated 2

B2-2 7:00 pm

	Trode 1		Trode 2		Trode 3		
depth (mm)	H2S uM	Fe (uM)	H2S uM	Fe (uM)	H2S uM	Fe (uM)	**Average H2S**
0.0	0.0	0.0	40.6	0.0	33.7	0.0	24.8
2.0	0.0	0.0	39.3	0.0	17.9	0.0	19.1
4.0	0.0	0.0	46.8	0.0	14.4	0.0	20.4
6.0	0.0	0.0	55.1	0.0	24.9	0.0	26.7
8.0	7.2	0.0	66.8	0.0	31.9	0.0	35.3
10.0	20.6	0.0	83.5	0.0	41.6	0.0	48.5
12.0	158.3	0.0	86.0	0.0	73.0	0.0	105.8
14.0	103.6	0.0	130.1	0.0	66.0	0.0	99.9
16.0	103.1	0.0	141.5	0.0	70.8	0.0	105.1
18.0	118.3	0.0	153.7	0.0	77.0	0.0	116.3
20.0	139.4	0.0	164.7	0.0	76.1	0.0	126.7
22.0	139.3	0.0	184.0	0.0	84.8	0.0	136.0
24.0	143.0	0.0	190.4	0.0	79.2	0.0	137.6
26.0	132.1	0.0	162.9	0.0	86.5	0.0	127.2
28.0	189.1	0.0	197.4	0.0	81.3	0.0	156.0
30.0	188.7	0.0	214.5	0.0	81.3	0.0	161.5
32.0	185.3	0.0	209.6	0.0	75.6	0.0	156.8
34.0	170.7	0.0	219.7	0.0	88.8	0.0	159.7
36.0	170.4	0.0	215.6	0.0	99.6	0.0	161.9
38.0	168.2	0.0	220.5	0.0	77.0	0.0	155.2
40.0	168.9	0.0	217.5	0.0	80.0	0.0	155.5
42.0	161.2	0.0	207.1	0.0	63.3	0.0	143.9
44.0	167.1	0.0	216.2	0.0	64.2	0.0	149.2
46.0	166.1	0.0	216.3	0.0	84.7	0.0	155.7
48.0	141.7	0.0	210.5	0.0	83.0	0.0	145.1
50.0	145.2	0.0	212.7	0.0	89.7	0.0	149.2
55.0	144.8	0.0	209.2	0.0	82.1	0.0	145.4
60.0	145.7	0.0	196.5	0.0	79.5	0.0	140.6
65.0	138.6	0.0	189.1	0.0	69.1	0.0	132.3
70.0	141.8	0.0	207.1	0.0	57.3	0.0	135.4
75.0	146.0	0.0	213.5	0.0	59.4	0.0	139.7
80.0	147.7	0.0	201.8	0.0	42.4	0.0	130.6
85.0	149.1	0.0	208.8	0.0	42.4	0.0	133.4
90.0	149.7	0.0	214.0	0.0	48.3	0.0	137.3
95.0	147.0	0.0	206.2	0.0	40.6	0.0	131.3
100.0	134.1	0.0	203.9	0.0	48.3	0.0	128.8
105.0	147.9	0.0	203.5	0.0	40.6	0.0	130.7
110.0	150.9	0.0	203.5	0.0	50.8	0.0	135.1
115.0	144.8	0.0	195.7	0.0	45.5	0.0	128.7
120.0	144.2	0.0	187.4	0.0	73.5	0.0	135.1
125.0	130.7	0.0	154.8	0.0	64.7	0.0	116.7
130.0	136.4	0.0	166.0	0.0	66.7	0.0	123.0
135.0	129.8	0.0	196.6	0.0	92.6	0.0	139.7
140.0	164.1	0.0	194.4	0.0	48.3	0.0	135.6
145.0	262.2	0.0	186.7	0.0	55.2	0.0	168.0
150.0	347.7	0.0	217.1	0.0	160.3	0.0	241.7

Unvegetated 2

B2-3 11:00 pm

	Trode 1		Trode 2		Trode 3		
depth (mm)	H2S uM	Fe (uM)	H2S uM	Fe (uM)	H2S uM	Fe (uM)	**Average H2S**
0.0	0.0	0.0	47.2	0.0	63.8	0.0	37.0
2.0	0.0	0.0	0.0	0.0	22.7	0.0	7.6
4.0	0.0	0.0	0.0	0.0	21.8	0.0	7.3
6.0	0.0	0.0	0.0	0.0	52.4	0.0	17.5
8.0	0.0	0.0	0.0	0.0	57.7	0.0	19.2
10.0	0.0	0.0	0.0	0.0	60.7	0.0	20.2
12.0	0.0	0.0	0.0	0.0	79.1	0.0	26.4
14.0	0.0	0.0	0.0	0.0	54.6	0.0	18.2
16.0	0.0	0.0	0.0	0.0	68.6	0.0	22.9
18.0	0.0	0.0	0.0	0.0	88.3	0.0	29.4
20.0	0.0	0.0	0.0	0.0	77.3	0.0	25.8
22.0	35.9	0.0	0.0	0.0	114.0	0.0	50.0
24.0	28.4	0.0	0.0	0.0	105.0	0.0	44.5
26.0	21.4	0.0	0.0	0.0	92.2	0.0	37.9
28.0	17.9	0.0	0.0	0.0	89.1	0.0	35.7
30.0	17.0	0.0	0.0	0.0	119.2	0.0	45.4
32.0	17.9	0.0	0.0	0.0	102.3	0.0	40.1
34.0	18.8	0.0	0.0	0.0	96.3	0.0	38.4
36.0	24.9	0.0	0.0	0.0	107.1	0.0	44.0
38.0	27.5	0.0	0.0	0.0	83.5	0.0	37.0
40.0	21.4	0.0	0.0	0.0	90.4	0.0	37.3
42.0	51.2	0.0	0.0	0.0	37.0	0.0	29.4
44.0	52.4	0.0	0.0	0.0	122.0	0.0	58.1
46.0	52.9	0.0	0.0	0.0	68.9	0.0	40.6
48.0	49.4	0.0	15.3	0.0	56.2	0.0	40.3
50.0	45.6	0.0	0.0	0.0	43.4	0.0	29.7
55.0	59.5	0.0	0.0	0.0	109.2	0.0	56.2
60.0	52.1	0.0	0.0	0.0	77.9	0.0	43.3
65.0	55.6	0.0	0.0	0.0	115.3	0.0	57.0
70.0	63.5	0.0	0.0	0.0	106.6	0.0	56.7
75.0	60.7	0.0	0.0	0.0	105.8	0.0	55.5
80.0	59.9	0.0	0.0	0.0	43.4	0.0	34.4
85.0	66.0	0.0	0.0	0.0	82.1	0.0	49.4
90.0	69.5	0.0	0.0	0.0	88.3	0.0	52.6
95.0	69.5	0.0	0.0	0.0	84.4	0.0	51.3
100.0	65.6	0.0	0.0	0.0	57.5	0.0	41.0
105.0	64.7	0.0	0.0	0.0	103.1	0.0	56.0
110.0	63.3	0.0	0.0	0.0	92.6	0.0	52.0
115.0	59.0	0.0	0.0	0.0	85.2	0.0	48.1
120.0	58.1	0.0	38.9		62.6	0.0	53.2
125.0	58.6	0.0	39.7	0.0	134.2	0.0	77.5
130.0	55.1	0.0	26.6	0.0	68.9	0.0	50.2
135.0	55.0	0.0	11.5	0.0	75.3	0.0	47.3
140.0	48.5	0.0	22.3	0.0	49.8	0.0	40.2
145.0	39.8	0.0	19.7	0.0	68.9	0.0	42.8
150.0	42.0	0.0	12.0	0.0	37.0	0.0	30.3

Unvegetated 2

B2-4 3:00

am	Trode 1		Trode 2		Trode 3		
depth (mm)	H2S uM	Fe (uM)	H2S uM	Fe (uM)	H2S uM	Fe (uM)	**Average H2S**
0.0	0.0	0.0	0.0	0.0	0.0	0.0	0.0
2.0	0.0	0.0	0.0	0.0	0.0	0.0	0.0
4.0	0.0	0.0	0.0	0.0	0.0	0.0	0.0
6.0	0.0	0.0	0.0	0.0	0.0	0.0	0.0
8.0	0.0	0.0	0.0	0.0	10.0	0.0	3.3
10.0	0.0	0.0	0.0	0.0	3.8	0.0	1.3
12.0	0.0	0.0	0.0	0.0	18.4	0.0	6.1
14.0	0.0	0.0	0.0	0.0	23.2	0.0	7.7
16.0	0.0	0.0	0.0	0.0	29.7	0.0	9.9
18.0	0.0	0.0	0.0	0.0	14.9	0.0	5.0
20.0	0.0	0.0	0.0	0.0	32.0	0.0	10.7
22.0	0.0	0.0	0.0	0.0	39.3	0.0	13.1
24.0	0.0	0.0	0.0	0.0	40.6	0.0	13.5
26.0	0.0	0.0	0.0	0.0	42.0	0.0	14.0
28.0	0.0	0.0	0.0	0.0	57.9	0.0	19.3
30.0	0.0	0.0	0.0	0.0	48.9	0.0	16.3
32.0	0.0	0.0	0.0	0.0	45.9	0.0	15.3
34.0	0.0	0.0	0.0	0.0	49.8	0.0	16.6
36.0	0.0	0.0	0.0	0.0	46.3	0.0	15.4
38.0	0.0	0.0	0.0	0.0	54.6	0.0	18.2
40.0	0.0	0.0	0.0	0.0	79.5	0.0	26.5
42.0	0.0	0.0	0.0	0.0	59.0	0.0	19.7
44.0	0.0	0.0	0.0	0.0	38.9	0.0	13.0
46.0	0.0	0.0	0.0	0.0	45.0	0.0	15.0
48.0	0.0	0.0	0.0	0.0	32.8	0.0	10.9
50.0	0.0	0.0	92.2	0.0	103.4	0.0	65.2
55.0	0.0	0.0	69.6	0.0	102.2	0.0	57.3
60.0	0.0	0.0	66.0	0.0	69.1	0.0	45.0
65.0	0.0	0.0	83.0	0.0	53.7	0.0	45.6
70.0	0.0	0.0	52.9	0.0	60.7	0.0	37.9
75.0	0.0	0.0	33.7	0.0	84.9	0.0	39.5
80.0	0.0	0.0	84.4	0.0	48.5	0.0	44.3
85.0	0.0	0.0	87.4	0.0	55.6	0.0	47.7
90.0	0.0	0.0	64.2	0.0	55.5	0.0	39.9
95.0	0.0	0.0	60.3	0.0	79.5	0.0	46.6
100.0	0.0	0.0	134.2	0.0	80.4	0.0	71.5
105.0	0.0	0.0	67.3	0.0	76.5	0.0	47.9
110.0	0.0	0.0	103.6	0.0	62.5	0.0	55.4
115.0	0.0	0.0	39.4	0.0	69.0	0.0	36.1
120.0	0.0	0.0	67.8	0.0	81.3	0.0	49.7
125.0	0.0	0.0	34.5	0.0	62.9	0.0	32.5
130.0	0.0	0.0	83.4	0.0	66.9	0.0	50.1
135.0	0.0	0.0	33.8	0.0	70.9	0.0	34.9
140.0	0.0	0.0	103.4	0.0	84.3	0.0	62.6
145.0	0.0	0.0	88.1	0.0	66.9	0.0	51.7
150.0	0.0	0.0	89.1	0.0	49.8	0.0	46.3

Unvegetated 2

B2-5 7:00 am

	Trode 1		Trode 2		Trode 3		
depth (mm)	H2S uM	Fe (uM)	H2S uM	Fe (uM)	H2S uM	Fe (uM)	**Average H2S**
0.0	0.0	0.0	14.0	0.0	0.0	0.0	4.7
2.0	0.0	0.0	0.0	0.0	0.0	0.0	0.0
4.0	0.0	0.0	0.0	0.0	0.0	0.0	0.0
6.0	0.0	0.0	0.0	0.0	0.0	0.0	0.0
8.0	0.0	0.0	0.0	0.0	27.1	0.0	9.0
10.0	0.0	0.0	0.0	0.0	25.8	0.0	8.6
12.0	0.0	0.0	0.0	0.0	28.0	0.0	9.3
14.0	0.0	0.0	0.0	0.0	30.6	0.0	10.2
16.0	0.0	0.0	0.0	0.0	33.8	0.0	11.3
18.0	0.0	0.0	0.0	0.0	33.6	0.0	11.2
20.0	0.0	0.0	62.6	0.0	44.6	0.0	35.7
22.0	0.0	0.0	93.5	0.0	38.5	0.0	44.0
24.0	0.0	0.0	78.2	0.0	35.9	0.0	38.0
26.0	0.0	0.0	57.2	0.0	40.7	0.0	32.6
28.0	0.0	0.0	34.5	0.0	38.4	0.0	24.3
30.0	0.0	0.0	56.8	0.0	40.2	0.0	32.4
32.0	0.0	0.0	42.1	0.0	41.5	0.0	27.9
34.0	0.0	0.0	30.6	0.0	47.3	0.0	26.0
36.0	0.0	0.0	67.3	0.0	49.0	0.0	38.8
38.0	0.0	0.0	51.2	0.0	48.5	0.0	33.2
40.0	0.0	0.0	32.4	0.0	55.1	0.0	29.2
42.0	0.0	0.0	79.5	0.0	64.6	0.0	48.0
44.0	0.0	0.0	40.6	0.0	67.3	0.0	36.0
46.0	0.0	0.0	0.0	0.0	65.9	0.0	22.0
48.0	0.0	0.0	59.5	0.0	69.9	0.0	43.1
50.0	0.0	0.0	69.5	0.0	76.4	0.0	48.6
55.0	0.0	0.0	79.1	0.0	76.0	0.0	51.7
60.0	0.0	0.0	45.2	0.0	78.6	0.0	41.3
65.0	0.0	0.0	36.8	0.0	84.3	0.0	40.4
70.0	0.0	0.0	42.1	0.0	58.1	0.0	33.4
75.0	0.0	0.0	80.4	0.0	57.7	0.0	46.0
80.0	0.0	0.0	39.1	0.0	50.3	0.0	29.8
85.0	0.0	0.0	52.9	0.0	46.8	0.0	33.2
90.0	0.0	0.0	48.3	0.0	50.7	0.0	33.0
95.0	0.0	0.0	42.1	0.0	52.0	0.0	31.4
100.0	0.0	0.0	75.3	0.0	52.0	0.0	42.4
105.0	0.0	0.0	46.6	0.0	48.1	0.0	31.6
110.0	0.0	0.0	0.0	0.0	46.0	0.0	15.3
115.0	0.0	0.0	0.0	0.0	39.1	0.0	13.0
120.0	0.0	0.0	0.0	0.0	39.1	0.0	13.0
125.0	0.0	0.0	0.0	0.0	57.5	0.0	19.2
130.0	0.0	0.0	85.2	0.0	48.3	0.0	44.5
135.0	0.0	0.0	73.8	0.0	48.8	0.0	40.9
140.0	0.0	0.0	43.4	0.0	41.6	0.0	28.3
145.0	0.0	0.0	26.3	0.0	40.9	0.0	22.4
150.0	0.0	0.0	0.0	0.0	37.5	0.0	12.5

Unvegetated 2

B2-6 11:00 am

	Trode 1		Trode 2		Trode 3		
depth (mm)	H2S uM	Fe (uM)	H2S uM	Fe (uM)	H2S uM	Fe (uM)	**Average H2S**
0.0	0.0	0.0	0.0	0.0	17.5	0.0	5.8
2.0	0.0	0.0	0.0	0.0	6.4	0.0	2.1
4.0	0.0	0.0	0.0	0.0	7.2	0.0	2.4
6.0	0.0	0.0	0.0	0.0	18.8	0.0	6.3
8.0	0.0	0.0	0.0	0.0	40.1	0.0	13.4
10.0	0.0	0.0	0.0	0.0	31.4	0.0	10.5
12.0	0.0	0.0	0.0	0.0	21.5	0.0	7.2
14.0	0.0	0.0	0.0	0.0	53.1	0.0	17.7
16.0	0.0	0.0	0.0	0.0	69.1	0.0	23.0
18.0	0.0	0.0	0.0	0.0	69.2	0.0	23.1
20.0	0.0	0.0	0.0	0.0	84.4	0.0	28.1
22.0	0.0	0.0	0.0	0.0	88.4	0.0	29.5
24.0	0.0	0.0	0.0	0.0	106.3	0.0	35.4
26.0	0.0	0.0	0.0	0.0	111.4	0.0	37.1
28.0	0.0	0.0	0.0	0.0	107.0	0.0	35.7
30.0	0.0	0.0	0.0	0.0	114.1	0.0	38.0
32.0	0.0	0.0	0.0	0.0	123.6	0.0	41.2
34.0	0.0	0.0	0.0	0.0	119.4	0.0	39.8
36.0	0.0	0.0	0.0	0.0	135.8	0.0	45.3
38.0	0.0	0.0	0.0	0.0	134.1	0.0	44.7
40.0	0.0	0.0	0.0	0.0	131.6	0.0	43.9
42.0	0.0	0.0	0.0	0.0	131.2	0.0	43.7
44.0	0.0	0.0	0.0	0.0	135.9	0.0	45.3
46.0	0.0	0.0	0.0	0.0	139.6	0.0	46.5
48.0	0.0	0.0	0.0	0.0	143.2	0.0	47.7
50.0	0.0	0.0	0.0	0.0	151.3	0.0	50.4
55.0	0.0	0.0	0.0	0.0	143.3	0.0	47.8
60.0	0.0	0.0	0.0	0.0	4.6	0.0	1.5
65.0	0.0	0.0	0.0	0.0	158.7	0.0	52.9
70.0	0.0	0.0	0.0	0.0	159.4	0.0	53.1
75.0	0.0	0.0	0.0	0.0	142.9	0.0	47.6
80.0	0.0	0.0	0.0	0.0	155.1	0.0	51.7
85.0	0.0	0.0	0.0	0.0	172.9	0.0	57.6
90.0	0.0	0.0	0.0	0.0	149.8	0.0	49.9
95.0	0.0	0.0	0.0	0.0	173.9	0.0	58.0
100.0	0.0	0.0	0.0	0.0	139.2	0.0	46.4
105.0	0.0	0.0	0.0	0.0	177.9	0.0	59.3
110.0	0.0	0.0	0.0	0.0	154.2	0.0	51.4
115.0	0.0	0.0	0.0	0.0	147.3	0.0	49.1
120.0	0.0	0.0	0.0	0.0	162.9	0.0	54.3
125.0	0.0	0.0	0.0	0.0	176.5	0.0	58.8
130.0	0.0	0.0	0.0	0.0	148.6	0.0	49.5
135.0	0.0	0.0	1.9	0.0	153.4	0.0	51.8
140.0	0.0	0.0	19.2	0.0	169.1	0.0	62.8
145.0	0.0	0.0	10.0	0.0	159.4	0.0	56.5
150.0	0.0	0.0	15.3	0.0	126.4	0.0	47.2

Reactive metals (mg/kg, cold HCl Analysis)

Sample id	Depth (cm)	Fe	Mn	Al	Ba	Ca	Cd	Co	Cr	Cu	K	Li	Mg	Ni	P	Sr	Ti	V	Zn
SG1 light	0-2	9860	60.5	36300	27	3060	<1.27	3.36	11.8	13.9	2540	9.63	5030	12.9	718	32.7	305	22.9	136
SG1 light	2-4	8280	57.4	76700	31	2170	<1.02	<2.55	11.6	14.9	1970	8.58	3830	15.3	725	23.8	264	24.5	134
SG1 light	4-6	8540	55.1	70700	26.7	5450	<0.784	2.67	11.3	8.97	1910	8.6	3830	12.3	671	35.6	273	24	98.6
SG1 light	6-8	7600	49.8	30500	23.7	2350	<1.19	3.53	10.5	27.8	1740	8.13	3660	11.4	697	23.1	273	18.8	99.2
SG1 light	8-10	7100	45	49700	19.1	1750	<0.816	2.63	9.44	8.97	1630	7.17	3350	11.2	504	19.9	240	19.1	74.4
SG1 light	10-12	7400	51.2	86500	19.7	1840	<1.19	<2.97	9.36	11.4	1610	7.33	3340	13.2	547	19.7	235	22.9	67.1
SG1 light	12-14	7900	48.6	67100	39.9	2460	<0.958	3.12	34	8.84	2030	8.47	5440	12.1	420	37.6	268	21	489
SG1 light	14-16	8050	53.6	86800	24.9	1680	<1.05	2.97	11	21.6	1840	8.17	4030	14	500	20.7	258	25.4	387
SG1 light	16-18	6990	46.3	52200	23.8	1720	<1.13	<2.83	11.3	9.08	1670	7.41	3720	12.4	429	20	251	19.7	401
SG2 light	0-2	9260	56.8	67500	24.6	2770	<0.858	3.37	12.7	12.5	2380	9.28	4970	13.1	491	30.5	310	25.8	335
SG2 light	2-4	9470	58.1	86200	27.9	2640	1.08	3.73	14.1	14	2210	9.51	4730	13.2	498	27.6	304	26.5	392
SG2 light	4-6	8910	59.2	85500	25.4	2440	<1.05	3.01	12.7	22.7	2010	9.3	4530	15.9	483	24.9	291	26.7	397
SG2 light	6-8	8400	54.1	144000	25.8	2040	<1.25	<3.11	15.6	12.4	1900	8.74	4380	11.7	410	24	297	32.9	467
SG2 light	8-10	7480	50.2	101000	16.8	1750	<1.01	<2.53	12.6	18.8	1680	7.59	3470	10.3	440	20.1	264	27.2	80.6
SG2 light	10-12	7360	50	75700	20.8	1700	<1.05	2.63	11.7	9.19	1500	7.48	3240	10.4	410	20.2	264	23.1	54.9
SG2 light	12-14	8170	51.3	18900	50.8	2110	<1.14	4.7	13.7	7.81	1720	8.68	3930	12.3	486	22.8	252	14.9	64.7
SG2 light	14-16	8090	51.2	46600	23.4	1640	<0.896	2.63	11.2	8.43	1750	8.82	3820	10.8	457	20.4	284	19.9	54.8
SG2 light	16-18	8210	55.8	113000	20.3	1590	<1.15	<2.86	12.5	13.5	1690	8.8	3700	11.3	493	19	270	28.9	63.4
SG2 light	18-20	6930	44.5	20400	21.2	9470	0.674	2.91	11.6	9.93	1510	7.73	3360	10.1	410	50.3	245	16	58.2
UV1 light	0-2	8870	57.1	9850	21.9	5250	<0.800	3.44	11.6	12.2	1810	9.31	4150	12.9	556	39.3	301	17.3	75.4
UV1 light	2-4	8850	59.3	86000	25.3	2500	<1.06	3.39	11	11	1670	8.64	3740	14.6	547	25.7	290	25.3	71.7
UV1 light	4-6	7950	54.3	79900	23	1970	<1.20	3.39	10.4	11.1	1600	8.45	3490	10.7	535	20.4	268	22.3	63.9
UV1 light	6-8	8690	54.6	164000	19.5	2230	2.06	<2.75	13.7	12.9	1750	8.53	3780	8.98	470	23.6	312	36.2	68.4
UV1 light	8-10	7720	46.3	124000	16.5	1330	<1.16	<2.89	11	9.71	1570	8.05	3370	9.79	436	17.6	260	29.1	53.2
UV1 light	10-12	7780	46.9	64600	17.3	1810	<1.17	<2.94	9.27	10.1	1640	8.06	3680	12.5	501	22.6	290	23.8	47.9
UV1 light	12-14	8660	59.3	78400	45.3	1700	<1.17	<2.92	9.88	15.8	1810	9.01	4050	12.9	456	21.5	298	26.6	68.1
UV1 light	14-16	8150	52.6	70200	22.3	1640	<0.948	3.04	12.5	10.1	1780	8.78	3790	12.2	447	20.4	288	24.1	45.4
UV1 light	16-18	7980	48.6	6640	21.6	2040	<0.983	3.09	13.6	12	1940	8.63	4480	11	460	26.3	303	17.2	51.1
UV1 light	18-20	7800	49.9	28500	20.4	2430	<0.673	3.27	13.1	7.63	1870	8.51	4290	11.1	446	26.9	283	19.1	56.7
UV2 light	0-2	8580	58.8	113000	26.4	3010	<1.10	3.1	12.6	18.7	1740	8.1	3870	9.99	716	29.6	273	29	108
UV2 light	2-4	9740	63.6	80500	29.2	5290	0.976	2.61	13.2	12.5	3190	9.46	8370	12.2	663	57.8	301	27.4	81.5
UV2 light	4-6	10400	66.7	21200	42.3	3450	<1.40	3.84	15.1	10.4	2260	9.57	5180	14.7	688	36.9	327	19.3	87.3
UV2 light	6-8	7820	51.2	68000	22.9	2150	<0.917	3.2	14.5	12.6	1640	7.43	3550	10.2	475	23.3	263	22	133
UV2 light	8-10	7600	51	52100	19.9	2080	<1.04	3.9	16.9	10.7	1630	7.55	3590	10.4	456	21	251	18.7	73.4
UV2 light	10-12	7320	49.5	59700	18.9	1510	<1.29	<3.22	11.3	13.1	1630	7.61	3460	11.6	465	18.8	260	19.2	67.1
UV2 light	12-14	7880	48.7	82500	39.6	2510	<1.12	3.7	10.4	8.75	3230	8.74	8860	10	517	47.4	286	25.1	89.2
UV2 light	14-16	7430	49.4	48400	20.8	1500	<1.03	3.52	11.5	8.9	1740	8.01	3950	12.4	426	20.1	277	20.7	46.3
UV2 light	16-18	7550	45.6	5510	18.8	2400	<1.03	3.86	18.4	8.05	1730	7.84	3690	11	414	23.7	280	17.7	67.3
UV2 light	18-20	7790	46.1	45100	25.9	1790	<0.945	3.88	12.2	9.22	1810	8	3840	9.56	498	22.3	285	21	80.7
SG1 dark	0-2	9700	68.2	97300	22.8	2760	<0.900	3.33	13.2	13	2030	9.13	4810	13.9	711	32.1	317	29.7	61.5
SG1 dark	2-4	7920	53.9	121000	20.4	1590	<0.943	2.63	11.8	14.8	1660	7.94	3650	12.4	518	19.7	270	30.2	53.8
SG1 dark	4-6	7650	53.7	122000	19.9	1480	<1.07	<2.67	12.1	13.7	1820	7.92	3980	11.9	490	20.7	284	30.6	55
SG1 dark	6-8	6670	44	83100	19.9	18600	1.02	2.93	10	7.77	1800	7.09	3330	8.3	516	75	247	25.1	52.7
SG1 dark	8-10	7120	44.1	88700	20.1	1590	<1.22	<3.04	11.2	6.66	1910	7.94	4190	10.8	551	22.3	286	22.8	46.8
SG1 dark	10-12	7840	51.5	47500	17.9	2570	<0.898	3.44	11.7	11.2	1860	8.08	4230	11.6	516	26.6	284	21.8	48.8
SG1 dark	12-14	7440	53.3	105000	28	1820	<0.885	2.68	11.6	14	2050	8.16	4650	11.1	416	25.9	280	29.5	61
SG1 dark	14-16	7400	51.6	89500	21.9	1590	<1.00	<2.50	10.9	7.9	1860	7.88	4140	10.1	452	21.6	269	25.6	44
SG1 dark	16-18	7510	47.8	59000	17.8	2080	0.773	4.2	11.7	8.2	2440	8.27	5880	11.1	438	30.7	280	23.2	44.7
SG1 dark	18-20	6880	43.3	21800	17.3	2580	<0.706	2.24	9.8	13.3	1860	7.51	4110	10.8	398	25.6	278	17.7	48
SG2 dark	0-2	8310	57.4	108000	21	3200	<1.07	3.23	10.8	15.9	1860	8.04	4000	13.3	655	28.3	290	29	65.6
SG2 dark	2-4	7680	49.6	62600	20.3	1950	0.852	2.51	9.71	11.7	2050	8.06	4410	11.2	492	26	283	21.7	52.4
SG2 dark	4-6	7060	49.5	67800	21.7	3740	<0.950	3.4	9.72	12.4	2240	7.39	5670	13.2	507	35.3	256	20.4	52
SG2 dark	6-8	7130	44.2	36000	19.7	1880	<0.949	3.44	8.93	12.6	1800	7.36	4070	11.5	483	23	256	15.9	50.5
SG2 dark	8-10	7770	49.1	75100	19.8	1700	1.15	2.17	10.6	10.5	1930	7.86	4080	10.5	437	22.2	280	24.4	46.1
SG2 dark	10-12	8140	50.7	114000	27.4	1850	<1.04	<2.59	10.5	28.5	1850	7.96	3840	9.39	461	22.8	304	31.7	48.5
SG2 dark	12-14	7540	47.3	95900	28.3	1750	1.3	2.8	11.4	9.72	1940	7.94	4120	8.44	446	22.7	277	27.2	50.2
SG2 dark	14-16	7100	46.4	84100	18	1430	1.47	3.11	9.87	9.47	1710	7.24	3390	8.42	411	18.2	252	22.6	41.8
SG2 dark	16-18	7310	46.7	131000	19.6	1630	<1.25	<3.12	11.6	9.54	1700	7.1	3460	12.7	498	20	259	28.4	49.1
SG2 dark	18-20	7240	46	132000	22.1	1620	1.32	<2.83	12.4	12.3	1690	7.37	3520	7.51	451	19.2	269	32.6	45.1
UV1 dark	0-2	9740	58.7	71300	23.7	3350	<1.11	<2.78	19.5	13.6	2340	9.32	4860	13.8	663	32.9	295	23.1	674
UV1 dark	2-4	8090	50.5	10200	36.8	2330	<1.10	3.91	15.2	7.14	1810	7.77	3700	13	579	23.8	260	13.9	333
UV1 dark	4-6	7870	48.8	48500	40.2	2520	<1.09	3.62	16.8	8.76	1730	7.41	3630	11.3	469	25.1	275	18.3	249
UV1 dark	6-8	8730	54.6	40200	27.1	3450	<1.14	3.38	17.7	8.95	1860	8.01	4080	11.1	531	29.1	289	18.6	347
UV1 dark	8-10	7040	41.9	4490	25.9	1720	<1.28	3.43	18.8	7.96	1670	7.11	3540	8.51	460	19.8	247	13.7	238
UV1 dark	10-12	7000	46.2	47400	17.9	2060	<1.25	3.75	121	25.4	1840	7.38	3520	10.4	544	20.2	259	18.6	412
UV1 dark	12-14	6810	40.6	21300	37.1	1470	<0.902	2.77	9.57	7.09	1610	6.89	3350	9.66	419	18.6	245	15.9	222
UV1 dark	14-16	8020	52.3	82800	24.4	1660	<1.12	<2.80	10.6	10.5	1830	8.07	3730	11.4	524	19.6	276	21.5	82
UV1 dark	16-18	7660	48	25400	23.9	1700	<1.39	<3.47	29.4	12	1780	7.79	3600	14.5	475	20.2	277	16.5	269
UV1 dark	18-20	7970	47.3	22000	42.3	1590	<1.29	<3.22	14.2	22.1	1930	8.02	3880	12.8	531	21.1	284	17.4	207
UV2 dark	0-2	10000	61.3	90200	25.9	3080	<1.15	<2.86	12.5	14.7	2400	9.36	5040	12.1	655	33.4	303	26.3	82.6
UV2 dark	2-4	9240	58.5	46300	19.9	3050	<0.980	3.36	12.2	13.3	2020	8.85	4200	11.8	584	29.4	287	17.4	71.6
UV2 dark	4-6	8980	55.6	49200	24.1	2420	<1.27	3.71	21.2	10.6	1920	8.62	4060	12	573	26.5	284	20	80.5
UV2 dark	6-8	8260	52.5	47200	19.3	2640	<1.03	2.6	13.4	11.5	1790	7.9	3900	11.8	529	26.7	281	20.1	79.8
UV2 dark	8-10	7260	45.7	47600	17.5	1980	0.728	3.17	11.2	7.99	1680	7.04	3500	9.58	430	21	241	17.5	52.2
UV2 dark	10-12	7860	47.5	86600	16.7	1870	1.2	<2.91	17.1	29.7	1820	7.91	3740	10.8	465	21.7	275	25.2	93.6
UV2 dark	12-14	7350	46.3	20000	21.2	1750	<0.751	2.8	10.6	10.1	1740	7.61	3600	11	467	19.9	258	15.1	75.6
UV2 dark	14-16	7360	46.3	5050	24	1500	<1.02	3.58	9.05	11.4	1710	7.79	3470	10.4	418	18.4	263	13.8	60.7
UV2 dark	16-18	7460	47.1	7220	18.1	1620	<0.957	3.27	11	8.4	1760	7.88	3670	11.4	455	21.1	287	14.4	74
UV2 dark	18-20	7590	48.2	63000	20.1	1800	<1.05	<2.64	11.6	11.6	1780	7.73	3700	9.51	501	21.6	277	21.7	71.2
HTSG	0-2	8560	49.7	79100	17.4	2960	<1.25	3.19	13.7	15.5	1810	8	4030	9.94	528	29	262	22.8	79.1
HTSG	2-4	7350	46.2	22300	15.3	2240	<1.01	3.53	10.4	8.84	1610	7.46	3460	9.93	455	20.7	242	13.2	63.3
HTSG	4-6	6620	39	3560	17	1900	<1.04	3.02	9.45	11.1	1460	6.83	3190	10.4	379	18.5	221	10.5	67.1
HTSG	6-8	6570	42.8	44300	19	2240	<1.01	2.67	10.1	9.01	1410	6.97	3100	9.22	438	19	221	15.2	69.9
HTSG	8-10	6650	40.1	14500	20.1	1800	<0.713	3.1	10.7	8.07	1470	6.88	3120	10.1	371	18.9	222	13.4	56.3
HTSG	10-12	6880	46.3	38600	14.5	1750	<1.12	3	12.3	7.55	1580	6.89	3260	9.88	497	18.9	224	15	72.1
HTSG	12-14	7300	46	19400	20.3	1750	<1.03	3.31	11.4	7.88	1640	7.65	3700	11.7	447	19.1	259	15	85.9
HTSG	14-16	7430	44.9	33500	17	1420	<0.964	2.46	10.9	5.44	1640	7.72	3420	11.6	466	16.4	252	15.4	59.4
HTUV	0-2	6490	35.9	62800	14	2030	0.902	2.29	13.3	8.41	1280	6.14	2840	7.96	596	19.9	198	17.5	280
HTUV	2-4	5780	32.5	26100	29	1760	<1.19	<2.97	9.93	7.14	1200	5.5	2530	7.22	486	17.5	186	10.6	310
HTUV	4-6	5970	34.8	4600	24.4	1890	<1.09	3.49	11.6	4.9	1210	6.15	2670	9.42	408	17	210	10.1	152
HTUV	6-8	5290	33.2	53400	16.6	1590	<1.24	<3.10	10.8	29.9	1110	5.34	2320	8.62	433	14.6	204	13.6	138
HTUV	8-10	5880	33.9	9910	16.6	1790	<1.20	<2.99	10.5	10.5	1250	5.8	2620	7.73	374	16.5	193	8.97	130
HTUV	10-12	5720	34.8	9420	14.5	1850	<1.19	<2.97	68.6	8.19	1260	5.95	2600	8.31	363	15.9	200	8.87	239
HTUV	12-14	6580	39.5	38900	31.6	1840	<1.17	<2.93	10.3	16.7	1450	6.85	2970	9.98	438	17.5	216	11.2	170
HTUV	14-16	6590	39	25500	16.8	1940	<1.25	3.33	8.87	31.4	1410	6.86	2950	9.8	453	17.7	222	11.6	93.6
HTUV	16-18	6030	36.4	5820	14.8	1920	<1.10	3.79	17.4	5.15	1360	6.34	2920	8.45	382	18.1	211	11.2	129
HTUV	18-20	6370	40.3	30300	24	10100	<1.07	<2.68	10.6	8.08	1380	6.56	2820	10.4	452	45.3	217	14.1	99.5

SG light	18-20	NAN	408.3	NAN	190.8	NAN	NAN	NAN	0.9	NAN	36.3	NAN	124.1	NAN	0.8	NAN	NAN	NAN	NAN	NAN	NAN	6.9
SG dark	0-2	329.8	319.0	131.8	152.5	41.9	4.5	1.2	1.3	58.2	46.9	173.7	148.8	1.2	1.0	0.5	8.0	19.4	3.4	0.8	0.056	7.1
SG dark	2-4	304.9	315.5	148.1	161.2	7.7	17.2	1.2	1.1	43.5	39.9	141.8	137.5	1.0	0.9	0.5	1.1	12.6	3.4	1.4	0.058	7.1
SG dark	4-6	295.7	463.0	152.3	165.6	6.2	5.2	1.6	1.2	39.4	36.2	137.0	126.4	1.0	0.9	0.3	0.0	1.1	2.2	3.2	0.052	7.1
SG dark	6-8	419.8	446.1	145.6	208.5	6.5	13.2	2.2	1.3	38.3	38.5	119.4	127.7	0.8	0.8	0.3	0.0	5.7	NAN	1.3	0.059	7.1
SG dark	8-10	435.9	610.7	199.0	222.9	7.9	12.6	1.4	1.8	34.6	42.3	127.5	139.1	0.8	0.9	0.3	NAN	3.4	2.2	4.4	NAN	7.2
SG dark	10-12	402.7	554.8	200.3	242.3	12.5	6.3	1.8	1.3	39.4	41.7	140.4	145.8	0.9	0.9	0.5	NAN	10.3	3.1	2.3	NAN	7.1
SG dark	12-14	464.7	511.0	192.1	230.7	3.0	5.5	1.3	1.3	35.5	41.4	133.2	135.0	1.0	0.9	NAN	NAN	NAN	4.3	2.1	NAN	7.2
SG dark	14-16	302.5	488.1	188.0	231.4	6.6	5.2	1.3	1.3	41.2	36.2	132.5	127.1	0.9	0.8	NAN	NAN	NAN	4.9	6.3	NAN	7.2
SG dark	16-18	447.2	484.7	177.6	207.3	5.3	6.1	1.2	0.9	36.7	36.5	134.5	130.9	0.9	0.9	2.2	0.0	69.6	5.1	0.8	0.056	7.2
SG dark	18-20	439.9	434.2	207.9	192.9	4.0	7.2	1.3	1.3	32.8	38.7	123.2	129.6	0.8	0.8	1.0	NAN	65.1	5.4	1.4	NAN	7.2
UV light	0-2	333.6	278.1	163.1	139.1	19.8	2.1	1.6	1.1	54.4	56.4	158.8	153.6	1.0	1.1	0.4	0.0	133.5	7.3	0.9	0.049	7.7
UV light	2-4	347.4	348.8	142.0	152.4	34.2	6.3	1.4	1.6	47.1	68.6	158.5	174.4	1.1	1.2	1.8	0.0	147.2	6.9	0.8	0.051	7.0
UV light	4-6	317.4	353.8	161.7	167.6	27.7	5.9	0.9	1.9	35.5	82.4	142.4	186.2	1.0	1.2	1.5	0.0	69.6	6.8	1.5	0.053	7.0
UV light	6-8	338.3	364.5	200.0	211.8	30.8	9.0	0.9	0.8	42.6	51.9	155.6	140.0	1.0	0.9	1.9	10.3	81.0	5.6	5.2	0.048	7.0
UV light	8-10	284.2	390.8	198.9	214.8	14.1	3.3	1.4	0.8	41.0	46.7	138.2	136.1	0.8	0.9	1.1	22.2	21.7	4.4	1.5	0.055	7.0
UV light	10-12	405.6	391.1	240.4	177.3	4.0	1.7	0.5	0.8	37.4	41.9	139.3	131.1	0.9	0.9	1.2	NAN	174.6	4.1	1.1	0.057	7.0
UV light	12-14	397.8	352.5	217.0	192.8	3.9	2.4	0.7	1.0	40.5	45.3	155.1	141.1	1.1	0.9	1.2	0.0	24.0	4.5	1.3	0.055	7.0
UV light	14-16	273.5	370.7	210.3	196.9	14.6	2.6	0.8	1.0	36.0	39.9	145.9	133.0	1.0	0.9	1.1	12.4	21.7	3.9	1.6	0.059	7.0
UV light	16-18	448.9	445.2	194.8	203.2	20.8	2.6	1.2	0.8	33.5	42.1	142.9	135.2	0.9	0.8	0.9	0.0	21.7	5.5	1.8	0.047	7.1
UV light	18-20	449.8	470.7	335.0	206.8	6.8	2.1	0.8	0.9	33.1	43.9	139.7	139.5	0.9	0.8	1.7	0.0	126.7	8.5	3.1	0.049	7.1
UV dark	0-2	368.1	385.4	209.6	213.8	4.2	2.4	1.6	2.1	40.3	45.3	174.4	179.1	1.1	1.1	1.4	0.0	309.3	10.5	1.3	0.047	7.2
UV dark	2-4	411.3	312.1	203.3	163.6	10.2	3.8	0.9	1.6	31.7	44.2	144.9	165.5	0.9	1.1	2.2	0.0	489.6	14.4	1.5	0.045	7.1
UV dark	4-6	374.9	324.4	176.6	180.1	18.5	6.0	1.0	1.7	26.7	33.7	140.9	160.8	0.9	1.0	1.4	0.0	204.3	6.2	1.1	0.040	7.1
UV dark	6-8	434.0	400.2	214.3	185.1	7.9	2.0	1.1	1.3	31.9	27.9	156.3	147.9	1.0	1.0	1.6	29.1	133.5	4.9	1.3	0.039	7.1
UV dark	8-10	457.9	405.0	220.0	216.5	19.2	1.5	0.8	1.0	25.6	25.4	126.1	130.0	0.8	0.8	0.8	27.3	106.1	4.7	0.9	0.043	7.1
UV dark	10-12	452.6	446.2	207.7	238.9	6.6	8.7	1.1	1.8	24.2	29.7	125.3	140.7	0.8	0.9	1.7	112.4	170.1	4.9	1.1	0.045	7.1
UV dark	12-14	400.5	461.8	188.1	223.7	3.7	1.4	3.2	1.0	21.7	30.8	121.9	131.6	0.7	0.8	1.6	7.8	213.4	NAN	0.8	0.042	7.1
UV dark	14-16	402.2	455.1	214.2	238.2	2.9	1.4	0.6	1.6	26.3	26.1	143.6	131.8	1.0	0.8	1.5	9.4	213.4	7.8	1.3	0.039	7.2
UV dark	16-18	484.4	457.8	229.6	223.7	1.3	0.7	1.2	1.0	31.0	25.1	137.2	133.6	0.9	0.9	0.9	0.0	142.7	7.2	1.0	0.046	7.1
UV dark	18-20	510.2	484.6	213.9	200.8	5.4	3.4	1.4	1.0	27.2	25.3	142.7	135.9	0.9	0.9	0.7	0.0	131.3	7.2	1.6	0.041	7.1
HTSG	0-2	268.8		118.5				1.9		30.6		153.3		0.2								
HTSG	2-4	251.6		153.2				1.3		25.6		131.6		0.2								
HTSG	4-6	235.0		118.5				0.6		17.9		118.5		0.1								
HTSG	6-8	256.8		112.2				0.6		18.4		117.6		0.2								
HTSG	8-10	269.3		124.2				0.8		18.4		119.1		0.1								
HTSG	10-12	314.4		154.1				1.9		23.3		123.2		0.2								
HTSG	12-14	277.3		150.1				0.7		20.6		130.7		0.2								
HTSG	14-16	268.0		168.1				0.9		20.1		133.0		0.2								
HTUV	0-2	200.8		104.8				0.6		21.5		116.2		0.2								
HTUV	2-4	193.7		105.5				0.5		21.7		103.5		0.2								
HTUV	4-6	182.6		123.0				0.4		18.4		106.9		0.1								
HTUV	6-8	193.8		145.2				0.3		14.8		94.7		0.1								
HTUV	8-10	225.3		162.9				0.5		19.0		105.3		0.1								
HTUV	10-12	306.9		280.7				0.3		16.2		102.4		0.1								
HTUV	12-14	260.4		220.7				0.6		22.2		117.8		0.1								
HTUV	14-16	249.0		150.7				0.5		21.7		118.0		0.1								
HTUV	16-18	229.4		133.6				0.8		17.1		108.0		0.1								
HTUV	18-20	267.0		147.5				0.6		19.0		114.1		0.1								

SG=seagrass, UV=unvegetated, HTSG= seagrass under high tide, and HTUV=unvegetated sediments under high tide

The numbers 1 and 2 refer to two adjacent cores taken at the same time, except for SRR where it is 3-hr and 12-hr incubations, respectively.

TRS, AVS, Fe, Mn = µmol/gdw

TOC = wt% organic carbon

SRR = mmol $SO_4^{2-} \cdot m^{-2} \cdot d^{-1}$

DIC, DOC, NH_4^+ = mM

NO_3^-, PO_4^{3-} =µM

NAN = no data

High tide data are supplement

VITA

ANDREW BRIAN HEBERT

Department of Oceanography	Office: 979.845.9633
3146 TAMU	Lab: 979.845.8179
College of Geosciences	Fax: 979.845.9631
Texas A&M University	Home: 979.260.2700
College Station, Texas 77843-3146	Email: hebert@ocean.tamu.edu
http://ocean.tamu.edu/~hebert	

EDUCATION

2002- Ph.D. Oceanography, Texas A&M University, College Station, TX
2002 M.Sci. Oceanography, Texas A&M University, College Station, TX
1998 B.Sci. Biology, chemistry minor, Northwestern State University, Natchitoches, LA

PROFESSIONAL EXPERIENCE

2001, 03 Graduate Assistant Teaching (Oceanography Laboratory), Texas A&M University. Designed course syllabi, exams, and lectures. Positive course evaluations.

1999- Graduate Assistant Research, Texas A&M University
Implemented research curriculum for seagrass sediment biogeochemistry and developed key methodology for *in situ* sediment sampling techniques using microelectrodes. Collaborated with EPA on seagrass-sediment biogeochemistry and aquatic stressors model through pore water chemical assessment. Managed undergraduate student workers.

1995-98 Math tutor, Northwestern State University. Mentored algebra through calculus level courses for the College of Science and Technology.

1995-98 Technician, North Texas Business Systems

SELECTED PUBLICATIONS

Hebert, A. B. and Morse, J. W. (2003) Microscale effects of light on H_2S and Fe^{2+} in vegetated (*Zostera marina*) sediments. *Marine Chemistry* **81**, 1-9.

Morse, J.W., DiMarco, S.F., Sell K.S., and **Hebert, A.B.** (2003) Determination of the optimum sampling intervals in sediment pore waters using the autocovariance function. *Aquatic Geochemistry* **9**, 41-57.

Morse, J.W., DiMarco, S.F., **Hebert, A.B.**, and Sell, K.S. (2003) A scaling approach to spatial variability in early diagenetic processes. *Hydrobiologia* **494**, 25-29.